CHARACTERIZING THE MURINE NASAL MICROBIOME

THE UPPER RESPIRATORY TRACT MICROBIOTA CONTRIBUTES TO SUSCEPTIBILITY TO STREPTOCOCCUS PNEUMONIAE INFECTIONS

By

L. PATRICK SCHENCK, M.Sc., B.Sc.

A Thesis Submitted to the School of Graduate Studies in Partial Fulfillment of the Requirements for the Degree

Doctor of Philosophy

McMaster University DOCTOR OF PHILOSOPHY (2019)
Hamilton, Ontario (Biochemistry and Biomedical Sciences)

TITLE: The upper respiratory tract microbiota contributes to susceptibility to *Streptococcus pneumoniae* infections

AUTHOR: L. Patrick Schenck, M.Sc, B.Sc (McMaster University)

SUPERVISOR: Dr. Michael G. Surette

NUMBER OF PAGES: 174, xvii

Lay Abstract

Bacteria living in the gut have been shown to benefit our health, but the role of bacteria living in our respiratory tract is relatively unknown. I describe the methods for characterizing the bacteria in the nose of a mouse as a model of the human nose. I found that pockets of the mouse nose are colonized by different bacteria. I also characterized a mouse model that had bacteria in the gut without nasal bacteria. I used this mouse model to understand infections with *Streptococcus pneumoniae,* the worldwide leading cause of bacterial pneumonia. The mice without nasal bacteria were protected from infections, which was due to a nasal bacteria helping *S. pneumoniae* escape from the nasal tissue. This work established new models for understanding how bacteria affect respiratory health, and identified new targets for protecting against infections.

Abstract

The upper respiratory tract (URT), including the nasal and oral cavities, is a reservoir for pathogenic and commensal microbial species, collectively known as the microbiota. Microbial colonization of the URT occurs right after birth, and URT microbial composition has been linked to development of respiratory infections, allergy, and asthma, though few direct mechanisms have been uncovered. Thus, I set out to establish animal models for characterizing the URT microbiota, and its role in infections. I found that nasal washes, a predominant method for measuring URT bacterial colonization, were insufficient for completely extracting the URT microbiota. The age and source of mice greatly affected the composition of the microbiota, which could be transferred to germ-free mice via cohousing. I also established that mice colonized with the Altered Schaedler's Flora in the gut microbiota have no cultivable URT microbiota. To test the function of the URT microbiota, I colonized mice with *Streptococcus pneumoniae,* the leading cause of bacterial pneumonia worldwide. I show that the presence of a nasal microbiota increases permissiveness to pneumococcal infection in murine models. Addition of a single URT isolate, *Actinomyces naeslundii*, increased pneumococcal adherence to human respiratory epithelial cells *in vitro* and increased pneumococcal dissemination *in vivo* in a sialidase-dependent manner. The microbiota affects expression of several host genes throughout the respiratory tract involved in pneumococcal

pathogenesis. Together, this work establishes new models for assessing the URT microbiota, and highlights the contribution of the URT microbiota to pneumococcal pathogenesis and identifies druggable targets to prevent and treat infections.

Acknowledgments

This work was supported by several grants, but I was personally funded by the Banting and Best Canada Graduate Scholarship from the Canadian Institutes of Health Research. I received a Michael Smith Foreign Study Supplement from the Canadian Institutes of Health Research. I am grateful for the opportunities that were made possible by these scholarships.

I would like to thank my supervisor, Dr. Mike Surette, for inspiring me as a scientist during my doctoral training. You provided the environment to learn in more ways than I could have imagined: learning to try new techniques and succeeding, or trying to learn new techniques and failing. I really appreciated your mentorship: you made complex problems seem really simple, and simple problems seem really complex. I have learned how to approach all projects better because of you, so thank you.

I would like to thank my mentor (and unofficial co-supervisor), Dr. Dawn Bowdish. You were instrumental in building me up as a scientist, learning my strengths and weaknesses, what I need to focus on, or when I just need to focus. Being a member of the Bowdish lab brought unrivalled camaraderie, and being surrounded by passionate scientists made this experience wonderful. You challenged me to see the world, and were the biggest supporter of my time in Scotland and England. I will be forever grateful for all of the time you gave me during my PhD.

To my committee members, Dr. Brian Coombes and Dr. Martin Stämpfli, thank you for guiding me along this PhD. I chose the two of you to be challenged by leading host-pathogen and respiratory immunity experts, and you definitely challenged me. I really appreciated the interest that you took in my development; you were always there for a smile, or a whiteboard, when I needed one.

I have to thank all of the members of the Surette and Bowdish labs. To the Surette lab members, thanks for trying really hard to make me a microbiologist, whether it was teaching me about sequencing analysis, culturing, or just putting memes of me around the lab. Thanks to Laura and Michelle for helping me whenever I needed, and for keeping the place running! To the Bowdish lab members, thanks for such a collaborative environment, learning my project along with me, or just being patient when I am coming down off of a coffee high. There are too many of you to individually thank, but this would be incomplete if I didn't thank my 'sass-ter' Daphnée Lamarche. You were ALWAYS there for me, whether it was a science question, a non-science question, a quick trip for a beer, or a quick trip to the hospital. This entire experience was what it was because of you, and I know you'll miss me correcting your English.

I fully appreciate and gained so much from the scientific community I m*et al*ong the way: Biochemistry grad students, Lisa and Allison from the Biochemistry office, Farncombe members, MIRC, IIDR, Dr. Mark

McDermott, Dr. Donald Davidson and his lab at the University of Edinburgh, Dr. Jo Konkel and her lab at the University of Manchester, as well as my friends at University of Calgary. The interactions, whether collaborative, competitive, or social, all contributed to my awesome graduate school experience.

Though this doesn't usually go in acknowledgments, I'd like to thank the Canadian healthcare system for getting me through this PhD. Universal healthcare is a blessing to those who need it, and I probably oversubscribed during my PhD. I'd like to acknowledge my senses of taste and smell, even though you weren't there for the whole PhD, it was nice knowing you.

Thank you to my parents, Babs and Lou Schenck, and my siblings Maureen and Tom, for supporting me in my passion to push scientific borders, even if you didn't know what I was doing. You helped me throughout this process and I appreciated all of the love along the way. Your encouraging words, card games, and laughs kept me sane through this process. Thanks to all of my friends and family near and far, and to the Ratelle's for supporting a 30 year old student. And last but certainly not least, thanks to my wife Constance. You were my pillar through all of this, challenging me to get what I wanted, or just challenging me to have fun. Though we spent the first half of this PhD separated by land (and water), your support was always there when I needed it, and I couldn't have done this without you.

Table of Contents

List of Figures and Tables

List of Abbreviations

16S rRNA	16S ribosomal ribonucleic acid
ASF	Altered Schaedler's Flora
ASF-CoH	Altered Schaedler's Flora cohoused with SPF
ASV	amplicon sequence variant
BgaA	β-galactosidase
BHI	brain heart infusion
CbpA	Choline binding protein A
CCL2/MCP-1	Chemokine (C-C motif) ligand 2/ monocyte chemoattractant protein 1
CFU	colony forming units
ChoP	phosphorylcholine
cNT	complete nasal tissue
DANA	2,3-didehydro-2-deoxy-N-acetylneuraminic acid
DMEM	Dulbecco’s modified Eagle’s medium
DNA	Deoxyribonucleic acid
FAA	fastidious anaerobe agar
GF	germ-free
HMP	Human Microbiome Project
IgA	immunoglobulin A
IL	interleukin
IPD	invasive pneumococcal disease
JAX	Jackson Laboratories

LDA	linear discriminate analysis
LEfSe	linear discriminate analysis effect size
MetaHIT	Metagenomics of the Human Intestinal Tract
MOI	multiplicity of infection
MUN	2'-(4-methylumbelliferyl)-α-D-N-acetylneuraminic acid sodium salt hydrate
N	Nested PCR
NanA	neuraminidase A
Nod2	nucleotide-binding oligomerization domain-containing protein 2
PAFR	platelet-activating factor receptor
PBS	phosphate buffered saline
PCR	polymerase chain reaction
PERMANOVA	Permutational multivariate analysis of variance
pIgR	polymeric immunoglobulin receptor
RNA	ribonucleic acid
S	Standard PCR
SPF	Specific pathogen-free
StrH	β-*N*-acetylglucosaminidase
T_H17	interleukin-17A-producing CD4+ T cells
TLR	Toll-like receptor
TSA	tryptic soy agar
UPGMA	unweighted pair group method with arithmetic mean
URT	Upper respiratory tract

Declaration of Academic Achievement

The work presented in the thesis is my own, though some aspects were done in collaboration. The research throughout was designed by me with inputs from Dr. Mike Surette and Dr. Dawn Bowdish.

In Chapter 3.1, I designed the experiments, completed the majority of the bench work, and completed the bioinformatic analysis, which is being prepared for submission with me as the primary author. At times, Michelle Shah and Laura Rossi helped with DNA extraction and PCR for high-throughput sequencing, and Daphnée Lamarche helped with bioinformatic analysis. Netusha Thevaranjan helped with the experiments with old mice, and coordinated the cohousing with germ-free mice. Josh McGrath performed the Buffer RLT nasal washes on naïve mice. The mice from Jackson Laboratories were ordered by Dr. Martin Stämpfli and collected in collaboration with Dr. Pam Shen.

In Chapter 3.2, I designed the experiments, completed the majority of the bench work, and completed bioinformatic analysis, which is being prepared for submission with me as the primary author. Dr. Dessi Loukov and Dr. Christian Schulz helped with flow cytometry. Dr. Christian Schulz isolated lung tissue to send to Dr. Alexander Misharin and his lab sorted alveolar macrophages for RNA-Seq, as well as align the sequences to the mouse genome. Dr. Janine Strehmel isolated the nasal tissue RNA prior to

sequencing at the Farncombe Genomics Facility, with gene alignment performed by Jake Szamosi.

The thesis was completely written by me, with editing notes from Dr. Mike Surette, Dr. Dawn Bowdish, Dr. Michael Dorrington, and Daphnée Lamarche.

Chapter 1: Introduction

1.1 The microbiota

The human body has been referred to as a superorganism, hosting a diverse microbiota in a balance with their host. This ecosystem includes many distinct niche for bacterial, archaeal, viral and fungal species to colonize and thrive. This microbial ecosystem, collectively called the microbiota or microbiome, has shaped the evolution of the human species and interacts with every aspect of life, from development and metabolism to immunity and infections (McFall-Ngai *et al.*, 2013). The microbiome has been intensely studied for centuries, with the discoveries in 1676 by Antonie van Leeuwenhoek of different “animalcules” from dental plaque (Porter, 1976). The role of the microbiota dominated debates at the turn of the 20th century, with prominent researchers, or famed cereal maker John Harvey Kellogg, arguing the microbiota contributed to ‘autointoxication’, poisoning the host (Kellogg, 1917). Élie Metchnikoff, who once said the colon was a useless appendage, made several contributions to the study of immune-microbiota interactions, demonstrating that *Lactobacillus* species were beneficial to health and counteracted some of the bad bacteria (Metchnikoff and Williams, 1912). Findings by Metchnikoff and others led to the development of many *Lactobacillus*-based probiotics that are still in use (Bested, Logan and Selhub, 2013).

Today, the microbiota is generally thought to be beneficial, if not essential, to human health; however, it can contain microbial species that can cause local or systemic disease. The microbiota contains more genetic content compared to its

host, resulting in the production of enzymes capable of modifying and producing nutritional metabolites, modifying xenobiotics, and stimulating the immune system (Jandhyala *et al.*, 2015). Due to the ability to alter the microbiota (especially relative to altering human genetics), the microbiota is being targeted for helping with current health crises, including diabetes, obesity, cancer, and antibiotic resistant infections. The excitement over the microbiota has increased over the past decade due to several contributing factors, namely the creation of larger human studies including the Human Microbiome Project (HMP), the decrease in DNA sequencing costs, and the success of microbiota-based therapies in clinical trials. In this section, I will summarize the current state of bacterial microbiota research, and highlight current strengths and drawbacks of methodologies.

1.1.1 Microbial community analysis

Understanding the tools and models of microbiome analysis is essential to developing mechanistic studies. Microbial communities are analyzed in culture-dependent and -independent methods. Culture-dependent methods allow for the isolation and characterization of individual microbes both *in vitro* and *in vivo*. Culture-dependent methods were long considered inadequate due to the thought that most bacteria were uncultivable (Hayashi, Sakamoto and Benno, 2002; Eckburg *et al.*, 2005; Stewart, 2012). The launch of HMP in 2009 stated that 20-60% of the human-associated microbiome was uncultivable, necessitating the dominance of culture-independent methods (Peterson *et al.*, 2009). Today, the microbiota from multiple tissue sites is considered cultivable via the use of nutrient-

rich media types and anaerobic culture conditions (Sibley *et al.*, 2011; Browne *et al.*, 2016; Lau *et al.*, 2016). Nonetheless, the ease and accessibility of culture-independent assessment of the microbiome predominates current literature.

Culture-independent assessment of microbial communities involves the study of selected marker genes, namely the 16S ribosomal ribonucleic acid (16S rRNA) gene, or metagenomic analysis, allowing for assessment of total genetic composition of a sample. The 16S rRNA gene is the predominant marker gene due to conserved regions across all bacteria with 9 variable regions that allow species-level identification; 16S rRNA databases exist for taxon classification (DeSantis *et al.*, 2006; Wang *et al.*, 2007; Quast *et al.*, 2013). Analysis of the 16S rRNA gene has been used for decades to characterize microbial communities via polymerase chain reaction (PCR) quantification of targeted groups, denaturing gradient gel electrophoresis, terminal restriction fragment length polymorphism bacteria, or direct sequencing of portions or the entire (Muyzer, de Waal and Uitterlinden, 1993; Liu *et al.*, 1997). The HMP set out to describe the microbial communities across multiple tissues, namely the nose, mouth, gastrointestinal tract, skin, and vaginal tract, in 250 “normal” volunteers; with “normal” being defined by lack of symptoms within the specific tissue (Peterson *et al.*, 2009). “Normal” and diseased microbial communities could then be contrasted to detect a shift in the microbial population, known as dysbiosis. Development of high-throughput sequencing technology, which dropped the cost of DNA sequencing from $1000 per million base pairs in 2004 to $0.25 per million base pairs in 2010, aided the development of the large

scale microbiota sequencing projects, including the Metagenomics of the Human Intestinal Tract (MetaHIT) and the HMP (Qin *et al.*, 2010; Mardis, 2011). The HMP and MetaHIT improved 16S rRNA gene databases, increased the number of available genomes, and improved functional analysis of the microbial communities. Marker gene studies have been used in innumerable research studies to compare healthy and diseased states; however short sequence lengths produced from sequencing technology often fail to fully identify taxa (Schloss, 2010). Metagenomic analysis can identify functional genes and also non-bacterial members of the microbiota. Nonetheless, metagenomics is complicated by bioinformatic pipelines, identification of complete genomes, and understanding the functions of newly identified genes within a sample, though this area is rapidly improving (Almeida *et al.*, 2019; Nayfach *et al.*, 2019; Pasolli *et al.*, 2019).

The increase in culture-independent analysis of the microbiota combined with the low cost has led to the development of many large microbiota datasets. Bioinformatic analysis of microbial sequencing data has continued to develop since the launch of the HMP and MetaHIT. Bioinformatic pipelines involve the cleaning and organizing sequencing reads, assignment of taxonomy, and community and taxonomy analysis (Schloss *et al.*, 2009; Caporaso *et al.*, 2010). Though new tools and statistical methods are constantly being developed, similar questions are asked of all datasets: identifying a compositional difference between healthy and diseased patient samples, and what is driving that difference. Assessment of microbial composition relies on the analysis of α-diversity, referring to the diversity

of the microbiota within a patient, and β-diversity, the diversity within a group of samples versus another. Altered α-diversity, measured by observed number of species, Shannon or Simpson diversity indices, has been reported in several diseases. The Shannon diversity index is a metric which accounts for the abundance of different bacteria, with a low Shannon diversity suggesting the microbiota is dominated by a few bacterial species, whereas a high Shannon diversity suggests many different taxa of even relative abundance (Jost, 2007). Statistical analysis of β-diversity metrics, including Bray-Curtis or UniFrac, give insight into the contribution of a specified factor (e.g. disease status, sex) to the diversity across all samples (Bray and Curtis, 1957; Lozupone, Hamady and Knight, 2006). Finally, taxonomic analysis reveals the bacterial sequences that can be driving the difference between two groups (Segata *et al.*, 2011; Mandal *et al.*, 2015).

Culture-independent and -dependent methods have strengths and drawbacks. Culture-independent methods allow for an inexpensive survey of the microbiota from many specimen types. Furthermore, culture-independent methods are accessible worldwide due to the large number of sequencing facilities, stability of DNA for storage and shipping purposes, and increased ease of bioinformatic analysis. Nonetheless, culture-independent analysis can be marred by sequencing errors and PCR bias, the inability to distinguish between live and dead bacteria, the inability to resolve bacterial identities from short sequencing reads, and incomplete reference databases (Kuczynski *et al.*, 2012). A current frustration

with microbiome research is the lack of functional studies, with culture-independent analysis unable to determine if microbial differences are a cause or consequence of disease. A recent meta-analysis identified that some microbial signatures may be common to many diseases, including obesity, *Clostridioides difficile* infections, and inflammatory bowel disease (Duvallet *et al.*, 2017). Functional microbiota research studies will require a combination of culture-dependent and independent methods to allow for improved identification and functional analysis of bacteria. Culture-dependent methods allow for the isolation of bacteria, which permits genomic and functional analyses of the isolates. Culture-dependent methods are improving to allow cultivation of most of the bacteria present in the human microbiota, though this often requires aerobic and anaerobic cultivation of fresh samples (Sibley *et al.*, 2011; Browne *et al.*, 2016; Lau *et al.*, 2016). Access to appropriate equipment, and development of media that enrich and isolate specific bacteria remain a challenge for culture-dependent methodologies. Intriguingly, culture-dependent methodologies have been shown to improve DNA sequencing quality and resolution, suggesting the combination of the two strategies will allow more powerful research analysis (Lau *et al.*, 2016).

1.1.2 Assessing the microbiome in animal models

Functional assessment of the contribution of the microbiota to health and disease uses animal models. The use of animals provides a natural niche for bacteria to colonize while also providing a platform to investigate the involvement of the host immune and metabolic responses to colonization and infection. The

majority of wildtype mice are housed under specific pathogen-free (SPF) conditions, allowing for the colonization of many bacteria that are not considered mouse pathogens. SPF mice can be compared to microbiota-free mice, also referred to as axenic or germ-free (GF) mice (Glimstedt, 1959; Bested, Logan and Selhub, 2013). GF mice display altered histological, immunological, and physiological attributes relative to SPF mice (Thompson and Trexler, 1971). GF mice have altered cecal sizes due to their inability to metabolize certain components of their diet. Furthermore, GF mice have deficits in several immune compartments, including reduced innate and adaptive immunity cells (Atarashi *et al*., 2013; Ivanov *et al*., 2009; D. Zhang *et al*., 2015). The behaviour of GF mice is also altered compared to SPF mice (Bercik *et al.*, 2011). The addition of individual, a minimal cocktail, or entire consortia of bacteria into GF mice allow for the interrogation of their respective contribution to a selected phenotype. SPF mice do not have a defined microbiota, but are rather defined by the lack of pathogens. As such, the gut microbiota of SPF mice can vary greatly depending on the source of the mice, which has an effect on immunology and susceptibility to infection (Gauguet *et al*., 2015; Ivanov *et al*., 2008; Rasmussen *et al*., 2019; Velazquez *et al*., 2019). Defined, simple microbial communities have been used for decades for simplistic investigation of the microbiota. Mice colonized with the Altered Schaedler's Flora (ASF), consisting of 8 anaerobic bacteria introduced to GF mice, have normalization of several deficits seen in GF mice (Dewhirst *et al.*, 1999; Feng *et al.*, 2010; Smith *et al.*, 2013; Collins *et al.*, 2014; Thevaranjan *et al.*, 2017). ASF

mice still share some characteristics of GF mice, as they do not have all microbial metabolic pathways replaced in a simplistic microbial consortia (Ivanov *et al.*, 2009; Norin and Midtvedt, 2010; Natividad *et al.*, 2012). This allows for the comparison of simple, defined microbial communities and more complex microbial communities to disease. This is further complicated by developmental windows, as timing of exposure to bacteria is important for microbial influence on immunology. A recent study identified that temporary microbial colonization of pregnant GF mice allowed for improved immune development of the offspring compared to naïve GF mice (Agüero *et al.*, 2016). As such, maintaining an ASF-microbiota colony allows for assessment of the impact of simple complex microbial communities without many of the deficits of GF mice.

There are very few investigations of the respiratory microbiota in mice. The majority of research investigating the microbiota and respiratory health has looked at the extraintestinal effects of the gut microbiota, referred to as the “gut-lung axis”. Antibiotic treatment of mice, and subsequent gut microbiota disturbances, have been linked to models of allergic asthma and influenza A virus susceptibility (Ichinohe *et al.*, 2011; Russell *et al.*, 2012, 2013). A recent mouse study suggests that the resident lung microbiota contributes to lung health (Dickson *et al*., 2018). The murine lung microbiota was found to be variable between mice, but antibiotic treatment altered these communities, and correlated with interleukin (IL)-1α abundance in the lung (Dickson *et al.*, 2018). The commercial source of the mice also affected the microbial community, which is known to affect the gut microbiota.

SPF mice underestimate the diversity naturally seen in the respiratory microbiota of wild-caught mice (Yun *et al.*, 2014). Changes in microbiota composition between SPF and wild-caught mice were linked to changes in alveolar structure in the lung.

The microbiota of the upper respiratory tract (URT) has been functionally linked to physiology, immunology, and infections. The first mechanistic study of the murine URT microbiota found that the resident bacteria afforded colonization resistance against *Bordetella pertussis,* but not *B. bronchiseptica*, but this could be overcome by antibiotic treatment of the URT (Weyrich *et al.*, 2014). Cultivation of bacterial isolates from the URT found multiple bacterial species capable of killing *B. pertussis in vitro*, which could confer protection *in vivo.* The URT microbiota plays a role in olfaction, as GF mice were found to have altered cilia on their olfactory epithelium, as well as prolonged responses to odorants, due to decreased production of xenobiotic metabolism enzymes (François *et al.*, 2016). The immunostimulatory capacity of the URT microbiota has been identified to promote the adjuvant activity of cholera toxin during vaccination studies in a nucleotide-binding oligomerization domain-containing protein 2 (Nod2) dependent manner (Kim *et al.*, 2016). The Nod2 stimulation from the URT also confers protection against bacterial infections in the lung (Brown, Sequeira and Clarke, 2017). Importantly, a few studies have assessed changes in the URT microbiota during *Streptococcus pneumoniae* colonization, which are discussed further later (Krone, 2014; Siegel, Tamashiro, & Weiser, 2015; Thevaranjan *et al*., 2016).

1.1.3 Tissue-specificity of the microbiome

The mucosal surfaces of the body provide distinct ecological niches for bacteria to colonize, allowing for extremely divergent communities. Multiple studies have set out to characterize the microbiota of different sites of the body, unveiling diverse communities underestimated by classic cultivation studies (Aas *et al*., 2005; Bik *et al*., 2006; Verhelst *et al*., 2004). Bacterial colonization is driven by nutrient availability, pH, oxygen and humidity levels within these tissues. The gastrointestinal tract contains many distinct niches throughout the stomach and intestines: the low pH of the human stomach restricts the growth of many bacteria, whereas the colon harbors the densest amount of colonization providing an anaerobic, nutrient-rich, neutral pH environment (Stearns *et al.*, 2011). The colonic microbiota has been intensely studied for decades for its contribution to local and systemic immunity, but the onset of the HMP allowed expanded assessment of other tissue sites.

The respiratory tract can be segmented into two major areas – the upper and lower respiratory tract. The major functions of the URT are to heat, humidify, and filter air through several compartments (i.e. nares/vestibules, nasal cavity/meatus, nasopharynx, oropharynx, and pharynx) before the air reaches the lungs (Sahin-Yilmaz and Naclerio, 2011). These different compartments provide a niche for colonization of pathogens, as differences in temperature, mucus secretion, and relative oxygen concentration throughout the URT may regulate colonization, as it does in the gastrointestinal tract (Rigottier-Gois, 2013; Siegel

and Weiser, 2015). The vestibules contain stratified squamous epithelial cells that transition into pseudostratified epithelial cells, as well as hairs that are important for trapping large particulate matter (Sahin-Yilmaz and Naclerio, 2011). Inspired air is heated and humidified within the turbinates of the nasal cavity, which also dehumidifies expired air. The nasal cavity has three turbinates that increase the surface area of the nose, and heat airflow entering the nasopharynx (Yu *et al.*, 2008). Glands and goblet cells are important for secreting the hydrated mucus layer, which contributes to humidifying incoming air and traps microparticles and microbes entering the URT from the environment. Finally, the humidified air enters the nasopharynx, which moves into the lungs for respiration within the alveolar space. Ciliated epithelial cells direct mucus flow towards the oesophagus to remove trapped particles, which is known as mucociliary clearance (Wanner, Salathe and O'Riordan, 1996). Thus, the URT protects the lower airways from temperature or particle-induced cellular damage. Air inspired into the URT impacts the inner ear since the Eustachian tubes contain air that is required for equalization of air pressure near the eardrum. Infections of the Eustachian tubes, known as acute or chronic otitis media, occur when pathogens evade physiological and immunological barriers of the upper respiratory tract (Faden *et al.*, 1997; Verhoeven, Nesselbush and Pichichero, 2013). Characterizing the microbiota of the deeper regions of the nasal cavity, including the sinuses, is challenging in routine clinical diagnostics; however, the more accessible regions of the nasal cavity have distinct microbiota profiles within an individual (Yan *et al.*, 2013).

In humans, the nasal microbiota is colonized by several bacterial genera, including *Staphylococcus, Streptococcus, Moraxella, Haemophilus, Prevotella, Enterococcus, Corynebacterium* and *Dolosigranulum* (Biesbroek *et al*., 2014; Stearns *et al*., 2015). A number of these bacterial species reside in the URT as potential pathogens, asymptomatically colonizing the tissue of many individuals, with the potential to cause disease is susceptible individuals (Round and Mazmanian, 2009). Early microbiome analysis of the URT involved targeted culture for pathogens, namely *Staphylococcus aureus, Streptococcus pneumoniae*, and *Haemophilus influenzae*. Culture-independent techniques have demonstrated compositional changes in microbial communities during healthy aging and diseases.

While the URT microbiota has long been recognized as a reservoir of pathogens, the lower respiratory tract has been thought to be sterile in healthy individuals. Studies from the 1960's failed to recover viable bacteria in the lower airways of healthy individuals in bronchial swabs (Laurenzi, Potter and Kass, 1961). When bacteria or bacterial DNA were recovered from the airways it was believed to be due to sampling contamination by the upper airways (Dickson *et al*., 2016). Consequently, the lungs were one of the few body sites which were not sampled as part of the HMP (Peterson *et al.*, 2009). Culture-independent approaches identified the presence of microbial DNA that originated primarily from the oral cavity (Segal *et al.*, 2013; Bassis *et al.*, 2015). The question of whether there was a unique microbial community in healthy adults was thoroughly

investigated in studies that used extremely careful sampling techniques (Hilty *et al.*, 2010; Morris *et al.*, 2013; Segal *et al.*, 2013; Venkataraman *et al.*, 2015). Neutral community modelling, which hypothesizes that the bacteria found in the lungs should match those found in the URT if it was contamination, suggested that the microbial community of the lungs was distinct from that of the URT (Venkataraman *et al.*, 2015). In chronic lower airway diseases such as cystic fibrosis, the lower airways are colonized by microbial communities clearly distinct from the URT (Rogers *et al.*, 2006).

Bacterial spread from or within individuals is facilitated through air flow, nasal secretions and saliva. Infections of the lower respiratory tract often originate from bacteria in the oral cavity, in a process called “microaspiration” (Dickson *et al*., 2016). Salivary excretions, which can be up to a litre a day, move bacteria from the tongue and throat/oropharynx towards the lower respiratory tract. Microaspiration is a frequent event, though this bacterial exposure is cleared in healthy adults, and likely only result in infections in those with impaired lung or immune function (Marik and Kaplan, 2003).

Investigative studies that assess bacterial interactions between potential pathogens and other naturally-colonizing members of the microbial community may lead to non-antibiotic based methods of clearing pathogens. A study by Yan *et al*. elegantly assessed different regions of the nasal cavity that would be exposed to the external environment (anterior nares), as well as drainage from the sinuses (middle meatus and sphenoethmoidal recess) in 6 *Staphylococcus aureus* carriers

and 6 non-carriers (Yan *et al.*, 2013). The middle meatus and sphenoethmoidal recess were dominated by *Corynebacterium* and *Staphylococcus* species, while anterior nares have a greater abundance of *Propionibacterium/Cutibacterium* species. When *S. aureus* sequences were removed from the microbiome analysis, carriers could not be distinguished from non-carriers based on overall diversity. However, *S. aureus* carriers had high rates of *Corynebacterium accolens* whereas non-carriers had high rates of *Corynebacterium pseudodiphtheriticum*, suggesting some levels of niche competition could be important for colonization by *S. aureus* (Yan *et al.*, 2013). This was corroborated with *in vitro* data showing the *C. accolens* and *S. aureus* support each other's growth, whereas *C. pseudodiphtheriticum* inhibited the growth of *S. aureus*. Clearly, the URT houses a diverse microbiota, where bacterial interactions can drive colonization success.

1.1.4 Respiratory microbiota throughout life

Colonization of the URT begins at birth and, importantly, early colonization events impact respiratory health throughout life. Correlations between the method of delivery (i.e. vaginal or caesarean) and breastfeeding with susceptibility to respiratory infections, asthma and allergy have been observed for decades (Arrieta *et al*., 2015; Dogaru *et al*., 2014; van Nimwegen *et al*., 2011); it is now believed that this due in part to the establishment of the URT microbiome. There is a negative correlation between wheezing and the relative abundance of *Dolosigranulum* species at 6 weeks of age. Infants colonized by *Haemophilus influenzae*, *Moraxella catarrhalis*, and *Streptococcus pneumoniae* within the first

month of life are more likely to demonstrate wheezing, but colonization status of these pathogens at one year of life did not correlate with wheezing (von Linstow *et al.*, 2013). Infants born via caesarean section are more likely to have reduced colonization of *Dolosigranulum* and *Corynebacterium* species (Bosch, Levin, *et al.*, 2016). Breastfeeding improves infant health in part because it facilitates the transfer of maternal antibodies which are then found in the infant's nasal secretions (Roberts and Freed, 1977; Taylor and Toms, 1984). A recent study established the role of exclusive breastfeeding versus exclusive formula feeding from 6 weeks of age up to an age of 6 months of life on the URT microbiota, including increased levels of *Corynebacterium* and *Dolosigranulum* species (Biesbroek *et al*., 2014; Stearns *et al*., 2015). A prospective cohort study involving 234 children demonstrated that nasopharyngeal colonization by *Streptococcus* at ~2 months of age was a strong predictor for asthma later in life (Teo *et al.*, 2015). Disruption of the microbiota via exposure to antibiotics increases the likelihood of colonization by *Streptococcus, Haemophilus* and *Moraxella* (Teo *et al.*, 2015).

Microbial succession patterns within the URT have been associated with allergic airway disease, starting from early infancy. A landmark study in 2014 assessed the URT microbiota and health outcomes from 1.5 months of age to 24 months (Biesbroek *et al*., 2014). The relative bacterial load and α-diversity did not change over time; however, the composition of the microbiota did change over time. At 1.5 months of age, 5 clusters were observed that were dominated by either *Streptococcus, Moraxella, Staphylococcus, Corynebacterium,* or

Corynebacterium/Dolosigranulum (Biesbroek *et al*., 2014). In the *Streptococcus* and *Staphylococcus* clusters, *Corynebacterium* and *Dolosigranulum* were found at very low abundance. As the infants progressed from 1.5 months to 24 months of age, those whose microbiota were dominated by *Moraxella* were likely to remain dominated by *Moraxella,* and infants who were colonized with *Corynebacterium/Dolosigranulum* were likely to become dominated by *Moraxella*. In contrast, microbial communities dominated by *Streptococcus* and *Staphylococcus* were not stable and would often have a completely different profile in subsequent samples, with no defined pattern (Biesbroek *et al*., 2014). The *Corynebacterium/Dolosigranulum* cluster was less likely to have URT infections, and was highly correlated with breastfeeding. This study demonstrated a repeatable pattern of ecological succession, and potentially identifies groups of infants that may be at risk for respiratory infections.

The URT microbiota transitions with increasing age, as noted by the reduced carriage of *S. pneumoniae* in adults. A cross-sectional study assessed composition of the nasopharyngeal and oral microbiota in 51 young children and 19 parents by both culture and 16S rRNA sequencing (Stearns *et al.*, 2015). Stearns *et al.* demonstrated that the oropharyngeal swabs had similar microbial communities regardless of age, and were dominated by *Streptococcus, Prevotella,* and *Veillonella*. Nasopharyngeal microbiota did cluster by age, with enriched of *Moraxella, Haemophilus,* and *Enterococcus* in children*,* whereas adult nasal microbiota were enriched with *Staphylococcus, Streptococcus, Prevotella,* and

Rothia. Cultivation of these bacteria allowed for species identification, including *Staphylococcus* (*S. epidermidis*), *Haemophilus* (*H. influenzae* and *H. parainfluenzae*), *Dolosigranulum pigrum* (member of Carnobacteriaceae), *Actinomyces*, and *Corynebacterium* (*C. durum* and *C. mucifaciens*) (Stearns *et al.*, 2015). The nasopharynx of children also had an increased cultivable bacterial density compared to healthy adults, indicating changing environmental niches with age could affect colonization.

The URT microbiota composition begins to deteriorate with age. Though no true definition of a “healthy” microbiota exists, the compositional distinction between tissue sites is a hallmark of the URT microbiota (Stearns *et al.*, 2015). The composition of the oropharyngeal microbiota did not differ between young adults (18-40 years old) and older adults (>65 years old), but the nasopharyngeal microbiota of older adults looked similar to the oropharynx, dominated by *Streptococcus, Prevotella,* and *Veillonella* species (Whelan *et al.*, 2014). These age-related changes may contribute to the increased susceptibility to respiratory infections (de Steenhuijsen Piters *et al.*, 2016).

1.1.5 Respiratory tract microbiota during disease

Genetic diseases affecting mucociliary clearance, such as cystic fibrosis and primary ciliary dyskinesia, affect the URT microbiota. Two recent studies have identified that infants with cystic fibrosis, which results in a thickened mucus layer, have an altered URT microbiota development compared to healthy infants including increased relative abundance of *Staphylococcus* species and decreased

abundance of potential beneficial bacteria (Mika *et al.*, 2016; Prevaes *et al.*, 2016). People with primary ciliary dyskinesia, a combination of diseases resulting in decreased ciliary action to clear mucus, also suffer from chronic rhinosinusitis, and there is a high reported rate of URT manifestations of disease, contributing to morbidity (Sommer *et al.*, 2011). While no studies have been completed to assess the total URT microbiota, cultivation or targeted PCR of pathogens from those suffering from primary ciliary dyskinesia have high levels of *H. influenzae, S. pneumoniae*, and *P. aeruginosa* (Møller *et al.*, 2017). The two diseases differ in their bacteriology, as *S. pneumoniae* has a very low prevalence in cystic fibrosis compared to primary ciliary dyskinesia (Møller *et al.*, 2017). The low prevalence of *S. pneumoniae* was replicated in a Canadian cohort of 318 cystic fibrosis patients repeatedly sampled over 34 years, in which only 15 patients had detectable *S. pneumoniae* (Thornton *et al*., 2015).

The prevalence of *S. pneumoniae* in the URT is important, as it is the leading cause of bacterial pneumonia worldwide. The very young and very old are typically impacted by pneumococcal infections, who have an altered immunity and distinct URT microbiota composition from healthy adults. The combination of low colonization rates and high incidence of pneumonia in the elderly implies that colonization is brief and proceeds swiftly to infection (Kellner *et al.*, 2009). In this study, pneumonia patients had a decrease in anaerobic bacteria, including *Prevotella*, and decreased lactic acid bacteria *Leptotrichia,* and an increased viral load. A human experimental pneumococcal carriage model has identified that

increased Shannon diversity in the URT microbiota of healthy adults correlates with permissiveness to colonization (Cremers *et al.*, 2014). Understanding the role of the URT microbiota during *S. pneumoniae* colonization, pathogenesis, and clearance is essential to discover new targets for prevention of pneumococcal infections.

1.2 *Streptococcus pneumoniae*

Streptococcus pneumoniae is an encapsulated, Gram-positive, human-adapted pathogen that is a leading cause of bacterial infections worldwide, resulting in the death of over 1,000,000 individuals annually (Demczuk *et al*., 2014). *S. pneumoniae* periodically and asymptomatically colonizes the upper respiratory tract (the nasal and oral passages) of young children and adults. Occasionally, colonization can progress to infections of the sinuses (sinusitis), ear (acute otitis media), and lung (pneumonia), or invasive pneumococcal disease (IPD) in which the bacteria is found in the blood (bacteraemia), brain or cerebrospinal fluid (meningitis). Canada experiences roughly 9 cases of IPD per 100,000 people annually, with the highest rates in children under the age of 1 (16.9 cases per 100,000 people annually) and adults over the age of 60 (21.5 cases per 100,000 people annually) (Demczuk *et al.*, 2014). Acute otitis media affects 32% of Canadian families, with *S. pneumoniae* being the causative agent in nearly half of these cases (Casey, Adlowitz and Pichichero, 2010; Dubé *et al.*, 2011; Ngo *et al.*, 2016). It is estimated the economic costs of pneumococcal infections are in excess of $132,000,000 annually within Canada (Earnshaw *et al.*, 2012). Clearly,

pneumococcal infections are a great burden on individuals, caregivers, and health funding within Canada. Vaccination strategies have begun to reduce the overall burden of IPD within Canada; however, further understanding of the progression from colonization to infection will identify new druggable targets to aid in the reduction of morbidity and mortality. This chapter will introduce the current understanding of pneumococcal pathogenesis, followed by an in-depth review of the host microbiota and its potential contribution to pneumococcal infections.

1.2.1 Modelling pneumococcal pathogenesis

The use of experimental pneumococcal colonization in humans has begun to assess different host factors involved in nasal colonization; however, human models are impractical to assess pneumococcal pathogenesis (Gritzfeld *et al*., 2013). Animal models have been used for decades to replicate pneumococcal infections (Webster, 1933; Wu *et al.*, 1997). A variety of animals, including mice, rats, rabbits, chinchillas, gerbils, and guinea pigs, have been used to model different aspects of pneumococcal pathogenesis (Chiavolini, Pozzi and Ricci, 2008). Some aspects of disease, especially pneumonia, are more adequately modelled in non-human primate models due to similarities is anatomy and physiology (Berendt, Long and Walker, 1975; Kraft *et al.*, 2014; Reyes *et al.*, 2016). The mouse model is most frequently used due to genetic tractability, ease of use, and low cost. Mouse models have been developed to evaluate colonization and transmission, pneumonia, bacteraemia, meningitis, and the host response to infection (Chiavolini, Pozzi and Ricci, 2008). Colonization and infections are

initiated by intranasal inoculation of *S. pneumoniae* to mice, remaining in the nose or reaching the lung depending on anaesthesia and inoculum volume (Southam *et al*., 2002; Wu *et al*., 1997). Susceptibility in mouse models is driven by both mouse and pneumococcal strains (Sandgren *et al.*, 2005). Susceptibility differences between mouse strains is potentially due to altered immune responses, specifically from neutrophils, though specific mechanisms are unclear (Gingles *et al.*, 2001). The following sections will address pneumococcal pathogenesis, much of which has been informed by mouse models.

1.2.2 *S. pneumoniae* colonization, immune evasion, and transmission

Approximately 30% of children are asymptomatically colonized by *S. pneumoniae* at any given time (Tocheva *et al.*, 2011). The URT acts as a reservoir for colonization, which can last weeks to months, allowing replication and transmission to other hosts. *S. pneumoniae* uses several virulence factors for adherence and immune evasion in order to successfully colonize the URT, which will be highlighted in this section.

The first barrier to pneumococcal colonization is the presence of a mucus barrier, which restricts access to the respiratory epithelial cells to all colonizing bacteria. Mucus is produced by goblet cells within the respiratory epithelium, with ciliated epithelial cells driving the mucus layer (and all trapped particles and microbes) towards the pharynx, where it is cleared into the gastrointestinal tract (Cohen, 2006). The pneumococcal capsular polysaccharides are essential throughout colonization, as unencapsulated mutants have a reduced density and

increased clearance in murine models (Nelson *et al.*, 2007). The negative charge present on capsular polysaccharides provides electrostatic repulsion of terminal sialic acids present on mucin proteins, allowing *S. pneumoniae* to escape entrapment in the mucus layer and interact with epithelial cells. Indeed, prevalence of pneumococcal serotypes correlates with their respective capsule charge (Li *et al*., 2013).

S. pneumoniae can utilize mucin as a nutrient source, possessing enzymes that can cleave sugar residues from mucins for nutrients and to expose residues for adherence, as depicted in Figure 1. Carbohydrates can act as the sole carbon source for *S. pneumoniae*, as it devotes nearly 30% of all transport mechanisms to carbohydrate import (Buckwalter and King, 2012). *S. pneumoniae* produces multiple neuraminidases (also known as sialidases), β-galactosidases, and β-*N*-acetylglucosaminidases, which release sialic acid, galactose, and *N*-acetylglucosamine, respectively, from mucins that can be imported and metabolized. While these enzymes disrupt mucin structure, *S. pneumoniae* also produces a multi-functional toxin called pneumolysin that disrupts mucociliary clearance by binding to cholesterol present on epithelial cell membranes, resulting in cell damage and reducing ciliary beating (Rayner *et al.*, 1995; Nöllmann *et al.*, 2004). *S. pneumoniae* has, in essence, made a career of turning the mucus barrier into a mucus carrier.

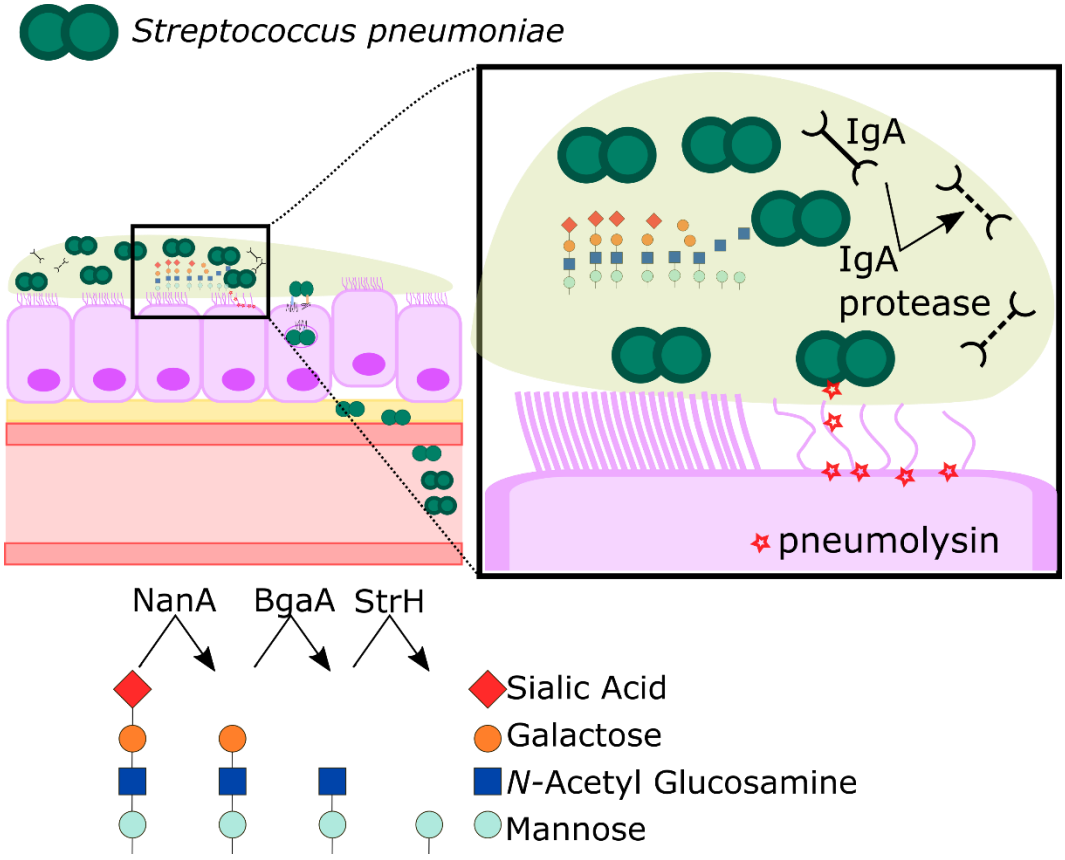

Figure 1 – Disruption of mucociliary clearance during *Streptococcus pneumoniae* colonization.

S. pneumoniae is protected by a negatively charged capsule, repelling mucus sialic acids. The expression of exo-glycosidases NanA, BgaA, and StrH allow for the breakdown of sugar residues within the mucus layer, providing nutrients to the bacteria. *S. pneumoniae* produces IgA protease to inactivate secreted IgA and pneumolysin which damages epithelial cells and ablates ciliary movement.

By dismantling mucociliary clearance, *S. pneumoniae* gains access to the respiratory epithelial layer. The pneumococcal exo-glycosidases can degrade glycoproteins present in mucin and on the epithelial surface for nutrient acquisition and access to adherence factors (King, Hippe and Weiser, 2006). Cleavage of glycoproteins occurs sequentially: 1) neuraminidase A (NanA) cleaves terminal sialic acids to expose galactose, 2) β-galactosidase (BgaA) cleaves galactose to

reveal *N*-acetylglucosamine, 3) β-*N*-acetylglucosaminidase (StrH) cleaves *N*-acetylglucosamine to expose mannose (King, Hippe and Weiser, 2006). Recently, NanA was shown to cleave sialic acid from 58 proteins present on endothelial cells surfaces, highlighting the broad specificity of the enzyme to promote adherence (McCombs and Kohler, 2016). Though several studies suggest increased adherence to human respiratory epithelial cells *in vitro*, investigating the role of NanA in murine models has been complicated (King, Hippe and Weiser, 2006). Triple exo-glycosidase knockout (Δ*nanA*Δ*bgaA*Δ*strH*) *S. pneumoniae* is able to colonize the murine nasal cavity as efficiently as wildtype after 5 days, whereas another study found *ΔnanA S. pneumoniae* had impaired nasal colonization 2 days after colonization (King *et al*., 2006; Orihuela *et al*., 2004). Recent work identified that the type of terminal sialic acid affects virulence; humans express more terminal *N*-acetylneuraminic acid residues than mice and most other mammals, which express more terminal *N*-glycolylneuraminic acid residues (Hentrich *et al.*, 2016). Pneumococcal NanA is upregulated in the presence of *N*-acetylneuraminic acid, and mice enriched for *N*-acetylneuraminic acid experience increased pneumococcal dissemination.

After moving past the mucus layer, *S. pneumoniae* must shed its capsule to allow cell wall-associated adhesins to bind to epithelial and extracellular matrix proteins. The alteration of capsular expression is referred to as phase variation, with opaque variants expressing a high amount of capsule and transparent variants expressing low capsule (Weiser *et al*., 1994. Transparent variants have stronger

epithelial adherence *in vitro* and *in vivo* (Cundell *et al*., 1995; Weiser *et al*., 1994). Expression of capsule reduces recognition and subsequent phagocytosis by macrophages; however, it also impedes adhesion to epithelial cells by shielding adhesion molecules. Phase variation between high and low capsule expression appears to be stochastic, though it has been attributed to changes in oxygen tension (Weiser *et al.*, 2001). A recent mechanism demonstrated epithelial-associated antimicrobial peptides can stimulate the release of pneumococcal autolysin, which triggers the release of capsule (Kietzman *et al*., 2016). Once the capsule is shed, adhesins are able to target their respective host receptors.

S. pneumoniae has many redundant mechanisms to adhere to host epithelial cells, as depicted in Figure 2. NanA and BgaA act as adhesins independent of their enzymatic activity (Limoli *et al*., 2011; Uchiyama *et al*., 2009). Choline binding protein A (CbpA, also known as PspC) is able to bind human polymeric immunoglobulin receptor (pIgR), but not rabbit pIgR, to facilitate adhesion and translocation across epithelial cells, though this may be strain and host specific (Brock *et al*., 2002; Zhang *et al*., 2000). Mice deficient for pIgR have decreased or unchanged nasopharyngeal colonization, whereas aged mice have increased pIgR and increased disease (Hinojosa *et al*., 2009; Sun *et al.*, 2004; Zhang *et al*., 2000). Phosphorylcholine (ChoP) moieties on the pneumococcal cell wall share similar structures to platelet-activating factor, allowing *S. pneumoniae* to interact with platelet-activating factor receptor (PAFR) on respiratory epithelial cells (Weiser *et al.*, 1994; Cundell *et al.*, 1995). Other adhesin/host adherence factors are

exhaustively reviewed elsewhere (Gamez and Hammerschmidt, 2012). The number of mechanisms by which *S. pneumoniae* uses to adhere to epithelial cells speaks to the importance of colonization in its life cycle.

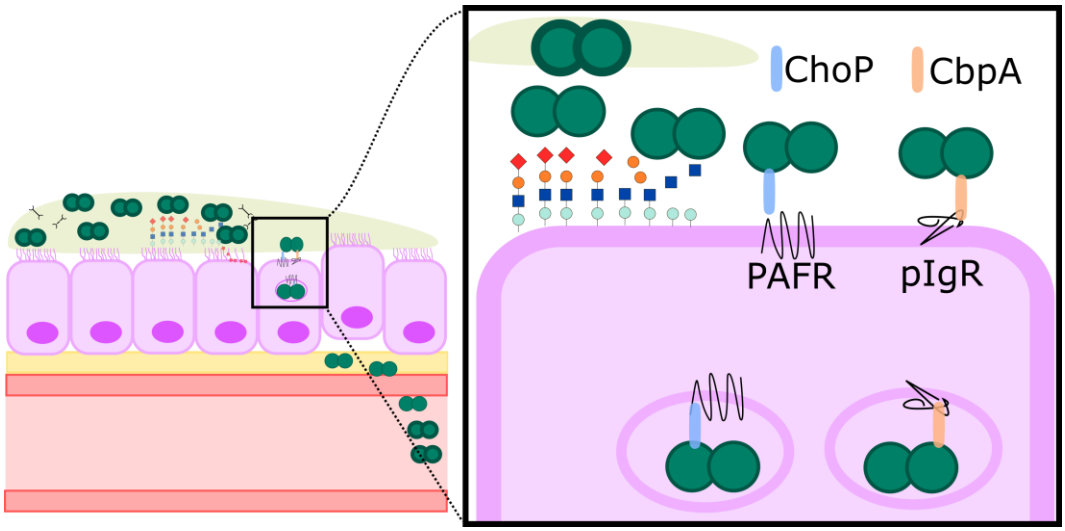

Figure 2 – *S. pneumoniae* adheres to epithelial cells via multiple mechanisms.
S. pneumoniae breaks down glycolipids and glycoproteins expressed on epithelial cells, exposing adherence residues such as mannose and *N*-acetyl glucosamine. *S. pneumoniae* sheds its capsule, resulting in exposure of ChoP and CbpA present on its cell wall, allowing adherence to PAFR and pIgR, respectively. The internalization of the receptors allows for pneumococcal invasion.

S. pneumoniae has evolved to respond to and take advantage of the host immune response during colonization. The host produces a wealth of cell- and protein-mediated responses that normally clear infections. Immunoglobulin A (IgA) is the most highly secreted immunoglobulin in the nasopharyngeal space, and can bind, neutralize and aggregate bacteria within the mucus layer to aid in mucociliary clearance and promote opsonization (Kirkeby *et al*., 2000). *S. pneumoniae*, similar

to other respiratory pathogens, produces an IgA1 protease that removes the Fc portion of IgA, with the hydrolyzed portion actually enhancing pneumococcal adherence to epithelial cells (Weiser *et al.*, 2003). The host produces a number of antimicrobial peptides, including lysozyme, lactoferrin, and cathelicidin that are capable of binding and promoting the killing of bacteria (Ganz, 2002; Bowdish, Davidson and Hancock, 2006). *S. pneumoniae* responds to the presence cathelicidin by shedding its capsule and increasing invasion of respiratory epithelial cells by 7-8 fold (Kietzman *et al.*, 2016). *S. pneumoniae* is able to modify its peptidoglycan structure to resist killing by lysozyme (Davis *et al.*, 2008). Lactoferrin, which normally sequesters iron away from bacteria, is inactivated by pneumococcal virulence factors (Mirza *et al.*, 2016). Lastly, while pneumolysin induces inflammation and recruitment of immune cells that can be beneficial to the host, *S. pneumoniae* utilizes this response to promote transmission to a new host (Zafar *et al.*, 2016). Furthermore, pneumococcal-induced inflammation upregulates host factors, including pIgR and PAFR, confirming that *S. pneumoniae* can modify its environment to enhance adherence (Hinojosa, Boyd and Orihuela, 2009; Rajendra *et al.*, 2017).

Inflammation protects the host against *S. pneumoniae* colonization, but is used by the pathogen for transmission to new hosts. Inflammation increases respiratory droplet production, which can be driven directly by pneumolysin, or indirectly through concomitant viral infections (Diavatopoulos *et al.*, 2010; Zafar *et al.*, 2016). Respiratory droplets are further increased in the cooler and drier months of winter

(Numminen *et al.*, 2015). This results in drastic spikes of pneumococcal disease in winter months, as children with high carriage rates and increased respiratory droplet production transmit *S. pneumoniae* to susceptible older adults around the holidays (Walter *et al.*, 2009; Numminen *et al.*, 2015). Transmission events are also related to crowding, which occurs in winter months but also at large gatherings, such as the Hajj (Memish *et al.*, 2015).

1.2.3 Clearance of *Streptococcus pneumoniae*

Capsule shedding, which promotes adherence to epithelial cells, also results in exposure of cell wall components, including peptidoglycan, to toll-like receptor 2 (TLR2) and Nod2 in resident macrophages and IL-17A-producing CD4+ T (T_H17) cells (Davis, Nakamura, & Weiser, 2011; Zhang, Clarke, & Weiser, 2009). T_H17 cells are important for the recruitment of monocytes, which differentiate into macrophages upon reaching the nasopharyngeal space and bind *S. pneumoniae* (Zhang *et al*., 2009). Pneumococcal binding and phagocytosis by macrophages are aided by the scavenger receptor macrophage receptor with collagenous structure (MARCO) recognition from which amplifies TLR2 and Nod2 signalling and production of monocyte chemoattractant protein-1 (MCP-1, also known as CCL2), initiating the recruitment of monocytes to the nasopharynx (Dorrington *et al.*, 2013). Resident macrophages and monocyte-derived macrophages are able to phagocytose and kill *S. pneumoniae* (Siegel, Tamashiro and Weiser, 2015; Puchta *et al.*, 2016). As previously mentioned, inflammation, specifically NF-κB downstream of TLR2 signalling, initiates clearance but also upregulates host

adherence factors allowing increased adherence and invasion of epithelial cells (Rajendra *et al.*, 2017).

Both pneumococcal vaccination and natural colonization can be immunizing events. Two vaccination strategies are used against *S. pneumoniae*: 1) a protein-conjugate vaccine targeting 13 of the most prevalent serotypes (PCV-13/Prevnar); and 2) a pneumococcal polysaccharide vaccine targeting CPS from 23 serotypes (PPV-23/Pneumovax). PCV-13 is conjugated to a carrier protein (diphtheria toxoid) resulting in strong T-cell responses, and has became a part of standard pediatric immunization in Canada in 2010 (Demczuk *et al.*, 2012). Due to a lack of protein carrier, immune activation by PPV-23 is T-cell independent, and therefore poorly immunogenic in children, being used primarily in at-risk elderly people (Demczuk *et al*., 2014). Vaccination results in the production of anti-capsular IgG capable of binding and agglutinating of *S. pneumoniae* cells, triggering the complement cascade and opsonization of the bacteria, resulting in opsonophagocytosis by macrophages and neutrophils (Dalia and Weiser, 2011). Agglutination of streptococci species was first described by Élie Metchnikoff in 1891 (Metchnikoff, 1891). Agglutination driven by pneumococcal-specific IgG, which is insensitive to the pneumococcal IgA protease, is sufficient to prevent initial pneumococcal colonization, though does little to eradicate established pneumococcal colonization (Roche *et al.*, 2015). As such, the combination of humoral and cellular immunity is essential to prevent and clear pneumococcal infections. The presence of anti-pneumococcal antibodies and antigen-specific T_H17 cells increase the rate of

clearance via recruitment and antibody-mediated recognition and destruction by neutrophils (Zhang *et al*., 2009).

1.2.4 Pneumococcal dissemination from the upper respiratory tract

Asymptomatic colonization progresses to infections in susceptible hosts, predominantly the very young and the very old. Multiple mechanisms contribute to susceptibility, including compromised immune systems, frailty, and potentially altered microbiota composition. Due to the production of pro-inflammatory cytokines, cellular invasion, and damaged epithelial layers permits the dissemination of *S. pneumoniae* from the URT. Mouse models have identified that infant mice are unable to produce an appropriate CCL2 gradient to recruit monocytes during pneumococcal colonization, resulting in prolonged colonization. Impaired innate immunity in the URT has been described in aged mouse models (Krone *et al.*, 2013; Puchta *et al*., 2016). Altered TLR and murine cathelicidin expression, as well as impaired monocyte recruitment in the response to pneumococcal colonization contributes to decreased pneumococcal clearance in aged mice (Krone *et al*., 2013). More recently, TNF-α was shown to be elevated in elderly mice, which promoted premature monocyte egress from the bone marrow and impaired bacterial clearance upon reaching the nasopharynx (Puchta *et al.*, 2016). These data correlate well with human data, demonstrating that elevated levels of circulating TNF-α and IL-6 are associated with increased risk for community-acquired pneumonia (Yende *et al.*, 2005). Elderly people are also less

responsive to pneumococcal vaccination and have reduced opsonophagocytic killing capacity (Romero-Steiner *et al.*, 1999).

Acute otitis media is one of the most common presentations of pneumococcal disease in children; causing over 90% of pneumococcal infections in the Canadian population in the pre-vaccination era (Morrow *et al.*, 2007) . *S. pneumoniae* can travel from the URT through the Eustachian tubes, where pneumolysin-mediated destruction of epithelial cells results in inflammation and pathology (Tuomanen, 2000). Acute otitis media also regularly presents with a concomitant viral infection (Pettigrew *et al.*, 2011).

Pneumonia is the second-most common presentation of pneumococcal disease, predominantly in people over 65 years of age. Impaired clearance and immunity allow *S. pneumoniae* to adhere to lung epithelial cells in a similar manner to URT epithelial cells; the resultant immune response bringing immune cells, increased host damage, and fluid to the lungs. This damage results in epithelial sloughing, which allows pneumococcal adherence to the basement membrane, extracellular matrix, and subsequently endothelial cells via multiple adherence factors (Pracht *et al.*, 2005; Jensch *et al.*, 2010). *S. pneumoniae* can bind to endothelial pIgR and PAFR to allow translocation into the bloodstream, with bacteraemia commonly co-occurring with pneumonia; a recent Canadian study identified that 30% of patients with community-acquired pneumococcal pneumonia also had pneumococcal bacteraemia (LeBlanc *et al.*, 2017).

Progression to bacteraemia is the initiation of invasive pneumococcal disease (IPD), which is defined as detection of *S. pneumoniae* in sterile sites outside of the respiratory tract (Demczuk *et al.*, 2014). The bloodstream allows dissemination to different organs, where expression of PAFR or pIgR on endothelial cells allow translocation out of the blood, including the heart and the brain (Brown, Sequeira and Clarke, 2017). *S. pneumoniae* begins to produce CPS within the bloodstream, where vaccine-derived IgG can bind and help clear the infection (Kietzman *et al.*, 2016). While bacteraemia results in increased mortality compared to pneumonia in the elderly, meningitis is the most devastating presentation of IPD, with a 27.6% mortality rate in Canadian adults over 18 years old (Morrow *et al.*, 2007). Furthermore, survivors of meningitis suffer from sequelae including deafness and neurological disabilities. Intriguingly, bacteremia is not a prerequisite for meningitis; *S. pneumoniae* can translocate directly through olfactory epithelium into olfactory nerves and progress to the brain (van Ginkel *et al.*, 2003). Addition of free sialic acid increased recovery of *S. pneumoniae* in the olfactory bulb (Hatcher, Hale and Briles, 2016). Understanding mechanisms that trigger pneumococcal translocation to the brain would greatly reduce the burden of meningitis.

1.3 Microbiota-pneumococcal interactions

Human studies have implicated a role for the microbiota during pneumococcal pathogenesis. Experimental human pneumococcal colonization identified that increased α-diversity in the URT microbiota increases the likelihood of colonization

(Cremers *et al.*, 2014). Shannon diversity of the URT microbiota is increased in elderly patients suffering from pneumonia compared to healthy elderly people (de Steenhuijsen Piters *et al.*, 2016). The increased α-diversity potentially indicates specific bacterial members could be influencing colonization, yet no studies have found bacterial synergy to increase pneumococcal colonization. Most studies have looked at correlations between *S. pneumoniae* and other resident pathogens, including *Staphylococcus aureus*, *Moraxella catarrhalis*, and *Haemophilus influenzae* (Margolis, Yates and Levin, 2010; Shak *et al.*, 2014). Successful colonization has also been linked to increased viral carriage (Glennie *et al.*, 2016). Mechanistic studies investigating microbial interactions within the URT could lead to new targets for prevention of colonization or subsequent infections.

1.3.1 Pneumococcal-viral interactions

Viral infections are a strong contributor to pneumococcal pneumonia and IPD. The “Spanish Flu” pandemic of 1918-1919 resulted in the death of 50-100 million people worldwide, including an estimated 50,000 Canadians (Johnson and Mueller, 2002). Mortality in the Spanish Flu and other influenza pandemics is driven by post-influenza bacterial pneumonia (Morens, Taubenberger and Fauci, 2008; Palacios *et al.*, 2009). Mechanistic studies have uncovered multiple pathways of viral-pneumococcal synergy preceding and during disease. Indeed, research from 70 years ago identified that viral infections increase pneumococcal survival in mouse lungs, likely due to the production of lesions by the virus (Harford, 1949). Viral colonization is also a strong predictor of successful pneumococcal

colonization in an experimental human model (Glennie *et al.*, 2016). Viral co-infections alter host susceptibility to *S. pneumoniae* by modifying the epithelial layer, immune response and bacterial virulence.

Influenza A virus, the main cause of flu pandemics, expresses two major enzymes: hemagglutinin and neuraminidase. Hemagglutinin binds terminal sialic acids on epithelial cell surfaces to promote cell adhesion and internalization, whereas neuraminidase cleaves terminal sialic acids to permit the release of new viral particles. As mentioned earlier, *S. pneumoniae* also produces its own neuraminidase NanA, which cleaves sialic acid to promote adherence to epithelial cells. Viral pre-treatment of epithelial cells increases pneumococcal adherence in a neuraminidase activity-dependent manner (Peltola, Murti and McCullers, 2005; Kash *et al.*, 2011). Viral co-infection leads to increased sialic acid production within the mucus layer, enhancing pneumococcal nasopharyngeal colonization, growth, and dissemination (Nelson *et al.*, 2007; Siegel, Roche and Weiser, 2014; Wren *et al.*, 2017). Independently, inhibition of neuraminidase activity improved host response in a co-infection model of pneumococcal pneumonia (McCullers and Bartmess, 2003). Viral infection also leads to disruption of the epithelial layer and exposure of the basement membrane, allowing pneumococcal adherence and increased bacteraemia (Kash *et al.*, 2011). Alterations and disruption of the epithelial layer by viral infections clearly enhance pneumococcal infections.

Although inflammation is key to remove infectious agents, the respiratory tract must restrain excessive responses in order to maintain proper organ function.

The immune response to a viral infection via multiple pattern recognition receptors infection results in the production of Type I interferons, interferon-α and interferon-β, which stimulate the production of interferon-stimulated genes that impair viral pathogenesis (Chen *et al.*, 2018). Influenza-induced interferon signalling results in a period of immune repression throughout the respiratory tract, impairing important cytokine responses to *S. pneumoniae* and worsening pathology (Shahangian *et al.*, 2009; Pettigrew *et al.*, 2014). Interferon-γ is produced 7 days after viral infection, leading to decreased expression of MARCO on alveolar macrophages and impaired pneumococcal clearance (Sun and Metzger, 2008). Alveolar macrophages enter a prolonged state of resolution, having dampened responses to inflammatory stimuli for up to 6 months after the viral infection (Didierlaurent *et al.*, 2008). Importantly, this impairs neutrophil recruitment during *S. pneumoniae* exposure, leading to increased pneumococcal pneumonia. Finally, co-infection results in increased pneumococcal transmission to new hosts, driven in part by the inflammatory response to influenza (Richard *et al.*, 2014). The immune response to viral infections increases individual susceptibility to and transmission of *S. pneumoniae*.

During asymptomatic pneumococcal colonization, *S. pneumoniae* can form biofilms within the mucus layer that are generally considered harmless to the host (Sanchez *et al.*, 2011). Disruption of epithelial cell-associated pneumococcal biofilms by viral exposure result in the release of planktonic *S. pneumoniae*, which are hypervirulent *in vivo* (Marks *et al.*, 2013). Biofilm disruption could be driven by

viral presence, epithelial cells, or extracellular ATP; however, the transcriptional profiles differ based on the disruption trigger (Marks *et al.*, 2013; Pettigrew *et al.*, 2014). In agreement, viral disruption of pneumococcal biofilms results in more virulent phenotypes compared to ATP-induced or planktonic bacteria grown in normal cell culture media.

Viral co-infections have been one of the largest contributors to bacterial pneumonia-related deaths worldwide. These co-colonizing events affect the local environment, immune response, and pneumococcal activity; however, viruses are only one of the many microbial members of the URT. Interactions between *S. pneumoniae* and other bacterial species have been identified for protection from disease. With the onset of inexpensive sequencing technologies and the development of the Human Microbiome Project, the past decade has been dominated by measuring the bacterial microbiota and its involvement in many diseases. Pneumococcal-bacterial interactions could control the switch from colonization to pathogenesis in certain individuals.

1.3.2 Pneumococcal-bacterial interactions

The majority of microbiota-pneumococcal interactions have implicated a role for the gut microbiota in systemic immunity, with disruption of the gut microbiota leading to an increase in susceptibility to pneumococcal pneumonia (Clarke *et al.*, 2010; Schuijt *et al.*, 2016; Wang *et al.*, 2018). The suggested mechanism includes the translocation of Nod and TLR ligands from the gut microbiota to stimulate bone marrow-derived immune cells or alveolar macrophages to improve responses to *S.*

pneumoniae and *Klebsiella pneumoniae*, and that antibiotic-mediated disruption of the gut microbiota impairs this protective signal. Mouse models of pneumococcal colonization have only recently started to investigate the role of the URT microbiota. The immune response to pneumococcal colonization in infant mice is impaired by the URT microbiota through reduced recruitment of monocytes to the nasopharyngeal space (Siegel *et al*., 2015). In this model, the neonatal URT microbiota contributed to high baseline chemokine expression, as antibiotic treatment decreased baseline chemokine expression. The URT microbiota of elderly mice experiences prolonged disruption in response to *S. pneumoniae* colonization (Krone *et al*., 2014; Thevaranjan *et al*., 2016). The contribution of individual microbial species to pneumococcal colonization is unknown, although co-colonization of *S. pneumoniae* with *S. aureus* and *H. influenzae* has identified several cooperative and inhibitory interactions (Margolis, Yates and Levin, 2010). Neonatal rodent models identify that *H. influenzae* and *S. pneumoniae* can co-colonize the host, though neutrophilic infiltration leads to selective clearance of luminal *S. pneumoniae* (Lysenko *et al.*, 2005; Margolis, Yates and Levin, 2010). This is due to *H. influenzae*-driven activation of neutrophils, leading to the targeted killing and clearance of *S. pneumoniae* (Lysenko *et al.*, 2005). Recent *in vitro* studies suggest that *Corynebacterium* species are able to liberate triacylglycerols from host epithelial cells that are toxic to *S. pneumoniae*, though this has not been tested *in vivo* (Bomar *et al.*, 2016). While there are several implications of potential

interactions between *S. pneumoniae* and other members of the URT microbiota, no studies have investigated these models extensively *in vivo*.

1.4 Central paradigm and hypothesis

The last decade has seen an explosion of microbiota research, primarily focussed on the role of the gut microbiota in various diseases. Despite clear evidence that viral interactions can increase *S. pneumoniae* pathogenesis, the influence of resident bacteria within the URT have not been definitively investigated. Due to antagonistic relationships between *S. pneumoniae* and other bacterial species *in vitro*, I hypothesized the URT microbiota of SPF mice would confer colonization resistance, reducing pneumococcal colonization and subsequent infection. Specifically, I hypothesize the URT harbors bacteria capable of inhibiting *S. pneumoniae* growth, and will prevent *S. pneumoniae* adherence. A combination of *in vivo* and *in vitro* analysis, including cultivation of bacteria isolated from the URT, is essential for mechanistic investigation of these interactions. To address this hypothesis, I proposed three aims:

Aim 1 – Optimize methodology for characterization of the murine URT microbiota.

Aim 2 – Determine the contribution of the URT microbiota to pneumococcal pathogenesis *in vivo*

Aim 3 - Investigate pneumococcal-bacterial interactions *in vitro* that could contribute to disease

Chapter 2: Methods

2.1 Animals

Age- and sex-matched C57BL/6J mice were obtained from Jackson Laboratories (Bar Harbor, ME) or from C57BL/6J mice bred within the McMaster Central Animal Facility. Mice were housed and bred in specific-pathogen free (SPF) conditions and had access to food and water *ad libitum* for up to 22 months. Germ-free (GF) and Altered Schaedler's flora (ASF) C57BL/6N mice were originally obtained from Taconic Biosciences (Germantown, NY) and bred within the Farncombe Family Axenic-Gnotobiotic Facility at McMaster University. GF mice were inoculated with frozen cecal contents from ASF mice via oral gavage, and bred for at least 2 generations within the gnotobiotic unit (Galipeau *et al.*, 2015). GF and ASF mice were exported and used immediately for experiments to maintain gnotobiotic status. To allow for microbiota transfer, mice were cohoused as indicated for 3-6 weeks, as previously described (Thevaranjan *et al.*, 2017). Female mice were used for cohousing experiments to reduce aggressive behaviours. Mice were anesthetized using isoflurane and euthanized by exsanguination. All experiments were approved by McMaster University's Animal Research Ethics Board, as per the recommendations of the Canadian Council for Animal Care.

2.2 Nasal tissue collection

Nasal wash was completed as per (Puchta *et al*., 2014). Briefly, a PE-20 polyethylene tube attached to a 26-gauge needle was inserted through a small

incision in the trachea. Lavages, performed with either 300 µL of sterilized phosphate buffered saline (PBS) or Buffer RLT (Qiagen), were flushed through the trachea and collected through the nares in a 1.7 mL microtube. Complete nasal tissue (cNT) was collected from lavaged or naïve mice via bisection of the skull with sterilized surgical tools (Zeppa *et al.*, 2016). Excised tissues were homogenized in 300 µL PBS in 2 mL screw-top tubes using 2.8 mm ceramic beads for 1 min at 2000 rpm (MoBio).

2.3 Histological Analysis

After nasal washes, mouse heads were placed into formalin for 24 hours before being placed in Shandon TBD-2 Decalcifier (Thermo Scientific, Kalamazoo, MI) for four days. Decalcified heads were placed in formalin for two days, followed by twice daily washes with PBS for an additional four days. Samples were washed with and placed in 70% ethanol prior to standard histological processing and embedded in paraffin wax. Cross-sectional slices (5 µm) were mounted on slides and stained with hematoxylin and eosin following standard protocols. Slides were randomized and scored in a blinded fashion. The integrity of the epithelial lining was measured by quantifying the area of intact/disrupt epithelium using ImageJ (Schneider, Rasband and Eliceiri, 2012).

2.4 DNA Extraction, Amplification, and Analysis of 16S rRNA gene

DNA was extracted from nasal wash and cNT homogenates as previously (Thevaranjan *et al.*, 2016). Samples were mechanically homogenized (2x 3min at 3000rpm) with 0.2 g of 0.1 mm glass beads and 0.2 g of 2.8 mm glass beads

(MoBio) in 800 µL of 200 mM $NaPO_4$ (pH 8) and 100 µL of guanidine thiocyanate-EDTA-*N*-lauroyl sarcosine. After homogenization, the sample was incubated with 50 µL of lysozyme (100 mg/mL) and 10 µL of RNase A (10 mg/mL) for 1 hour at 37°C, followed by incubation with 25 µL sodium dodecyl sulphate (25%), 62.5 µL NaCl (5 M), and 25 µL proteinase K (20 mg/mL) for 1 hour at 65°C. Samples were centrifuged for 5 minutes at maximum speed and the supernatant was transferred to 900 µL of buffered phenol:chloroform:isoamyl alcohol (25:24:1). Samples were vortexed and centrifuged for 10 minutes at maximum speed prior to transferring the aqueous phase to DNA Clean and Concentrator-25 columns (Zymo) as per manufacturer's instructions, except samples were eluted with 50 µL ultrapure water. Negative controls included PBS exposed to surgical tools, cage bedding, drinking water, were extracted in a similar fashion.

PCR amplification of the 16S rRNA variable region 3 (V3) gene involved a two-step, nested polymerase chain reaction, which improves efficiency in the presence of high host DNA (Stearns *et al.*, 2011). The first step involved amplification of the 16S rRNA gene region spanning V1-V5 using universal primers 8F (AGAGTTTGATCCTGGCTCAG) and 926R (CCGTCAATTCCTTTRAGTTT) for 15 cycles (94°C for 30 sec, 56°C for 30 sec, 72°C for 60 sec). This product was used as template in the second reaction for 25 cycles (94°C for 30 sec, 50°C for 30 sec, 72°C for 30 sec) to amplify the V3 region of the 16S rRNA gene. Barcoded primer sequences were adapted similar to previous work (Bartram *et al*., 2011). All reactions, including extraction negatives and no-template control, were performed

in triplicate to reduce PCR bias and pooled prior to sequencing using the MiSeq sequencing platform (Illumina, Inc., San Diego, CA) at the Farncombe Genomics Facility at McMaster University. Sequences were trimmed using CutAdapt (Martin, 2011) prior to analysis with DADA2 (Callahan *et al.*, 2016) to organize sequences into amplicon sequence variants (ASVs). Taxonomy was assigned using the Silva database (Quast *et al.*, 2013). Relative abundance, α- and β-diversity, and rarefactions were completed using the Phyloseq package (McMurdie and Holmes, 2013) in R version 3.5.2 (R Core Team, 2018). A dendrogram based on unweighted pair group method with arithmetic mean (UPGMA) hierarchical clustering using Bray-Curtis distances using the phangorn package (Schliep, 2011) and plotted with iTOL (Letunic and Bork, 2016). Differences between bacterial communities were tested using a permutational multivariate analysis of variance (PERMANOVA) within the vegan package (Oksanen *et al.*, 2019). Differences in taxon abundance were assessed using linear discriminate analysis (LDA) effect size (LEfSe) (Segata *et al.*, 2011).

2.5 Bacterial culture and identification

All media reagents were purchased from Fisher Scientific (Burlington, ON). Nasal wash and tissue homogenates were incubated overnight on brain heart infusion (BHI) agar or on pre-reduced fastidious anaerobe agar (FAA) in an anaerobic chamber (5% CO_2, 5% H_2, 90% N_2; Shel Labs, Cornelius, OR). Colonies were counted prior to picking and re-streaking to confirm purity. A portion of the collected colonies were stored in 10% glycerol at -80°C, while the remainder were

prepared for genomic DNA extraction. For liquid culture, bacterial cells were streaked from frozen glycerol stocks onto BHI agar plates and grown for 16-48 hours in 5% CO_2 at 37°C. Colonies were picked into BHI liquid for overnight growth in 5% CO_2 at 37°C. For use in all subsequent assays, cells would be diluted to a pre-determined OD_{600} value to 10^8 colony forming units (CFU)/mL, pelleted at 15,000 x *g* for 1 minute and resuspended in PBS. Bacterial concentrations were confirmed via dilution and plating onto BHI agar, followed by incubation for 16-48 hours in 5% CO_2 at 37°C.

Pure cultures were identified via colony PCR of the 16S rRNA gene. Single colonies were picked into 5% Chelex (Bio-Rad Laboratories, Mississauga, ON) and boiled for 15 minutes to lyse cells. Colony PCR to amplify the 16S rRNA gene was performed using 8f (5'- AGAGTTTGATCCTGGCTCAG-3') and 927r (5'- CCGTCAATTCCTTTR AGTTT-3') primers. PCR conditions consisted of an initial denaturation step at 94°C for 2 minutes, followed by 32 cycles of 94°C for 1 minute, 56°C for 1 minute, and 72°C for 2 minutes, with a final elongation of 72°C for 10 minutes. PCR products were sequenced via Sanger sequencing (GENEWIZ, South Plainfield, NJ) using the 8f primer. Taxonomy was assigned to isolates using the Human Oral Microbiome Database (Escapa *et al.*, 2018).

2.6 *Streptococcus pneumoniae* culture

S. pneumoniae strain P1547 (serotype 6A), a mouse-virulent strain obtained from Dr. Jeff Weiser (NYU School of Medicine) as previously described (Puchta *et al*., 2014). Frozen glycerol stocks were streaked onto tryptic soy agar (TSA)

supplemented with 5% sheep's blood and neomycin (10 µg/mL) and incubated in 5% CO_2 at 37°C. Colonies were picked into tryptic soy broth and grown in 5% CO_2 at 37°C until cultures were in late-log phase (OD_{600} = 0.5). Cultures were spun down at 15000 x *g* for 1 minute and resuspended at a concentration of 10^9 CFU/mL in PBS.

2.7 *Streptococcus pneumoniae* mouse models

For nasal exposure, mice were colonized by depositing 10 µL containing 10^7 CFU of *S. pneumoniae* P1547 directly in the nares. For lung exposure, mice were anaesthetized with isoflurane prior to depositing 30 µL containing 10^3 CFU intranasally. Bacterial inoculums were confirmed via dilution and plating onto TSA, followed by incubation for 16 hours in 5% CO_2 at 37°C. Mice were monitored for signs of infection (weight changes and activity level) and were removed from study if showing signs of disease (weight loss, altered breathing rate, reduced activity). At designated time points, mice were anaesthetized using isoflurane and sacrificed via exsanguination. Nasal wash and tissue were collected, followed by brain, spleen, and lung collection. Nasal and lung tissue were homogenized in a bead beater prior to dilution. Brain and spleen tissue were homogenized manually with syringes on scored 12-well plates. Brain homogenates were collected with cut micropipette tips and briefly centrifuged at 1000 rpm for 30 seconds to allow for separation of debris prior to dilution. Dilutions of homogenates were spotted onto TSA containing 5% sheep's blood and neomycin. Remaining homogenates were stored at -80°C for genomic DNA extraction and storage.

2.8 Epithelial Cell Culture

Detroit-562 (ATCC #CCL-138) cells and A549 (ATCC #CCL-185) cells were maintained in complete Dulbecco's modified Eagle's medium (DMEM) supplemented with 10% heat-inactivated fetal bovine serum, 2 mM L-glutamine, 100 U/mL penicillin, and 100 mg/mL streptomycin at 37°C in 5% CO_2. Cells were grown to ~95% confluency, washed with pre-warmed PBS prior to treatment with trypsin to lift cells for seeding. Cells were counted and assessed for viability using a haemocytometer and trypan blue staining. Cells were replenished from frozen aliquots before the passage number reached 25.

2.9 Pneumococcal adherence assays

Adherence assays were completed as published previously with slight modifications (Romero-Steiner *et al.*, 2003). Detroit-562 or A549 cells were seeded at a density of 40,000 cells/well into 96-well plates and allowed to grow for 2 days to reach confluency. Cells were washed and replenished with DMEM with L-glutamine. Washed bacterial isolates from liquid cultures were added to wells (multiplicity of infection [MOI] 10 bacterial cells : 1 epithelial cell) prior to plate centrifugation at a low speed (8 x *g* for 1 minute) to ensure bacteria-epithelial interactions. Plates were incubated for 1 hour at 37°C followed by addition of *S. pneumoniae* P1547 (MOI 10:1), centrifugation at low speed and 2 hours of incubation at 37°C. Cells were washed five times with PBS to remove non-adherent *S. pneumoniae* prior to trypsinization and plating on TSA supplemented with 5% sheep's blood and neomycin (10 µg/mL). Outer wells of the 96-well plates were not

used for assays to reduce temperature variance and served as sterility controls. For the purposes of sialidase activity inhibition, 2,3-didehydro-2-deoxy-N-acetylneuraminic acid (DANA) was added to wells (final concentration 0.5 mM) immediately prior to addition of commensal bacteria.

2.10 Sialidase activity measurement

Sialidase activity was measured via modification of previously published protocols (Chen *et al.*, 2014). Activity was measured using 2'-(4-methylumbelliferyl)-α-D-N-acetylneuraminic acid sodium salt hydrate (MUN; Sigma Aldrich M8639, Oakville, ON). Bacterial colonies were picked and re-suspended in MUN (final concentration 7.5 µM) in 50 µL sodium phosphate (50 mM, pH 5.2) in black 96-well plates at 37°C for 30 minutes in the dark. Reactions were stopped via addition of 150 µL stop buffer (0.25 M glycine-NaOH, pH 10.4) prior to measurement of fluorescence (excitation 360 nm; emission 460 nm) on a SpectraMax M3 microplate reader (Molecular Devices, San Jose, CA, USA). Inhibition of sialidase activity was measured with increasing concentrations of DANA dissolved in H_2O, with the IC_{50} determined using GraphPad Prism 6. *S. pneumoniae* was used as a positive control for sialidase activity, and negative controls were bacteria and buffer without addition of MUN. Background fluorescence was subtracted from each bacteria's respective negative control.

2.11 *Actinomyces naeslundii* culture and mouse colonization

Actinomyces naeslundii was streaked from frozen glycerol stocks onto TSA and grown in 5% CO_2 at 37°C for 48 hours. Bacterial colonies were picked and

cultured in BHI liquid media overnight. Cells were diluted to an OD_{600} of 0.55 which equates to ~10^7 CFU/mL and were pelleted via centrifugation at 15000 x *g* for 2 minutes. Cells were resuspended in PBS at a concentration of 10^8 CFU/mL prior to mouse exposure. Mice were colonized by depositing 10 µL containing 10^6 CFU of *A. naeslundii* intranasally 24 hours prior to pneumococcal exposure. *A. naeslundii*-exposed mice had no change in weight or activity levels over the course of the experiment.

2.12 Blood flow cytometry and pneumococcal binding

S. pneumoniae P1547 was labelled with tetramethylrhodamine (TRITC) and heat-killed at 65°C for 10 minutes. TRITC-*S. pneumoniae* was incubated with 100 µL whole blood from SPF and ASF mice (MOI 50:1) for 1 hour at either 4°C (binding) or 37°C (binding and internalization). Binding and internalization were arrested by incubation at 4°C for 30 minutes, with concomitant labelling of cells with a monoclonal antibody cocktail (suspended in 50 µL of FACS wash). The monoclonal antibody cocktail consisted of CD45 (eFluor 450), Ly6-C (BV510), CD11b (PerCP-Cy5.5), and Ly6G (Alexa Fluor 700), all from eBioscience (San Diego, CA, USA). Samples were then incubated with 1x Fix/Lyse Buffer (eBioscience) for 10 minutes with frequent inversion and centrifuged at 4°C, washed and resuspended with FACS wash. Samples were run on a LSR2 cytometer (BD Biosciences, Franklin Lake, NJ, USA) and analyzed with FlowJo 10 software (Treestar, Ashland, OR, USA). Monocytes were gated as $CD45^+CD11b^+Ly6C^+Ly6G^-$ and neutrophils were gated as $CD45^+CD11b^+Ly6C^-$

Ly6G$^+$. The proportion of cells with bound and/or internalized bacteria were TRITC$^+$ and the number of bacteria per cell was quantified by geometric mean fluorescence intensity.

2.13 RNA Sequencing

Nasal tissue was collected and placed into RNAlater (ThermoFisher Scientific) at 4°C for 24 hours prior to storage at -80°C. Samples were thawed and RNA was extracted using the TRIzol method following standard protocols (ThermoFisher Scientific). RNA was treated with DNase following the DNA-free™ DNA removal kit (#AM1906, ThermoFisher Scientific). Library preparation and sequencing on a MiSeq platform (Illumina) were performed at the Farncombe Genomics Facility at McMaster University. Sequences were checked for quality with FastQC (Andrews, 2010), aligned to the mouse genome using STAR (Dobin *et al.*, 2013) and binned into counts with QoRTs (Hartley and Mullikin, 2015).

PBS-perfused lungs were collected and sent to Dr. Alexander Misharin's group at Northwestern University for single alveolar cell sorting. Cell sorting, RNA extraction, library preparation, and initial data analysis were performed by the group at Northwestern University, as previously described (Misharin *et al.*, 2013, 2017).

Aligned sequences and differential gene expression were analyzed with edgeR (Robinson, McCarthy and Smyth, 2010). Genes with less than 1 normalized read count across half of the samples were removed from analysis. Genes of

interest to pneumococcal infections in murine models were identified via literature search. Heatmaps were generated in R using gplots (Warnes *et al.*, 2019).

2.14 Statistical Analysis

GraphPad Prism 6 and R were used for statistical analysis. Non-parametric tests were used for comparison of histology scoring and bacterial plate counts. Differences of $p<0.05$ were considered statistically significant. Microbial community composition differences were determined using the Adonis function (PERMANOVA) with 10,000 permutations within the vegan package. Correlation analysis between bacterial genera was performed using the R packages Hmisc (Harrell Jr. and Dupont, 2019) and corrplot (Wei and Simko, 2017)c, using the Spearman's rank correlation coefficient. Differences of $p<0.05$ were considered statistically significant.

Chapter 3: Results

3.1 The murine upper respiratory tract microbiota

Little is known about the murine URT microbiota. Bacterial colonization has been assessed via collection of nasal washes (retrotracheal lavages collected through the nares), nasal swabs, and nasal tissue collection. I set out to compare nasal washes and nasal tissue collection for their ability to extract the nasal microbiota, and the impact on subsequent high throughput sequencing results. Nasal washes are currently the predominant methodology for assessing nasal colonization during experimental models.

3.1.1 Nasal washes do not completely disrupt nasal surfaces

Nasal washes are traditionally used to assess host and bacterial cell numbers; however, the area affected by a nasal wash is unknown. I performed nasal washes using a gentle (PBS) or harsh buffer (Buffer RLT) followed by histological assessment of the nasal tissue via hematoxylin and eosin staining. PBS does not affect the epithelial architecture of the nasal cavity (Figure 4A-C), whereas Buffer RLT disrupts the epithelial layer, nasal-associated lymphoid tissue, and surrounding tissues near the base of the cavity (Figure 4E,F) but not the upper turbinates (Figure 4D). Nasal washes with harsh buffers were unable to disrupt a large majority of the epithelial layer in the nasal cavity, implying that nasal washes do not accurately sample the complete surface area of the nasal tissue (Figure 4G).

3.1.2 Nasal tissue extraction recovers more bacteria compared to nasal washes

Seeing as nasal washes fail to sample the majority of the nasal cavity, I set out to compare the microbial profiles of nasal washes and tissues. Nasal washes and tissue were homogenized and incubated aerobically on BHI agar and anaerobically on FAA. Overall, the bacterial load is low in both cNT and nasal wash (~10^3 CFU/mouse). Nasal tissue has a significantly higher bacterial load and diversity of colony morphotypes compared to nasal washes (Figure 5A). Consistent with this observation, analysis of 16S rRNA gene sequencing revealed that nasal tissues and nasal washes were distinct from each other (Figure 5B; PERMANOVA $p<0.05$, $R^2 = 0.181$). *Streptococcus* and *Staphylococcus* species were dominant in nasal tissue and wash samples (Figure 5C). Nasal tissues contained significantly more Neisseriaceae, *Actinomyces*, and *Bifidobacterium* species, while nasal washes contained more Erysipelotrichaceae and Cyanobacteria (Figure 5D). When comparing the α-diversity between nasal wash and tissue, Shannon diversity index ($p=0.26$) and observed species ($p=0.42$) did not differ between washes and tissues. Cultivation of URT microbiota identified several bacterial families, including Streptococcaceae, Enterococcaceae, Enterobacteraceae, Staphylococcaceae, and Corynebacteriaceae (Figure 6). Identified isolates included *Actinomyces naeslundii, Klebsiella pneumoniae,* and several *Staphylococcus* species as well as some species that could not be resolved to the genera level (Table 1).

3.1.3 Nested PCR improves bacterial yield in sequencing

Degenerate PCR primers for broad amplification of bacterial 16S rRNA gene are impacted by low bacterial biomass in the presence of host DNA, and can interfere with the efficacy of PCR as well as the percentage of sequencing reads that are assigned to bacteria (Yu *et al*., 2015). Nested PCR is a two-step reaction that reduces non-specific binding; an initial reaction to improve the yield of the gene of interest followed by a more targeted second amplification. Nested PCR has been used to examine low biomass microbial communities including gut biopsies, respiratory and skin surfaces (Glendinning *et al*., 2016; Li *et al*., 2014; Stearns *et al*., 2011; Yu *et al*., 2015). I compared standard PCR to nested PCR to investigate the murine nasal tissue microbiota. Nested PCR resulted in better yield of the V3 region of 16S rRNA gene compared to standard PCR (35 cycles) Figure 7. Amplicon yield, as measured by gel band intensity, improved after nested PCR (Figure 7A). Nested PCR increased the number of bacterial reads (Figure 7B) and decreased the number of eukaryotic reads (Figure 7C), while total read counts were unchanged per sample Figure 7D). Indeed, the relative abundance of sequenced reads greatly improved after nested PCR per mouse (Figure 7E). Nested PCR was used for the rest of the study to assess the nasal microbiota.

3.1.4 Mouse nasal microbiota is distinct from the gut microbiota

It has been reported that bacterial DNA found in the URT originate from environmental contamination, rather than due to resident microbes (Dickson *et al*., 2018). In mice, contaminating DNA can come from exposure to fecal matter and

environmental exposure (bedding, drinking water). To determine the degree to which microbial profiles are influenced by fecal exposure, I compared the nasal tissue microbiota to the paired gut microbiota. The nasal microbiota was distinct from the gut microbiota (Figure 8A;PERMANOVA $p<0.001$, $R^2 = 0.383$). The gut microbiota had significantly increased α-diversity compared to the nasal microbiota (Figure 8B). Additionally, the dominant families in the gut (Muribaculaceae, Lactobacillaceae, Lachnospiraceae, Erysipelotrichaceae) are different from the dominant species in the nasal tissue (Streptococcaceae, Staphylococcaceae, Enterococcaceae) microbiota (Figure 8C).This indicates a selective niche within the URT for bacteria to colonize that is distinct from the gut.

3.1.5 Mouse nasal microbiota is distinct from extraction and sequencing controls

Sequencing and extraction controls are essential for analyzing low biomass microbiota analysis, as reagents and tissue handling have been shown to influence the community composition of low biomass communities (Salter *et al.*, 2014; de Goffau *et al.*, 2018). I assessed the contribution of reagent contamination via the inclusion of negative controls. In this study, a negative extraction (surgical tools dipped in PBS, then exposed to the same extraction process as tissues; cage bedding; drinking water) and a PCR negative (elution water used instead of DNA template) were included to determine the impact of contaminating DNA. The negatives are distinct from the nasal tissue microbiota, though the axes explain only a small amount of the variance in the dataset. (Figure 9A; PERMANOVA

$P<0.05$, $R^2 = 0.138$). A UPGMA tree is a hierarchical clustering method that demonstrates the distance between samples. A UPGMA-tree based on Bray-Curtis distances again demonstrates the separation between negatives and samples (Figure 9B). The dominant taxa in the nasal tissue, namely *Streptococcus* and *Staphylococcus*, are not present in the negative samples (Figure 9C). The inclusion of negatives in every extraction is still worthwhile to distinguish low abundance communities from reagent contamination.

3.1.6 Mouse source affects the composition of the nasal microbiota

Differences in the murine gut microbiota from various commercial breeders has been identified as a source of experimental variability (Alegre, 2019). In order to determine if vendor affected the URT microbiota, I compared nasal tissue microbiota from mice bred in the McMaster facility (in-house = 30) to those ordered from Jackson Laboratories (JAX, n=15). JAX mice have a distinct nasal microbiota composition compared to in-house mice (Figure 10A,B; PERMANOVA $P<0.0001$, $R^2=0.226$). While both mice are dominated by Streptococcaceae, JAX mice have several other dominant taxa (Figure 10C). Furthermore, JAX mice had increased α-diversity (Shannon Diversity Index, Simpson Diversity, and observed species) within the nasal tissue microbiota compared to in-house mice (Mann-Whitney $P<0.001$, Figure 10D). LEfSe analysis revealed 109 genera were significantly different between JAX and in-house mice (Table 3), including *Mycoplasma* (Figure 10E) and *Lactobacillus* (Figure 10F).

3.1.7 Young and old mice have a distinct nasal tissue microbiota, which can be transferred to germ-free mice

We have previously published the murine nasal microbiota is distinct between old and young SPF mice, as measured by nasal wash (Thevaranjan *et al.*, 2016). I sought to compare the nasal tissue microbiota of young (3-4 month old) and old (18-22 months old) SPF mice. Similar to the nasal wash, nasal tissue microbiota were distinct based on age (Figure 11A;PERMANOVA $p<0.00001$, $R^2 = 0.133$).

Cohousing of young and old mice with germ-free (GF) mice results in the transfer of the gut microbiota, as well as phenotypes associated with the microbiota (Thevaranjan *et al.*, 2017). It is unknown if the URT microbiota can be transferred by cohousing. To determine if the nasal microbiota is transferred to germ-free mice, I cohoused GF mice with young and old SPF mice (1:1 per cage) for 6 weeks before collecting nasal tissue. Nasal tissue microbiota of the germ-free mice closely resembled their cage-mate, and maintained the distinction between old and young microbiota (Figure 11B,C). This suggested that the microbiota can be transferred via cohousing.

3.1.8 Summary of results

Nasal washes were insufficient for surveying the majority of the nasal cavity. A large biomass of bacteria remained within the tissue, resulting in distinct bacteria being detected within the nasal tissue, including enriched *Neisseria* and *Actinomyces* species. Low bacterial biomass in the presence of high host DNA

impairs sequencing results, but this can be overcome by nested PCR. The nasal microbiota is distinct from the communities in the gut, indicating that select bacteria can colonize the nasal cavity. Age and source of mice, which have been demonstrated to affect the gut microbiota, also impacts the nasal microbiota. Cohousing of SPF mice with GF mice allows for the transfer of a URT microbiota profile similar to the SPF cage mate.

3.2 URT microbiota contributes to *Streptococcus pneumoniae* infections

In the previous section, I established methods for studying the composition of the murine URT microbiota. To investigate the functional role of the URT microbiota, I used an experimental colonization model using *Streptococcus pneumoniae*. We and others have previously shown how the respiratory microbiota changes in response to pneumococcal colonization, though this was measured via nasal wash (Krone *et al*., 2014; Thevaranjan *et al*., 2016). Furthermore, increased microbial diversity has been shown to increase pneumococcal colonization. I sought to measure both the impact of pneumococcal exposure on the URT microbiota, and the impact of the URT microbiota on pneumococcal colonization. I used Altered Schaedler's Flora (ASF) mice, colonized by a minimal, defined microbiome during pneumococcal infection models. ASF mice have similar bacterial loads in the gut as SPF mice, but reduced microbial enzyme complexity (Norin and Midtvedt, 2010; Natividad *et al.*, 2012). The respiratory microbiota of ASF mice has never been assessed.

3.2.1 *Streptococcus pneumoniae* dominates the nasal microbiota

Streptococcus pneumoniae colonization of the URT disrupts pre-existing microbial communities prior to causing respiratory and invasive infections. Investigation into microbial interactions between *S. pneumoniae* and other nasal microbiota members has been primarily studied by analyzing nasal washes which may overlook the interactions occurring within the nasal turbinates, adhering to the mucosa, and in the submucosa. Mice were intranasally colonized with *S.*

pneumoniae and nasal wash and tissue were collected 3 days post-colonization (n=9). The nasal tissue had significantly more *S. pneumoniae* CFU compared to the paired nasal wash (Figure 12A). The nasal tissue and wash microbiota of *S. pneumoniae*-colonized mice were distinct (Figure 12B). *Streptococcus* ASVs become the most dominant taxa within the nasal microbiota (Figure 12B,C). Individual mice had varied microbiota profiles, but nasal tissues were routinely dominated by *Streptococcus* ASVs (Figure 13). LEfSe analysis revealed 24 significantly different genera between the two sampling methods, indicating bacterial interactions may be location dependent (Figure 14).

3.2.2 Strong correlation between culture-dependent and culture-independent detection of *S. pneumoniae*

PCR-based detection of *S. pneumoniae* has been suggested to be superior to traditional culture based detection (Virolainen *et al.*, 1994; Wyllie *et al.*, 2014). All mice were culture-positive 3 days post-pneumococcal inoculation, though colonization success varied between the mice (Figure 12A, Figure 13). To determine the correlation between cultured and sequenced *S. pneumoniae*, I completed paired analysis of pneumococcal CFU and relative abundance of *Streptococcus* ASVs. The culture-based detection of *S. pneumoniae* was in strong agreement with the culture-independent *Streptococcus* detection. *S. pneumoniae* CFU strongly correlated with *Streptococcus* ASV relative abundance in the nasal tissue ($R = 0.9$, $p = 9.4 \times 10^{-5}$) and nasal wash ($R = 0.95$, $p = 8.8 \times 10^{-5}$) samples (Spearman correlations; Figure 15A,B). This correlation indicates the culture-

independent measurement of the microbiota is representative of the cultivable microbiota. *Streptococcus* ASV relative abundance (Figure 15C) correlated between nasal tissue and wash (R = 0.88, p = 0.0016), and nasal tissue *S. pneumoniae* CFU (Figure 15D) correlated with nasal wash CFU (R = 0.95, $p = 8.8 \times 10^{-5}$). The strong correlation between nasal wash and tissue does not suggest either can be used interchangeably, as different microbial species inhabit the two sampling sites, and previous studies have found discordance in *Haemophilus*-*Streptococcus* interactions when comparing the two methods (Lysenko *et al.*, 2005; Margolis, Yates and Levin, 2010). Further investigation of pneumococcal-bacterial interactions in the two sampling methods are required.

3.2.3 URT bacterial interactions are tissue site-specific

Staphylococcus species have been shown to have a negative correlation with *Streptococcus pneumoniae* during colonization, as sampled by nasal wash (Krone *et al*., 2014; Thevaranjan *et al*., 2016). *Staphylococcus and Streptococcus* species were negatively correlated in the nasal wash (R = -0.72, p = 0.03; Figure 16A); however, there was no significant correlation in the nasal tissue microbiota (R = -0.32, p = 0.41; Figure 16B). *Corynebacterium* species are overrepresented in nasal microbiota of children and adults negative for pneumococcal colonization, and have recently been identified to inhibit the growth of *S. pneumoniae in vitro* (Bomar *et al.*, 2016). No correlation was found between *Corynebacterium species* in the nasal wash microbiota (R = 0.36, p = 0.35; Figure 16C); however, a strong negative correlation (R = -0.95, $p = 8.8 \times 10^{-5}$) between *Corynebacterium* species

and *Streptococcus* species existed in the nasal tissue (Figure 16D), suggesting that interactions between these species could occur within regions not affected by nasal washes. These correlations imply that both sampling techniques may be necessary to uncover microbial interactions that are site specific. Furthermore, niche-specific interactions may be driving antagonism or cooperation between *S. pneumoniae* and other bacterial species in the URT.

3.2.4 ASF mice are less susceptible to *S. pneumoniae* infection

To determine if microbial interactions within the URT affect pneumococcal colonization, I compared ASF mice to SPF mice during colonization. Age- and sex-matched SPF and ASF mice (n=9) were intranasally inoculated with *S. pneumoniae* P1547 (10^7 CFU/10 µL) and monitored for 7 days. Unexpectedly, SPF mice exhibited a higher mortality rate compared to ASF mice during the course of infection (Figure 17A). Within this cohort, all male SPF mice reached endpoint during the course of *S. pneumoniae* exposure (Figure 17B). Addition of a separate cohort of male SPF and ASF mice demonstrated a significant difference in survival between the two groups (Figure 17C). Due to increased susceptibility seen over 7 days of colonization, nasal colonization rates were assessed during earlier timepoints. Similar to lower susceptibility, ASF mice had significantly lower pneumococcal colonization at day 1 (Figure 17D) and day 3 (Figure 17E) after inoculation. Surviving ASF and SPF mice had similar levels of pneumococcal colonization by day 7 (Figure 17F).

3.2.5 SPF mice have increased pneumococcal translocation

All mice that reach endpoint had detectable *S. pneumoniae* in the spleen, lungs, and brain, indicating *S. pneumoniae* had spread systemically. To determine the importance of the microbiota on pneumococcal translocation, ASF and SPF mice were cohoused for three weeks prior to pneumococcal lung instillation. ASF, SPF, and cohoused ASF mice (n=4-5 mice) were anaesthetized and intranasally instilled with a low dose of *S. pneumoniae* P1547 (10^3 CFU/30µL) to allow lung exposure, monitored for 3 days, and sacrificed prior to collection of nasal, lung, splenic, brain, and heart tissues. Nasal and lung tissues were *S. pneumoniae* culture-negative, but pneumococcal translocation was detected in the heart, brain, and spleen. One cohoused-ASF mouse was removed on day 2 due to decreased activity, and had high pneumococcal density in the spleen, heart, and brain (Figure 18A). SPF mice were more likely to have *S. pneumoniae* in the heart (4/5 SPF vs ASF 0/4; p=0.0476, two-tailed Fisher's exact test) compared to ASF mice (Figure 18C). SPF and ASF mice had similar translocation to the brain (Figure 18B; 5/5 SPF vs 4/4 ASF) though only one ASF mouse exhibited translocation to the spleen (Figure 18D; 4/5 SPF vs ASF 1/4; p=0.206, two-tailed Fisher's exact test). Interestingly, cohoused ASF mice had high incidence in the spleen (5/5; 4/4 surviving mice) and heart (4/5; 3/4 surviving mice). No difference was seen in overall pneumococcal burden in the brain (Figure 18B), heart (Figure 18C), or spleen (Figure 18D) of mice that experienced translocation. Increased susceptibility during colonization, in addition to increased incidence of translocation

of *S. pneumoniae* after cohousing, suggested the involvement of the microbiota in enhancing invasive pneumococcal disease. This finding was intriguing, as previous studies had suggested a decreased complexity of the gut microbiota (via antibiotic treatment) increases susceptibility to pneumococcal pneumonia ((Schuijt *et al.*, 2016; Brown, Sequeira and Clarke, 2017; Wang *et al.*, 2018). ASF mice have similar bacterial loads in the gut compared to SPF mice, but the composition of the URT microbiota is unknown.

3.2.6 ASF mice have a low diversity gut microbiota and no nasal microbiota

ASF mice have a defined minimal gut microbial community composed of only 8 facultative anaerobic species, but whether they colonize the respiratory tract is not known. I assessed the gut and nasal microbial communities of ASF mice via culture-independent and -dependent methods. As described earlier, SPF mice have distinct nasal and gut microbial communities (Figure 8A). Surprisingly, the cecal and nasal tissue microbiota completely overlapped (Figure 19A). Despite having a low diversity microbiota, different microbial compositions are found along the gastrointestinal tract; the small intestine microbiota is distinct from the cecal tissue microbiota, likely due to nutrient and oxygen availability, as well as pH differences (Figure 19C). As such, the lack of differentiation between the cecal and nasal microbiota was an unexpected result. ASF mice have greatly reduced Shannon diversity in both their gut and nasal tissue microbiota compared to SPF mice, but again, no distinction between to two tissue sites (Figure 19B). Furthermore, the relative abundances of several bacterial groups were nearly

identical between nasal and cecal tissues, which are greatly distinct from the composition of the small intestine (Figure 19D). To confirm our sequencing results, I used anaerobic cultivation to recover bacteria from the gut and nasal tissues. Cultivation of the gut microbiota resulted in expected community members and density of microbes (~10^9 CFU/mL), the nasal tissue was culture-negative (1 CFU detected in 1/5 mice; 0 CFU in 4/5; Figure 19E). This suggested that the microbial sequencing was the result of contaminating DNA from cage exposure to fecal matter. Bacterial DNA, as measured by qPCR of the 16S rRNA gene, was detectable in the ASF nasal tissue (Figure 19F). Therefore, I concluded that ASF mice have a low diversity, high density gut microbiota with no viable nasal microbiota. This indicates that members of the URT microbiota in SPF mice could be contributing to pneumococcal colonization and translocation.

3.2.7 *Actinomyces naeslundii* enhance pneumococcal adherence to human respiratory cells

Pneumococcal adherence and invasion of epithelial cells initiates bacterial translocation from the respiratory tract. As incubation of influenza virus with respiratory epithelial cells *in vitro* enhances pneumococcal adherence, I sought to determine if bacterial isolates from the URT could act in a similar fashion. Bacterial isolates were collected from SPF nasal tissue cultured on TSA, FAA, and BHI agar plates, with distinct bacterial morphotypes selected for phenotypic screening assays (Figure 20A). Detroit-562 cells, an adherent human pharyngeal carcinoma cell line, were incubated with bacterial isolates for 1 hour prior to exposure to *S.*

pneumoniae P1547 for 2 hours. Fourteen microbiota isolates were initially screened, and had varying ability to impact pneumococcal adherence (Figure 20B). Initial hits that initially increased the adherence of *S. pneumoniae* were re-screened with more replicates to determine reproducibility. Isolate C13 reproducibly increased pneumococcal adherence to Detroit-562 cells (Figure 20C). Full length 16S rRNA gene sequencing identified C13 as *Actinomyces naeslundii*. *Actinomyces naeslundii* is found normally in the oral cavity, but has been detected in the nasal cavity at low levels (Laufer *et al.*, 2011; Whelan *et al.*, 2014). Interestingly, *Actinomyces* species were enriched in nasal tissue compared to nasal wash, suggesting they reside within the nasal turbinates or closely adherent to the epithelial layer (Figure 5). Filtered supernatants of *Actinomyces naeslundii* cultures were unable to enhance pneumococcal adherence, suggesting the effect was not due to a secreted metabolite or enzyme (Figure 20D).

3.2.8 *Actinomyces naeslundii* expresses an active sialidase enzyme

Viral neuraminidase activity has been previously linked to enhanced *S. pneumoniae* adherence to epithelial cells (McCullers and Bartmess, 2003). Neuraminidase, also known as sialidase, has homologues in the eukaryotic and bacterial kingdoms (Lewis and Lewis, 2012). The murine nasal microbiota collection, *Escherichia coli*, a *Pseudomonas aeruginosa* clinical isolate, and *S. pneumoniae* were assessed for sialidase activity (Figure 21A). *S. pneumoniae* is known to have sialidase activity via the expression of multiple sialidases (NanA, NanB, and NanC) and was used as a positive control. Interestingly, only isolate

C13, *Actinomyces naeslundii,* possessed sialidase activity from the murine nasal microbiota isolate collection. Sialidase activity was present in *A. naeslundii* cultures, and activity was preserved after freeze-thaw cycles, but diminished in heat-killed preparations and filtered supernatants (Figure 21B). Sialidase activity was inhibited with the pan-sialidase inhibitor 2,3-didehydro-2-deoxy-N-acetylneuraminic acid (DANA). The IC_{50} of DANA towards *A. naeslundii* sialidase activity was determined to be 3.66 µM (Figure 21C).

3.2.9 Sialidase from *Actinomyces naeslundii* enhances pneumococcal adherence to human respiratory cells

Given that inhibition of sialidase activity blocks viral-enhanced pneumococcal adherence, I sought to determine the impact on *A. naeslundii*-enhanced adherence. A549, a human lung epithelial cell line, and Detroit-562 cells were exposed to *A. naeslundii* with or without DANA (500 µM) for 1 hour prior to pneumococcal exposure. *S. pneumoniae* exhibited a stronger adherence to A549 cells compared to Detroit-562 cells (Figure 21D). As before, *A. naeslundii* enhanced pneumococcal adherence to Detroit-562 cells, but this potentiation was inhibited with DANA (Figure 21E). Similarly, *A. naeslundii* enhanced pneumococcal adherence to A549 cells, which was significantly inhibited by DANA, though not to baseline levels (Figure 21F). This indicated that potentiation of pneumococcal adherence by *A. naeslundii* was, at least in part, sialidase activity dependent.

3.2.10 Sialidase activity is conserved among *Actinomyces*

The finding that *Actinomyces naeslundii* was the only bacteria in our murine microbiota screen to have activity was of interest. Sialidase activity is known to be expressed by gut bacteria for the purposes of nutrient liberation from mucins; however, there are few reports of bacteria from the respiratory tract expressing sialidase (Juge, Tailford and Owen, 2016). I screened 150 bacterial isolates from a lab collection of respiratory tract microbial isolates. Interestingly, all *Actinomyces* species that were tested, including *A. naeslundii, A. odontolyticus,* and *A. graevenitzii*, expressed abundant sialidase activity (Figure 22). *Staphylococcus* species (*S. aureus, S. warneri, S. epidermidis, S. capitis*), *Streptococcus* species (*S. gordonii, S. australis*, *S. salivarus*), and *Bacillus subtilis* had no sialidase activity. This suggests that sialidase activity is conserved within *Actinomyces* species, but is not abundant in other bacterial members from the respiratory tract.

3.2.11 *Actinomyces naeslundii* enhances translocation during murine *S. pneumoniae* nasal colonization

Due to *Actinomyces naeslundii* enhancing pneumococcal adherence *in vitro*, I investigated if *A. naeslundii* could enhance pneumococcal pathogenesis *in vivo*. Mice were intranasally inoculated with *A. naeslundii* (10^6 CFU/10 µL) or PBS 24 hours prior to pneumococcal inoculation (10^7 CFU/10 µL). Mice were sacrificed at 1 and 3 days post pneumococcal colonization to assess nasal colonization burden and translocation to other organs. *A. naeslundii*-colonized mice did not have a difference in nasal pneumococcal density compared to PBS pre-treated

mice (Figure 23A). However, translocation was seen to the brain (Figure 23B) and spleen (Figure 23C) in *A. naeslundii*-colonized mice 1 day after *S. pneumoniae* colonization. By day 3, *A. naeslundii*-colonized mice maintained increased pneumococcal load in the brain but had similar splenic pneumococcal spread to PBS-treated mice. This indicated that *A. naeslundii* accelerated pneumococcal translocation from the nasal cavity; however, introduction of *Actinomyces naeslundii* did not recapitulate all differences of pneumococcal pathogenesis between ASF and SPF mice. In particular, increased mortality and nasal colonization were not altered by *A. naeslundii* colonization.

3.2.12 Neutrophils from ASF mice have slightly increased pneumococcal binding

The microbiota contributes to the differentiation and abundance of cells involved in innate and adaptive immunity (Ivanov *et al*., 2009; Zhang *et al*., 2015). Neutrophils and monocytes are the initial cells recruited during *S. pneumoniae* nasal colonization and limiting systemic infection (Dorrington *et al.*, 2013). Furthermore, microbial products can influence neutrophil and monocyte function (Clarke *et al.*, 2010; Thevaranjan *et al.*, 2017). I examined the monocytes and neutrophils in the blood of ASF and SPF mice via flow cytometry. ASF and SPF mice had similar counts and proportions of neutrophils (Figure 24A,B) and monocytes (Figure 24C,D). Monocyte and neutrophil cell function were assessed by their ability to bind and internalize fluorescently labelled *S. pneumoniae* (Figure 25). We have previously shown that monocytes from old mice (18-22 months old)

have a reduced ability to bind *S. pneumoniae ex vivo* (Puchta *et al.*, 2016). Interestingly, more neutrophils from ASF mice were able to bind *S. pneumoniae* compared to SPF mice ($p = 0.043$; Figure 26A). Neutrophils from ASF mice bound similar amounts of *S. pneumoniae* as compared to SPF mice (Figure 26C). No difference was seen in pneumococcal internalization by neutrophils, or monocyte binding and internalization (Figure 26A-D). Increased pneumococcal binding by neutrophils may help limit pneumococcal dissemination in ASF mice, though these differences were small.

3.2.13 The microbiota alters expression of host genes within the respiratory system important for *S. pneumoniae* infections

Actinomyces naeslundii increased pneumococcal adherence to respiratory epithelial cells *in vitro*, but did not affect nasopharyngeal burden *in vivo*. Due to ASF and SPF having different pneumococcal burdens, I sought to determine if host factors were altered by microbial presence within the URT. To determine the impact of microbiota colonization on respiratory gene expression, I analyzed RNA sequencing of nasal and lung tissues from germ-free (GF) and SPF mice. Gene expression profiles of GF and SPF nasal tissue were distinct (Figure 27A). I investigated genes of interest for pneumococcal pathogenesis, specifically those previously identified in mouse pneumococcal colonization and infection studies (Table 1). SPF nasal tissue had higher gene expression of *Pigr,* and lower expression of *Lgals8* compared to GF nasal tissue (Figure 27B). *Pigr* expression

has been demonstrated to increase pneumococcal density within the murine URT (Zhang *et al.*, 2000).

I further explored the impact of microbial colonization on genes within the lower respiratory tract. SPF and GF lung tissue transcriptomic profiles were distinct (Figure 27C). SPF mice had 8 genes with higher expression in the lungs (*Snai1, Ptger3, Ccr2 , Tlr1, Il1b, Ptafr, Plau, Cd8a*) and 2 genes with lower expression (*Marco, Pten*) compared to GF mice (Figure 27D). Finally, alveolar macrophages were sorted from SPF and GF mice prior to RNA sequencing. Alveolar macrophages gene expression profiles differed between SPF and GF mice (Figure 27E;) and data not shown). Alveolar macrophages from SPF mice had 6 genes with higher expression (*Tlr4, Il1b, Lgals3, Plau, Ccr2, Tlr2*) and 2 genes with lower expression (*Lgals8, Irak2*) compared to alveolar macrophages from GF mice (Figure 27F). This implies that the presence of a microbiome can alter several host receptors important for response to pneumococcal infections.

3.2.14 Summary of results

In this chapter, I identified that pneumococcal exposure leads to dominance of *Streptococcus* within the URT microbiota. Pneumococcal interactions within the URT microbiota were site specific, as distinct patterns were found when assessing nasal wash and nasal tissue samples. SPF mice experienced significantly worse pneumococcal disease compared to ASF mice, including increased mortality, pneumococcal burden, and pneumococcal translocation. ASF mice do not have a cultivable URT microbiota, which implicated the URT microbiota as a potential

driver of pneumococcal infections in SPF mice. *Actinomyces naeslundii*, a URT isolate from SPF mice, was able to increase pneumococcal adherence to respiratory epithelial cells in a sialidase dependent manner. Nasal colonization of *A. naeslundii* accelerated pneumococcal dissemination from the URT. Neutrophils from ASF mice bound more *S. pneumoniae* compared to neutrophils from SPF mice. Finally, GF mice have many differentially expressed genes within the respiratory tract compared to SPF mice. Several genes identified in pneumococcal colonization and infection models are altered, implicating the lack of a microbiota can impact several aspects of pneumococcal infections.

Chapter 4: Discussion

4.1 Summary of contribution to the field

This thesis explored the URT microbiota in murine models, and discovered novel roles during pneumococcal infections. The URT microbiota is a low bacterial biomass community, with bacteria colonizing in unique niches throughout the URT. Nasal washes, which have been used to quantitate bacteria, do not completely sample the URT. The murine nasal microbiota can be shaped by intrinsic and extrinsic factors, including age and source of mice. I explored the impact of pneumococcal colonization on the URT microbiota, and found that, although *S. pneumoniae* dominates the nasal wash and tissue microbiota, its relationship with other bacteria depended on sampling method. To establish a causal role for the URT microbiota, I initially used mice colonized with a minimal microbiota to simplify the URT microbiota community. I discovered that using these Altered Schaedler's Flora mice provided a model of a complete (albeit simple) gut microbiota with a 'germ-free' nasal tissue in an immunologically developed host. I screened for bacteria that could enhance pneumococcal adherence *in* vitro, identifying that *Actinomyces naeslundii* was able to increase pneumococcal adherence to Detroit-562 cells and A549 cells. *A. naeslundii* enhanced pneumococcal adherence in a sialidase-dependent manner, similar to viral infections. This is the first study to uncover pneumococcal-bacterial cooperation to cause an infection. Lastly, the microbiota can alter response to infections by altering neutrophil function and expression of host genes throughout the respiratory tract. Together, these data

establish reproducible methods to study the contribution of the URT microbiota to health and disease in mouse models.

4.2 Modelling URT microbiota interactions

The URT microbiota has been increasingly studied over the past decade for its role in health, respiratory infections, allergy and asthma. Humans have 5 major nasal microbiota profiles, depending on what genera the subject is dominated by, namely *Streptococcus, Staphylococcus, Moraxella, Corynebacterium* or *Corynebacterium/Dolosigranulum* (Biesbroek *et al*., 2014). Children with *Corynebacterium* and *Dolosigranulum*-dominated profiles are reported to have decreased respiratory infections, as well as decreased pneumococcal colonization (Biesbroek *et al*., 2014; Bomar *et al*., 2016); however, very few mechanistic studies have investigated the direct impact of the nasal microbiota. Associations between respiratory events and these microbial profiles are complicated by the fact that individuals can vary between profiles over time, likely due to seasonal changes and exposures to other microbial species.

Human studies involve swabbing, washing, or scraping different sites of the nasal and oral cavity. Sampling methodology can be problematic, as comparisons of nasal washes and swabs, or even swabbing different locations, yield different detection of pathogens (Goggin *et al*., 2018; Gritzfeld *et al*., 2011; Li *et al*., 2013). The combination of changing microbial profiles with variable detection of pathogens make mechanistic studies challenging within the human population.

Animal models provide an avenue to controllable environments and exposures, though few examples of modelling the URT microbiota exist.

At the onset of this thesis, only two groups had assessed the murine nasal microbiota using different techniques, revealing very different profiles (Krone *et al*., 2014; Weyrich *et al*., 2014). It was unknown whether these differences were due to sampling methodology or different animal vivaria. As such, the primary aim was to compare the two sampling methodologies for their ability to extract the URT microbiota. Nasal wash and tissue extraction revealed distinct microbial communities, including increased bacterial yield in the nasal tissue. This difference was largely attributable to the nasal wash not completely sampling the nasal cavity, specifically the nasal turbinates and the olfactory epithelial layer. Additionally, PBS washes do not disrupt the epithelial layer, meaning that tightly adherent/submucosal bacteria are not detected in nasal washes. The incomplete sampling of the URT was not surprising, as some colonizing pathogens, including *Streptococcus pyogenes*, cannot be detected in nasal washes but are in high abundance of nasal tissue of the same mice (Kasper *et al.*, 2014).

Little is known about the impact of microbial communities or pathogen colonization within the olfactory turbinates. Pathogens, such as *Streptococcus pneumoniae*, have been suggested to disseminate from the URT via olfactory neurons, indicating that localization of bacteria may impact pathogenesis (van Ginkel *et al.*, 2003). *Actinomyces* species were enriched in nasal tissue microbiota, which led to identifying their involvement in pneumococcal pathogenesis discussed

later in the thesis. Localization of specific bacterial groups would identify potential microbe-microbe or microbe-host interactions, though this is challenging due to the low bacterial load (~10^3 CFU/mouse) and the large surface area of the nose. While I assessed the complete nasal tissue, microdissection of specific regions would enhance the assessment of microbial composition.

These results suggest that nasal tissue collection is superior to nasal wash for complete assessment of the microbiota; nonetheless, nasal washes carry some advantages over nasal tissue for microbiota assessment. Nasal washes may detect bacteria that are more likely to be transmitted to other mice, due to ease of removal by washing and proximity to the nares. Nasal wash samples also result in decreased presence of host DNA being released. High levels of host DNA, especially in combination with low bacterial biomass, complicate culture-independent analysis of the microbiota by decreasing PCR efficiency of the 16S rRNA gene, which uses primer degeneracy to detect a broad range of bacterial groups. The presence of host DNA was overcome in this study via nested PCR, using selective primers which enhanced bacterial DNA amplification and sequencing results. Previous studies have reduced host DNA in nasal wash samples by centrifugation at low speeds (~300 x *g*) for a short period of time to pellet host cells (Krone *et al*., 2014); however, this method is not applicable to total tissue extraction. As such, choice of sampling methodology depends on the research question being asked.

Cohousing SPF mice with GF mice allowed for the transfer of the nasal microbiota. Consistent with previously published studies from our group and others using nasal wash, I found that old and young mice had distinct nasal microbial compositions when extracting nasal tissue (Krone *et al*., 2014; Thevaranjan *et al*., 2016). These distinct microbial communities could be transferred to GF mice via cohousing, with recipient mice (GF) having a similar community to the donor mice (old or young SPF). Cohousing mice has been used for gut microbiota normalization, as mice are coprophagic, allowing for a natural transfer of the gut microbiota. It was recently shown that cohousing allows a transfer of the lung microbiota as well, though no previous reports have looked at the URT microbiota (Dickson *et al*., 2018). Additionally, although not presented in this thesis, I was part of the team to first demonstrate that the oral microbiota can be transferred by cohousing (Krishnan *et al.*, 2018). In our study, mice were cohoused for 6 weeks, so understanding the minimum amount of time needed for URT microbiota transfer would be of interest. The use of cohousing has been debated recently, as it was shown to dramatically shift fecal microbiota profiles while having little effect on small intestine and colonic tissue microbiota profiles (Robertson *et al.*, 2019). Specifically, that study used mice from two vendors with distinct microbiota profiles, which implies that cohousing is inefficient at displacing a resident microbiota. Designing a similar study investigating the impact of cohousing SPF and GF mice, and multiple tissue sites, would be of interest, though our research suggests it effectively transfers the majority of the URT microbiota when the recipient is sterile.

Though differences were found between sampling methods, mice from different sources had drastically different URT microbial compositions. When comparing mice shipped directly from Jackson Laboratories to mice bred in-house at McMaster, 109 genera were significantly different between the two groups. Differences in vendor-associated gut microbiota affect murine health, immune cells populations, and susceptibility to bacterial infections (Ivanov *et al*., 2008; Velazquez *et al*., 2019). While I did not explore the differences in disease susceptibility between Jackson Laboratories and in-house mice, the presence of specific bacterial groups may protect or make them more permissive to colonization by respiratory pathogens. Intriguingly, while SPF mice from different sources have vastly different microbiota, this likely pales in comparison to wild-caught mice. It was recently identified that the gut microbiota from wild-caught mice was more distinct than vendor-based differences (Rosshart *et al.*, 2017). GF mice colonized with the gut microbiota from wild-caught mice had improved resistance to influenza infections compared to GF mice recolonize with the SPF gut microbiota. Furthermore, wild-caught mice have a distinct lung microbiota, which influences alveolar morphology and mucus production (Yun *et al.*, 2014). This highlights that distinct microbial composition can affect lung and gut health, and likely upper respiratory health as well. As such, careful attention should be paid to source of mice when making assumptions about the role of the URT microbiota.

4.3 Pneumococcal-URT microbiota dynamics

S. pneumoniae colonizes the nasopharyngeal space by disrupting the mucus layer, followed by adherence and invasion of the respiratory epithelial layer. I assessed pneumococcal burden in colonized mice by nasal wash and nasal tissue, and found that a significant portion of *S. pneumoniae* remained in the nasal tissue after washing. Murine models have established that pneumococcal burdens can differ between nasal wash and tissue collection, though these differences are strain specific (Briles *et al*., 2005). They discovered that *S. pneumoniae* isolated from nasal tissue is often opaque-phase, suggesting upregulation of capsule after tissue invasion. Due to the pneumococcal burden differences, I assessed the microbiota composition during colonization via nasal wash and nasal tissue extraction. *S. pneumoniae* disrupted the nasal microbiome and became the dominant bacteria in both nasal wash and tissue, though the composition between the two sampling methods were distinct. This suggested that different bacterial interactions could occur at different sites within the URT.

Pneumococcal vaccination studies have identified decreased pneumococcal carriage leads to an increase in staphylococcal colonization (Bosch, van Houten, *et al.*, 2016). We and others have previously shown that as *S. pneumoniae* colonizes the nasopharynx, proportions of *S. aureus* decrease in nasal washes (Krone *et al*., 2014; Thevaranjan *et al*., 2016). In my study, *Staphylococcus* had a significant negative correlation with *Streptococcus* only in nasal wash samples, but not in nasal tissue samples. *S. pneumoniae* can produce

hydrogen peroxide that results in the lysis of *S. aureus* by activation of endogenous bacteriophages (Selva *et al.*, 2009).

Corynebacterium have recently been identified to be underrepresented in children colonized with *S. pneumoniae* (Bomar *et al.*, 2016). *Corynebacterium* species had a negative correlation with *Streptococcus* species in the nasal tissue microbiota, and *Corynebacterium* were barely detectable in nasal wash samples. *Corynebacterium* species release toxic triacylglycerols from epithelial sources that result in the killing of *S. pneumoniae in vitro* (Bomar *et al.*, 2016). This suggests that *Corynebacterium* would only be capable to inhibiting *S. pneumoniae* in close contact with the epithelial layer. Extracting the microbiota by only one method would have missed one of these interactions, implying that potentially both methodologies should be used to assess bacterial interactions. This is in agreement with co-colonization experiments between *Haemophilus influenzae* and *Streptococcus pneumoniae*, where antagonism was only seen in nasal wash samples, but not nasal tissue samples (Lysenko *et al.*, 2005; Margolis, Yates and Levin, 2010).

In order to determine the effect of microbiota interactions during *S. pneumoniae* exposure, I investigated the composition of the URT microbiota of ASF mice. Culture-independent analysis was completed first, which suggested that the composition looked virtually identical to the cecal microbiota; however, no cultivable bacteria were found in the URT of ASF mice, suggesting that the sequencing data was contamination from fecal matter exposure. This finding gave

us the opportunity to assess the impact of the an essentially “germ-free” URT microbiota with the presence of a gut microbiota. I initially hypothesized that ASF mice would be more permissive to colonization, predominantly due to their lack of URT microbiota. To my surprise, ASF mice were protected from pneumococcal-induced mortality seen in SPF mice. This difference was linked to lower colonization and lower dissemination in ASF mice. Cohousing ASF mice with SPF mice increased pneumococcal dissemination from the respiratory tract compared to naïve ASF mice. I hypothesized that resident bacteria within the respiratory tract are enhancing pneumococcal colonization and invasion.

The URT microbiota has been linked to increased susceptibility during pneumococcal colonization. Human experimental pneumococcal colonization models identified that individuals with an increased α-diversity in their URT microbiota were more likely to be colonized (Cremers *et al.*, 2014). The human experimental pneumococcal colonization study failed to find specific bacteria associated with colonization, mostly due to inter-subject variability. Clearly, ASF mice have a low α-diversity by not having any microbial species within the URT. A microbial species identified with enhancing pneumococcal infections is influenza A virus, which increases pneumococcal adherence to epithelial cells *in vitro* and pneumococcal pathogenesis *in vivo*. As such, I investigated whether members of the URT microbiota from SPF mice could enhance pneumococcal adherence to epithelial cells *in vitro*. I selected Detroit-562 cells for adherence studies as they represent human pharyngeal cells. While several bacteria impacted pneumococcal

adherence, *Actinomyces naeslundii* was among the most reproducible hits to increase pneumococcal binding to epithelial cells. *Actinomyces naeslundii* is commonly found in the human oral cavity and occasionally in the nasal cavity. *A. naeslundii* has been shown to co-aggregate with *Streptococcus* species within saliva, but does not co-aggregate with *S. pneumoniae* (Kitada and Oho, 2012). Intriguingly, heat-killed, but not freeze-thawed *A. naeslundii*, lost the ability to enhance pneumococcal adherence. This suggested that viable bacteria were not necessary for the augmentation of pneumococcal adherence.

Neuraminidase activity from influenza viruses can increase pneumococcal adherence by cleaving terminal sialic acid residues from host glycoproteins (McCullers and Bartmess, 2003; Peltola, Murti and McCullers, 2005) . Current nomenclature refers to neuraminidases as sialidases, though the term neuraminidase remains commonly used for viruses. Sialidase activity is detected in many eukaryotic and prokaryotic species; *S. pneumoniae* expresses 3 sialidases: NanA, NanB, NanC (Xu *et al.*, 2011). I screened the bacterial collection used in pneumococcal adherence assays for sialidase activity using a 96-well plate based assay. *Actinomyces naeslundii* was the only bacteria in the collection to have sialidase activity, which was actually stronger in activity compared to *S. pneumoniae*. *A. naeslundii* has previously been reported to have sialidase activity (Moncla and Braham, 1989). I examined the impact of sialidase activity from *A. naeslundii* on pneumococcal adherence via the use of a pan-sialidase inhibitor DANA. The addition of DANA blocked *A. naeslundii*-potentiated adherence, but,

importantly, did not impact baseline pneumococcal adherence. I was able to recapitulate this finding with a different human respiratory epithelial cell line, A549 cells. Intriguingly, the potentiation of pneumococcal adherence by *A. naeslundii* was greater on A549 cells (~10-fold increase) that was partially, but not completely, reduced by sialidase inhibition. This suggests that *A. naeslundii* may have multiple mechanisms of enhancing pneumococcal adherence depending on the tissue site.

A. naeslundii colonization accelerated pneumococcal pathogenesis *in vivo*. Mice colonized with *S. pneumoniae* had similar nasal burdens of *S. pneumoniae*, but experienced heightened dissemination to the brain and spleen at earlier timepoints compared to *S. pneumoniae*. In combination with our *in vitro* data, *A. naeslundii* likely promotes increased pneumococcal invasion across the epithelial layer. The *in vivo* targets of *A. naeslundii* sialidases are unknown, so this could be due to modifications of sialic acid residues on the mucus layer or epithelial cells. Beyond exposing adherence receptors, sialidase activity would also liberate sialic acid into the nasal cavity. A recent study demonstrated that addition of sialic acid increased pneumococcal invasion of the brain from the nasopharynx, though the exact mechanism is unclear (Hatcher, Hale and Briles, 2016). Based on recent findings, *S. pneumoniae* has increased expression of virulence factors in the presence of free sialic acid, so *A. naeslundii* could be altering *S. pneumoniae* as well as the host by producing sialidase. Further exploration of this hypothesis could include *in vitro* testing with an epithelial layer and *S. pneumoniae* with or without *A. naeslundii*, with measurement of *S. pneumoniae* virulence or total gene

expression. This work would benefit from microscopy of *in vivo* interactions between *A. naeslundii – S. pneumoniae* interactions, as well as staining to monitor exposure of sugar residues the URT. Clearly, sialic acid metabolism could affect multiple facets of *S. pneumoniae* pathogenesis.

This is the first report of microbial synergy between *S. pneumoniae* and a bacterial member of the URT microbiota. The potential use of sialidase by *A. naeslundii* is similar to enhanced pneumococcal adherence in the presence of influenza neuraminidases (McCullers and Bartmess, 2003). Sialidases are expressed by several bacteria genera, as it liberates a carbon source from mucins and mucosal surfaces, while also promoting adherence and immune evasion (Lewis and Lewis, 2012). It was recently demonstrated that sialidases from URT microbiota members had the capacity to restore growth of viruses in the presence of a neuraminidase inhibitor (Nishikawa *et al.*, 2012). I hypothesize that the augmentation of pneumococcal adherence and invasion is not limited to *A. naeslundii* sialidase activity. Nonetheless, *Staphylococcus, Haemophilus, Moraxella, Dolosigranulum,* and some *Streptococcus* species do not express sialidase, whereas *Actinomyces, Corynebacterium*, *Klebsiella*, *Pasteurella* and *Mycoplasma* species have abundant presence of sialidase in their genome, according to the Carbohydrate Active Enzymes database (Lombard *et al*., 2014). I confirmed the widespread sialidase activity within *Actinomyces* with our larger screen of human respiratory tract bacterial isolates. Screening human nasal microbiota members for functional sialidase activity, or completing

metagenomic/metatranscriptomic sequencing of URT microbiota to determine the abundance, prevalence, and distribution of sialidase enzymes would be of great interest. Additionally, the development of sialidase screens in this study were an inexpensive, high throughput methodology that could be used to screen many cultured isolates. It would be of interest to determine sialidase activity in direct clinical samples, including swabs or nasal washes, from subjects to determine if this would be a viable assay to detect if they were at risk for pneumococcal infections. The role of sialidase inhibition should be explored as a therapeutic option in patients suffering from pneumococcal pneumonia to prevent dissemination from the respiratory tract.

4.4 Microbiota impacts on host response

Addition of *A. naeslundii* did not completely recapitulate the differences in pneumococcal susceptibility between ASF and SPF mice. Neutrophils are important in the response to *S. pneumoniae*, and microbial products have been shown to enhance binding of *S. pneumoniae* by neutrophils (Clarke *et al.*, 2010). While ASF and SPF mice have similar levels of neutrophils, pneumococcal binding by neutrophils from ASF mice was slightly but significantly enhanced. Defects in neutrophils have been previously seen in antibiotic treated mice, but functional studies with ASF neutrophils have not been completed (Clarke *et al.*, 2010; Schuijt *et al.*, 2016). Alveolar macrophages and neutrophils from antibiotic-treated mice have a reduced ability to phagocytose *S. pneumoniae* (Schuijt *et al.*, 2016). As neutrophils from ASF mice had no deficit in their ability to phagocytose *S.*

pneumoniae, reduction in phagocytosis in antibiotic-treated mice appears to be driven by the gut microbiota density, as opposed to complexity. Future studies should fully characterize tissue-resident immune cells, including alveolar macrophages, from ASF mice in comparison to SPF mice to determine the impact of low and high complexity microbiota, as opposed to altered microbial load, on cellular function.

I hypothesized that the presence of a microbiota would alter gene expression within the respiratory mucosa, thus contributing to the host susceptibility to pneumococcal infection. To explore the impact of microbiota colonization on respiratory gene expression, I looked at transcriptomic data from naïve SPF and GF nasal tissues. Transcriptomic analysis revealed that SPF and GF gene expression patterns were distinct. The polymeric immunoglobulin receptor gene, *Pigr*, was significantly increased in SPF mice compared to GF mice. *Pigr* knockout mice have decreased pneumococcal colonization, and pIgR is a target for pneumococcal adherence and invasion of epithelial cells (Zhang *et al.*, 2000). Indeed, antibody-mediated blocking of pIgR leads to reduced pneumococcal binding and invasion of Detroit-562 cells (Zhang *et al.*, 2000; Iovino, Molema and Bijlsma, 2014). Furthermore, aged mice, which have increased susceptibility to pneumococcal infections, have increased *Pigr* expression in the lungs (Hinojosa, Boyd and Orihuela, 2009). Expression of *Pigr* is regulated by a combination of inflammatory and microbial pathways. Activation of TLR3 and TLR4 are known to increase *Pigr* expression in the intestinal epithelium, and systemic

administration of TNF-α results in increased expression of *Pigr* in the lungs (Schneeman *et al.*, 2005; Hinojosa, Boyd and Orihuela, 2009). It is unknown if the URT microbiota can contribute to *Pigr* expression locally.

I further explored microbiota colonization impacts on respiratory health by assessing transcriptomic data from lung tissue and alveolar macrophages from GF and SPF mice. Again, gene expression patterns were distinct between GF and SPF mice. Galectin-8, encoded by *Lgals8*, was decreased in GF mice in the nasal tissue, lung tissue, and alveolar macrophages. Galectin-8 has been demonstrated to be involved in the ubiquitination of intracellular Group A streptococci, leading to enhanced clearance of the bacteria (Cheng *et al.*, 2017). Galectin-8 can also promote bacterial clearance by binding host glycans on damaged vacuoles containing *Salmonella* (Thurston *et al*, 2012). The recognition of damaged vacuoles by galectin-8 results in increased recruitment of host factors important for autophagosome formation, and subsequent killing of the bacteria. Future studies should investigate the importance of galectin-8 and killing of intracellular *S. pneumoniae,* and the regulation of *Lgals8* expression by microbial factors within the respiratory tract.

Lung tissue from GF mice had decreased expression of *Ptafr,* the gene encoding platelet activating factor receptor (PAFR), compared to SPF mice. PAFR has been repeatedly associated with *S. pneumoniae* infections via multiple mechanisms. *Ptafr* knockout mice have reduced pneumococcal dissemination from the lungs compared to wildtype mice, and expression on epithelial cells

promote pneumococcal invasion (Rijneveld *et al.*, 2004; Radin *et al.*, 2005). Furthermore, *Ptafr* knockout mice also have reduced inflammation in response to *S. pneumoniae*, resulting is lessened pathology in both pneumococcal pneumonia and post-influenza pneumococcal pneumonia, and decreased shedding in transmission models (Rijneveld *et al.*, 2004; Sluijs *et al.*, 2006; Zafar *et al.*, 2016). Nonetheless, PAFR involvement in pneumococcal disease is not completely understood. Some groups have reported that inhibition of PAFR signalling has no effect on post-influenza pneumococcal infections, and deletion of *Ptafr* does not affect nasopharyngeal burden (McCullers and Rehg, 2002; Zafar *et al.*, 2016). Cigarette smoke has mixed effects on *Ptafr*, with increasing lung expression and decreasing nasal expression during smoke exposure compared to room-air exposed mice, though *Ptafr*-knockout mice are still equally susceptible to cigarette-smoke augmented pneumococcal infections (Shen *et al.*, 2016). As such, the role of PAFR may be tissue-specific during pneumococcal infections. Understanding the factors controlling *Ptafr* expression in different tissues may elucidate the potential effect of microbiota colonization. I hypothesize that specific microbial members, either from the respiratory or gut microbiota, could affect *Ptafr* expression, thus altering outcomes during pneumococcal infections. Addition of two probiotic species, *Lactobacillus helveticus* and *Bifidobacterium longum* subspecies *infantis,* along with TLR3 stimulation increased *Ptafr* expression on intestinal epithelial cells (MacPherson *et al*., 2017). This could be tested by incubation of multiple respiratory cell lines with bacterial and viral ligands, or

association of wild-type and *Ptafr* knockout mice with specific microbes, to determine the impact of the microbiota on respiratory *Ptafr* expression and pneumococcal infection outcomes.

The increased expression of *Marco*, the gene encoding the macrophage receptor with collagenous structure (MARCO), in GF lungs compared to SPF lungs was intriguing for multiple reasons. MARCO has been demonstrated to be important for binding and phagocytosis of *S. pneumoniae* by macrophages, leading to enhanced TLR2 signalling and improved clearance from the nasopharynx, as well as improved clearance from the lung (Sun and Metzger, 2008; Dorrington *et al.*, 2013). MARCO is known to be predominantly expressed by resident macrophages, including alveolar macrophages, though no difference in *Marco* expression in alveolar macrophages was observed between GF and SPF mice. This is supported by published evidence that *Marco* expression in alveolar macrophages is not altered by antibiotic treatment in mice (Schuijt *et al.*, 2016). The *Marco* signature is unlikely to be derived from non-resident macrophages, as recently recruited macrophages express much less *Marco* compared to alveolar and other embryo-derived macrophages (Lavin *et al.*, 2014; Gibbings *et al.*, 2015). Dendritic cells also produce MARCO, which aids in their TLR activation during stimulation similar to macrophages (Kissick *et al.*, 2014). Further investigation into the cellular source of *Marco* expression may yield a better understanding of lung physiology, especially in regard to pneumococcal pneumonia.

GF mice express less *Ptger3* and *Plau* in their lungs and alveolar macrophages, respectively, both of which have been identified in murine pneumococcal pneumonia studies. *Ptger3* encodes a prostaglandin receptor, E-prostanoid receptor 3, and *Ptger3* knockout mice have improved responses to pneumococcal pneumonia, including decreased pneumococcal burden (Aronoff *et al.*, 2009). Urokinase plasminogen activator, encoded by *Plau*, affects neutrophil recruitment during pneumococcal pneumonia (Rijneveld *et al.*, 2002). *Plau* knockout mice have improved neutrophil recruitment, and decreased pneumococcal load, compared to wild-type mice. These phenotypes could be contributing to the differences seen between ASF and SPF mice, though confirmation of these gene expression differences should be tested.

The lung tissue and alveolar macrophages from GF mice exhibited several decreased innate immune genes, including TLR1, TLR2, TLR4, and IL-1β, compared to SPF mice. TLR2 signalling and production of IL-1β are essential for the control and clearance of pneumococcal infections (Zhang, Clarke and Weiser, 2009). IL-1β expression is upregulated by NF-κB signalling downstream of several TLRs, and the lack of microbial ligands within the respiratory tract of GF mice would likely lead to diminished baseline TLR signalling. Gut microbiota colonization is known to increase intestinal expression of TLR2 (Hörmann *et al.*, 2014). Thus, it would be worthwhile to examine the impact of gut colonization of ASF mice on alveolar macrophage TLR2 expression. Nonetheless, TLR2-deficient mice have increased susceptibility to pneumococcal infections , which would imply that GF

mice would have increased susceptibility to pneumococcal infections (Zhang, Clarke and Weiser, 2009). These differences in innate immune signalling receptors and molecules need to be confirmed in ASF mice to determine their contribution to susceptibility differences, as well as the contribution of the URT microbiota. Nonetheless, the pattern of increased gene expression of factors important for pneumococcal binding , combined with decreased expression of genes important for pneumococcal-driven inflammation, would increase clearance and decrease the deleterious, exacerbated inflammatory response during pneumococcal infection.

In summary, I found that ASF mice lack URT bacteria affecting pneumococcal invasion that may change their susceptibility to *S. pneumoniae* infections. The lack of a microbiota could be contributing to multiple aspects of pneumococcal infections including direct microbial interactions, altered host cellular function and gene expression, as summarized in Figure 3. *Actinomyces naeslundii* exhibit sialidase activity, allowing for the cleavage and release of terminal sialic acids from extracellular proteins. This metabolism increases pneumococcal adherence to epithelial cells via exposure of residues for pneumococcal adhesins; furthermore, the presence of free sialic acids increase pneumococcal virulence. The alteration of several important host genes likely alters pneumococcal adherence and invasion within the respiratory tract. *S. pneumoniae* is known to bind to and invade respiratory epithelial cells via ChoP binding to PAFR, and CbpA binding to pIgR, and mice without a microbiome had decreased expression of PAFR and pIgR. The

decreased transcript expression correlates with the decreased pneumococcal colonization within the URT, and decreased pneumococcal dissemination seen in ASF mice. Thus, I propose a multi-faceted model, in which the microbiome affects multiple aspects of the host, increasing its susceptibility to pneumococcal pathogenesis. These individual aspects could all contribute to the final phenotype of increased colonization, dissemination, and mortality, and as such warrant further study in dedicated animal models.

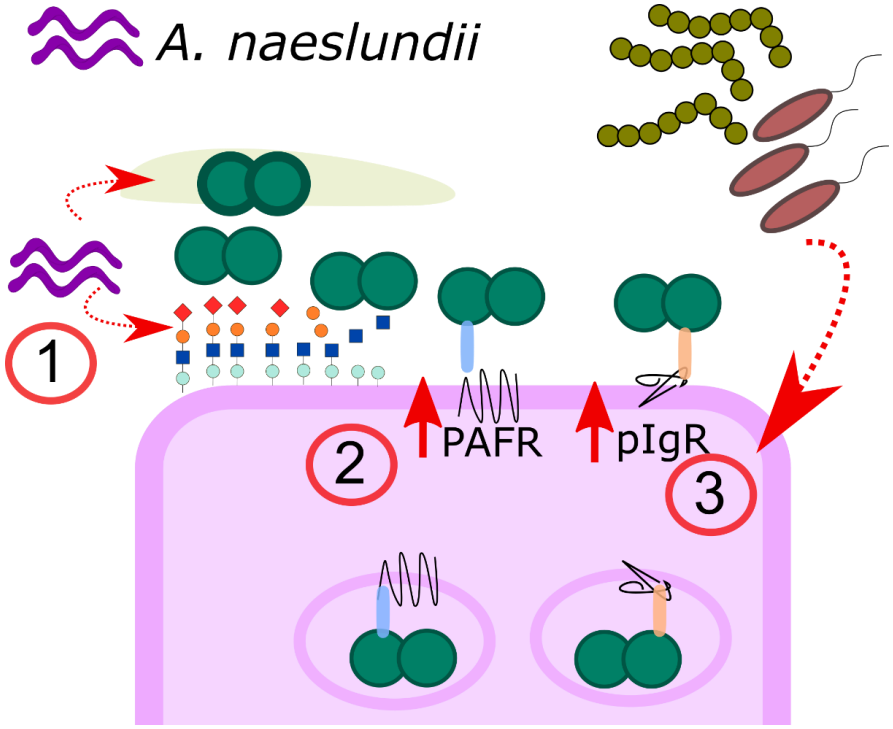

Figure 3 – Proposed mechanisms for microbiome-induced potentiation of pneumococcal pathogenesis.

Adherence of *Streptococcus pneumoniae* to respiratory epithelial cells occurs via binding to surface sugars and specific receptors. Cleavage of terminal sialic acids by *Actinomyces naeslundii* increases pneumococcal adherence to epithelial cells, with the potential additive effect of changing pneumococcal virulence. Additionally, the presence of a microbiome increases the expression of PAFR and pIgR, thus increasing the ability of *S. pneumoniae* to bind and invade epithelial cells via its own adhesins.

Delineation of individual genetic contributions may be difficult in traditional models, but genetic knockout mice with an ASF microbiome would contribute to the understanding of bacterial synergy compared to genetic susceptibility. Altered expression of adherence factors and immune responses may allow for increased colonization, dissemination, and transmission of *S. pneumoniae*, though this thesis focussed primarily on disease within the host. The URT microbiota, as well as gut microbiota complexity, could be playing a role in lung gene expression. The gut-lung axis for immune development has been supported by several studies, though recent work has suggested the contributions of local microbiota to gene expression should not be overlooked (Dickson *et al*., 2018; Siegel *et al*., 2015). A number of these genes are known to be under the control of inflammatory stimuli, but further understanding of microbial signals controlling expression would help elucidate the mechanistic pathways for treating or preventing pneumococcal infections.

4.5 ASF mice as a model organism for respiratory microbiota impact on host health

While ASF mice were investigated for their pneumococcal infection susceptibility, the finding of their “germ-free” nasal microbiota status extends beyond their use in this thesis. Due to the occasional irreproducibility seen from SPF mice from different commercial sources, or even different rooms within an institution, defined microbial consortia provide a controllable environment for experimental models (Moon *et al.*, 2015). ASF mice have been used for decades to assess microbial involvement in physiological and immunological development

(Brand *et al.*, 2015). ASF mice have been predominantly used to study gut immunology and development, though their use have also highlighted the role of the gut microbiota in systemic immunity and behavioral responses (Brand *et al.*, 2015). ASF mice are colonized by 8 bacteria originally isolated from SPF gut bacteria, with each species colonizing at a different efficiency along the gastrointestinal tract depending on pH, oxygen, and nutrient availability. The applications of this model are far reaching, allowing the understanding of the contribution of the URT microbiota in colonization resistance against or cooperation during infections. Murine models of *Staphylococcus aureus, Bordetella pertussis,* and *Corynebacterium tuberculostearicum* nasal colonization are aided by intranasal antibiotic pretreatment, suggesting that colonization resistance can be afforded by the URT microbiota (Kiser, Cantey-Kiser and Lee, 1999; Abreu *et al.*, 2012; Weyrich *et al.*, 2014). ASF mice would be a valuable tool to provide a controllable environment for measurement of bacterial competition and cooperation within the URT.

While ASF mice do have a gut microbiota, it does not contain the vast functional capacity seen in an SPF gut microbiota. ASF mice lack the Proteobacteria phylum, which are involved in various gut pathologies, and often bloom after an inflammatory event (Zeng, Inohara and Nuñez, 2017). The lack of several metabolic pathways provided by the gut microbiota may be important for baseline function or nutrient availability. ASF mice specifically lack T_H17 cells in their small intestine (Ivanov *et al*., 2009). Several attempts have been made to

improve defined, minimal microbial consortia and their impact on mouse health and colonization resistance. Research groups have inoculated mice with communities ranging from 2-91 bacteria to normalize responses, including colonization resistance against pathogens and immune cell development (Elzinga *et al.*, 2019). The development of minimal microbial consortia should depend on the research question. ASF mice are an exemplary intermediary between GF and SPF, as they recapitulate stimulation of the immune system by bacterial ligands, short chain fatty acid production, and normalization of cecum size (and therefore nutrient absorption) compared to GF mice. The differences in respiratory immunity between ASF, GF, and SPF mice remain unknown, in part due to undetermined “normal” functions of the respiratory microbiota during health. For example, germ-free mice have altered olfactory epithelial function, including prolonged responses to olfactory stimuli (François *et al.*, 2016). It is unclear if this is due to a lack of a respiratory microbiota, a gut microbiota, or lack of exposure to stimuli (including microbial byproducts). ASF mice provide a blank slate to allow colonization of individual or collections of bacteria to examine the impact on respiratory immunity and function.

4.6 Limitations of animal models

Mouse models allow for control over environment, though do not perfectly replicate human diseases. Many pathogens, including *S. pneumoniae* have adapted to their primary host, and only interact with the human versions of proteins

and environment. *S. pneumoniae* has evolved to produce multiple virulence factors that help it evade complement, including CbpA that binds human Factor H and enolase that binds human C4b-binding protein, but neither of these virulence factors bind their mouse homologue (Lu *et al.*, 2008; Agarwal *et al.*, 2012). CbpA also shows greater affinity for human pIgR over sheep pIgR (Zhang *et al.*, 2000). Human-specific mutations, including the deletion of an exon in cytidine-monophosphate-N-acetylneuraminic hydroxylase that converts N-acetylneuraminic acid into N-glycolylneuraminic acid, create an environment that results in upregulation of pneumococcal virulence factors; this environment is not present in mice (Hentrich *et al.*, 2016). Humanization of specific proteins in mice has been successfully used for other respiratory pathogens, including *Neisseria meningitidis* and *Streptococcus pyogenes* (Johswich *et al.*, 2013; Kasper *et al.*, 2014). No humanized mouse models have been used in *S. pneumoniae* studies, though several studies have used human antibodies to assess IgA protease activity and immunization strategies (Janoff *et al.*, 2014). Mouse models can complicate the addition of non-pathogens, as introducing bacterial species isolated from human samples may not colonize within the mouse URT. Exploration of species-specific interactions will continue to be a challenge in mouse models.

Sampling of the murine URT microbiota is challenged by the inability to serially sample the nasal cavity. Studies assessing the murine gut microbiota can use fecal pellets from multiple timepoints to monitor changes of the microbiota composition during interventions including cohousing and antibiotic treatment

(Russell *et al.*, 2012; Thevaranjan *et al.*, 2017). The murine nasal cavity is inaccessible to repeated swabs due to tiny nares and the potential for damage to the animal, which is not a problem in human studies. Some research groups have attempted to repeatedly sample murine nasal colonization by “nasal taps”, directly tapping a mouse nose onto agar plates to detect specific bacteria (Zafar *et al.*, 2016). This methodology is efficient to detect bacterial shedding, but is unlikely to properly sample the microbiota, especially biofilm- or turbinate-associated bacteria.

It was determined during this thesis that SPF mice were from a C57BL/6J background, whereas mice within the gnotobiotic unit were a C57BL/6N background. These mouse strains share a similar lineage, being separated by breeding facilities in 1951, meaning they have been separated for more than 230 generations (Simon *et al.*, 2013). This detail is often overlooked, with many papers stating the use of “C57BL/6” mice (Fontaine and Davis, 2016). A characterization of the two substrains of mice identified 34 coding and 146 non-coding single nucleotide polymorphisms, as well as 2 coding and 54 non-coding insertion/deletions (Simon *et al.*, 2013). Nicotinamide nucleotide transhydrogenase is a well-documented deletion in C57BL/6J mice compared to C57BL/6N, resulting in decreased insulin secretion and altered glucose metabolism in C57BL/6J mice (Freeman *et al*., 2006). A point mutation in *Nlrp12* was also discovered, but initially dismissed. Recent evidence has shown this point mutation results in a non-functional NLRP12 protein in C57BL/6J mice, impacting neutrophil recruitment

during *Staphylococcus aureus* and *Pseudomonas aeruginosa* lung infections (Ulland *et al.*, 2016). The differences between these two substrains are not clean-cut: one group reported increased susceptibility of C57BL/6J mice to influenza A infection compared to C57BL/6N, whereas another study found *Nlrp12* deficiency and C57BL/6J mice were protected from influenza A virus infections (Eisfeld *et al*., 2019; Hornick *et al*., 2018). *Nlrp12* deficiency has not been linked to altered pneumococcal disease, though this does not rule out that it could contribute to a difference between C57BL/6J and C57BL/6N mice. This issue is not simply solved by ordering SPF C57BL/6N mice, as these mice will likely have distinct microbial communities compared to current SPF mice, as was found for the Jackson mice in this study. In this study, I cohoused the SPF C57BL/6J mice with ASF C57BL/6N, and thus exposing them to microbial species from SPF C57BL/6J mice. This cohousing exhibited increased pneumococcal dissemination from the respiratory tract compared to ASF mice, demonstrating this phenotype had a bacterial and non-genetic component. Furthermore, the addition of *A. naeslundii* accelerated pneumococcal disease, further implying a microbial-driven phenotype. This is in agreement with other studies showing that differences in microbiota composition overcome differences in genetics between the two substrains during infectious models (Ivanov *et al*., 2008; Velazquez *et al*., 2019). Going forward, the ideal situation is to use genetically identical mice for comparisons, but this did not affect the major phenotype discussed in this thesis.

Lastly, the use of gnotobiotic animals is not without complications. ASF mice are known to be deficient in different cell types, including T_H17 cells, which could impact the outcome of different experimental models, and should be considered during research design (Ivanov *et al*., 2008). Additionally, mice bred within a gnotobiotic unit are expensive to maintain due to the careful breeding, handling, and monitoring protocols. The cost of housing and breeding minimal microbiota mice, including ASF mice, needs to be factored into research design. These mice also breed at reduced rates compared to SPF mice, with litters occasionally being eaten by the mother. Indeed, other studies have determined that litter sizes can range from 1 to 6 pups (Palma *et al.*, 2015). These erratic litters can limit availability of proper cohort sizes for experiments. Development of *in vitro* functional studies to complement *in vivo* experiments aids microbiome research. The development of *in vitro* microbiome models is a rapidly growing field. Use of *ex vivo* organs and organ-on-chip technology allow the complexity of the microbiota-host interactions to be modelled (Yissachar *et al.*, 2017; Jalili-Firoozinezhad *et al.*, 2019). In this study, I used functional enzyme screens in combination with cell culture-based screens to detect microbe-host interactions. Development of functional, cost-effective screens allow for mechanisms to be tested within animal models.

4.7 Concluding Remarks

This thesis set out to characterize the murine URT microbiota, and further leverage that as a model to examine pneumococcal-microbiota interactions. The characterization of the murine microbiota revealed niche-specific microbial

interactions, highlighting the importance of tissue sampling and source of mice during research design. The finding that ASF mice had a reduced susceptibility led us to discover sialidase activity from URT microbiota members, namely *Actinomyces naeslundii*, promote pneumococcal infections. Moving forward, sialidase from various bacterial sources should be explored for their ability to alter pneumococcal pathogenesis. The impact of the URT microbiota on host health presents an interesting avenue for exploring host susceptibility to pneumococcal infections, one of the leading causes of death worldwide.

Chapter 5: References

Aas, J. A. A. *et al.* (2005) 'Defining the normal bacterial flora of the oral cavity', *Journal of clinical microbiology*, 43(11), pp. 5721–5732. doi: 10.1128/jcm.43.11.5721-5732.2005.

Abreu, N. A. *et al.* (2012) 'Sinus microbiome diversity depletion and Corynebacterium tuberculostearicum enrichment mediates rhinosinusitis', *Sci Transl Med*, 4(151), p. 151ra124. doi: 10.1126/scitranslmed.3003783.

Agarwal, V. *et al.* (2012) 'Enolase of Streptococcus pneumoniae Binds Human Complement Inhibitor C4b-Binding Protein and Contributes to Complement Evasion', *The Journal of Immunology*, 189(7), pp. 3575–3584. doi: 10.4049/jimmunol.1102934.

Agüero, M. G. de *et al.* (2016) 'The maternal microbiota drives early postnatal innate immune development', *Science*, 351(6279), pp. 1296–1302. doi: 10.1126/science.aad2571.

Alegre, M. L. (2019) 'Mouse microbiomes: Overlooked culprits of experimental variability', *Genome Biology*, 20(1), p. 108. doi: 10.1186/s13059-019-1723-2.

Almeida, A. *et al.* (2019) 'A new genomic blueprint of the human gut microbiota', *Nature*, 568(7753), pp. 499–504. doi: 10.1038/s41586-019-0965-1.

Andrews, S. (2010) 'FastQC: a quality control tool for high throughput sequence data'. Available at: http://www.bioinformatics.babraham.ac.uk/projects/fastqc.

Aronoff, D. M. *et al.* (2009) 'E-Prostanoid 3 Receptor Deletion Improves Pulmonary Host Defense and Protects Mice from Death in Severe Streptococcus

pneumoniae Infection', *The Journal of Immunology*, 183(4), pp. 2642–2649. doi: 10.4049/jimmunol.0900129.

Arrieta, M. C. *et al.* (2015) 'Early infancy microbial and metabolic alterations affect risk of childhood asthma', *Sci Transl Med*, 7(307), p. 307ra152. doi: 10.1126/scitranslmed.aab2271.

Atarashi, K. *et al.* (2013) 'Treg induction by a rationally selected mixture of Clostridia strains from the human microbiota', *Nature*, 500(7461), pp. 232–236. doi: 10.1038/nature12331.

Bartram, A. K. *et al.* (2011) 'Generation of multimillion-sequence 16S rRNA gene libraries from complex microbial communities by assembling paired-end Illumina reads', *Applied and Environmental Microbiology*, 77(11), pp. 3846–3852. doi: 10.1128/AEM.02772-10.

Bassis, C. M. *et al.* (2015) 'Analysis of the upper respiratory tract microbiotas as the source of the lung and gastric microbiotas in healthy individuals', *mBio*, 6(2), p. e00037. doi: 10.1128/mBio.00037-15.

Bercik, P. *et al.* (2011) 'The intestinal microbiota affect central levels of brain-derived neurotropic factor and behavior in mice', *Gastroenterology*, 141(2), pp. 599-–609. doi: 10.1053/j.gastro.2011.04.052.

Berendt, R. F., Long, G. G. and Walker, J. S. (1975) 'Influenza alone and in sequence with pneumonia due to Streptococcus pneumoniae in the squirrel monkey', *The Journal of infectious diseases*, 132(6), pp. 689–693. doi: 10.1093/infdis/132.6.689.

Bested, A. C., Logan, A. C. and Selhub, E. M. (2013) 'Intestinal microbiota, probiotics and mental health: from Metchnikoff to modern advances: Part I - autointoxication revisited', *Gut pathogens*, 5(1), p. 5. doi: 10.1186/1757-4749-5-5.

Biesbroek, Giske *et al.* (2014) 'Early respiratory microbiota composition determines bacterial succession patterns and respiratory health in children.', *American journal of respiratory and critical care medicine*, 190(11), pp. 1283–92. doi: 10.1164/rccm.201407-1240OC.

Biesbroek, G *et al.* (2014) 'The impact of breastfeeding on nasopharyngeal microbial communities in infants', *Am J Respir Crit Care Med*, 190(3), pp. 298–308. doi: 10.1164/rccm.201401-0073OC.

Bik, E. M. *et al.* (2006) 'Molecular analysis of the bacterial microbiota in the human stomach', *Proceedings of the National Academy of Sciences of the United States of America*, 103(3), pp. 732–737. doi: 10.1073/pnas.0506655103.

Bomar, L. *et al.* (2016) 'Corynebacterium accolens Releases Antipneumococcal Free Fatty Acids from Human Nostril and Skin Surface Triacylglycerols', *MBio*, 7(1), pp. e01725-15. doi: 10.1128/mBio.01725-15.

Bosch, A. A., Levin, E., *et al.* (2016) 'Development of Upper Respiratory Tract Microbiota in Infancy is Affected by Mode of Delivery', *EBioMedicine*, 9, pp. 336–345. doi: 10.1016/j.ebiom.2016.05.031.

Bosch, A. A., van Houten, M. A., *et al.* (2016) 'Nasopharyngeal carriage of Streptococcus pneumoniae and other bacteria in the 7th year after implementation of the pneumococcal conjugate vaccine in the Netherlands',

Vaccine, 34(4), pp. 531–9. doi: 10.1016/j.vaccine.2015.11.060.

Bowdish, D. M. E., Davidson, D. J. and Hancock, R. E. W. (2006) 'Immunomodulatory properties of defensins and cathelicidins.', *Current topics in microbiology and immunology*, 306, pp. 27–66. Available at: http://www.ncbi.nlm.nih.gov/pubmed/16909917 (Accessed: 27 July 2019).

Brand, M. W. *et al.* (2015) 'The Altered Schaedler Flora: Continued Applications of a Defined Murine Microbial Community', *ILAR Journal*, 56(2), pp. 169–178. doi: 10.1093/ilar/ilv012.

Bray, J. R. and Curtis, J. T. (1957) 'An Ordination of the Upland Forest Communities of Southern Wisconsin', *Ecological Monographs*, 27(4), pp. 325–349. doi: 10.2307/1942268.

Briles, D. E. *et al.* (2005) 'Nasal Colonization with Streptococcus pneumoniae Includes Subpopulations of Surface and Invasive Pneumococci', *Infection and Immunity*, 73(10), pp. 6945–6951. doi: 10.1128/iai.73.10.6945-6951.2005.

Brock, S. C. *et al.* (2002) 'The human polymeric immunoglobulin receptor facilitates invasion of epithelial cells by Streptococcus pneumoniae in a strain-specific and cell type-specific manner', *Infection and Immunity*, 70(9), pp. 5091–5095. doi: 10.1128/IAI.70.9.5091-5095.2002.

Brown, R. L., Sequeira, R. P. and Clarke, T. B. (2017) 'The microbiota protects against respiratory infection via GM-CSF signaling', *Nature communications*, 8(1), p. 1512. doi: 10.1038/s41467-017-01803-x.

Browne, H. P. *et al.* (2016) 'Culturing of "unculturable" human microbiota reveals

novel taxa and extensive sporulation', *Nature*, 533(7604), pp. 543–546. doi: 10.1038/nature17645.

Buckwalter, C. M. and King, S. J. (2012) 'Pneumococcal carbohydrate transport: food for thought', *Trends in microbiology*, 20(11), pp. 517–522. doi: 10.1016/j.tim.2012.08.008.

Callahan, B. J. *et al.* (2016) 'DADA2: High-resolution sample inference from Illumina amplicon data', *Nature Methods*. doi: 10.1038/nmeth.3869.

Caporaso, J. G. *et al.* (2010) 'QIIME allows analysis of high-throughput community sequencing data', *Nature methods*, 7, pp. 335–336. doi: 10.1038/nmeth.f.303.

Casey, J. R., Adlowitz, D. G. and Pichichero, M. E. (2010) 'New patterns in the otopathogens causing acute otitis media six to eight years after introduction of pneumococcal conjugate vaccine', *The Pediatric infectious disease journal*, 29(4), pp. 304–309. doi: 10.1097/inf.0b013e3181c1bc48.

Chen, G. *et al.* (2014) 'Broad and direct interaction between TLR and Siglec families of pattern recognition receptors and its regulation by Neu1', *eLife*, 3, p. e04066. doi: 10.7554/eLife.04066.

Chen, X. *et al.* (2018) 'Host Immune Response to Influenza A Virus Infection', *Frontiers in Immunology*, 9, p. 320. doi: 10.3389/fimmu.2018.00320.

Cheng, Y. *et al.* (2017) 'Galectin-3 Inhibits Galectin-8/Parkin-Mediated Ubiquitination of Group A Streptococcus', *mBio*, 8(4), pp. e00899-17. doi: 10.1128/mbio.00899-17.

Chiavolini, D., Pozzi, G. and Ricci, S. (2008) 'Animal models of Streptococcus pneumoniae disease', *Clinical microbiology reviews*, 21(4), pp. 666–685. doi: 10.1128/cmr.00012-08.

Clarke, T. B. *et al.* (2010) 'Recognition of peptidoglycan from the microbiota by Nod1 enhances systemic innate immunity', *Nature Medicine*, 16(2), pp. 228–231. doi: 10.1038/nm.2087.

Cohen, N. A. (2006) 'Sinonasal mucociliary clearance in health and disease', *The Annals of otology, rhinology & laryngology. Supplement*, 196, pp. 20–26. Available at: https://www.ncbi.nlm.nih.gov/pubmed/17040014.

Collins, J. *et al.* (2014) 'Intestinal microbiota influence the early postnatal development of the enteric nervous system', *Neurogastroenterology & Motility*, 26(1), pp. 98–107. doi: 10.1111/nmo.12236.

Cremers, A. J. H. *et al.* (2014) 'The adult nasopharyngeal microbiome as a determinant of pneumococcal acquisition', *Microbiome*, 2(1), p. 44. doi: 10.1186/2049-2618-2-44.

Cundell, D. R. *et al.* (1995) 'Streptococcus pneumoniae anchor to activated human cells by the receptor for platelet-activating factor', *Nature*, 377(6548), pp. 435–438. doi: 10.1038/377435a0.

Dalia, A. B. and Weiser, J. N. (2011) 'Minimization of bacterial size allows for complement evasion and is overcome by the agglutinating effect of antibody', *Cell host & microbe*, 10(5), pp. 486–496. doi: 10.1016/j.chom.2011.09.009.

Davis, K. M. *et al.* (2008) 'Resistance to mucosal lysozyme compensates for the

fitness deficit of peptidoglycan modifications by Streptococcus pneumoniae.', *PLoS pathogens*, 4(12), p. e1000241. doi: 10.1371/journal.ppat.1000241.

Davis, K. M., Nakamura, S. and Weiser, J. N. (2011) 'Nod2 sensing of lysozyme-digested peptidoglycan promotes macrophage recruitment and clearance of S. pneumoniae colonization in mice', *J Clin Invest*, 121(9), pp. 3666–76. doi: 10.1172/JCI57761.

Demczuk, W. H. *et al.* (2012) 'Serotype distribution of invasive Streptococcus pneumoniae in Canada during the introduction of the 13-valent pneumococcal conjugate vaccine, 2010', *Can J Microbiol*, 58(8), pp. 1008–17. doi: 10.1139/w2012-073.

Demczuk, W. H. B. *et al.* (2014) *National Laboratory Surveillance of Invasive Streptococcal Disease in Canada – Annual Summary 2014*. Available at: https://www.canada.ca/en/public-health/services/publications/drugs-health-products/national-laboratory-surveillance-invasive-streptococcal-disease-canada-annual-summary-2014.html.

DeSantis, T. Z. *et al.* (2006) 'Greengenes, a chimera-checked 16S rRNA gene database and workbench compatible with ARB', *Applied and environmental microbiology*, 72(7), pp. 5069–5072. doi: 10.1128/aem.03006-05.

Dewhirst, F. E. *et al.* (1999) 'Phylogeny of the defined murine microbiota: altered Schaedler flora', *Applied and environmental microbiology*, 65(8), pp. 3287–3292. Available at: https://www.ncbi.nlm.nih.gov/pubmed/10427008.

Diavatopoulos, D. A. *et al.* (2010) 'Influenza A virus facilitates Streptococcus

pneumoniae transmission and disease', *FASEB J*, 24(6), pp. 1789–1798. doi: 10.1096/fj.09-146779.

Dickson, R. P. *et al.* (2016) 'The Microbiome and the Respiratory Tract', *Annu Rev Physiol*, 78, pp. 481–504. doi: 10.1146/annurev-physiol-021115-105238.

Dickson, R. P. *et al.* (2018) 'The Lung Microbiota of Healthy Mice Are Highly Variable, Cluster by Environment, and Reflect Variation in Baseline Lung Innate Immunity', *American Journal of Respiratory and Critical Care Medicine*, 198(4), pp. 497–508. doi: 10.1164/rccm.201711-2180oc.

Didierlaurent, A. *et al.* (2008) 'Sustained desensitization to bacterial Toll-like receptor ligands after resolutionof respiratory influenza infection', *The Journal of Experimental Medicine*, 205(2), pp. 323–329. doi: 10.1084/jem.20070891.

Dobin, A. *et al.* (2013) 'STAR: Ultrafast universal RNA-seq aligner', *Bioinformatics*, 29(1), pp. 15–21. doi: 10.1093/bioinformatics/bts635.

Dogaru, C. M. *et al.* (2014) 'Breastfeeding and childhood asthma: systematic review and meta-analysis', *Am J Epidemiol*, 179(10), pp. 1153–67. doi: 10.1093/aje/kwu072.

Dorrington, M. G. *et al.* (2013) 'MARCO is required for TLR2- and Nod2-mediated responses to Streptococcus pneumoniae and clearance of pneumococcal colonization in the murine nasopharynx', *J Immunol*, 190(1), pp. 250–258. doi: 10.4049/jimmunol.1202113.

Dubé, E. *et al.* (2011) 'Burden of acute otitis media on Canadian families.', *Canadian family physician Medecin de famille canadien*, 57(1), pp. 60–5.

Available at: http://www.ncbi.nlm.nih.gov/pubmed/21252135 (Accessed: 12 July 2019).

Duvallet, C. *et al.* (2017) 'Meta-analysis of gut microbiome studies identifies disease-specific and shared responses.', *Nature communications*, 8(1), p. 1784. doi: 10.1038/s41467-017-01973-8.

Earnshaw, S. R. *et al.* (2012) 'Cost-effectiveness of 2 + 1 dosing of 13-valent and 10-valent pneumococcal conjugate vaccines in Canada', *BMC Infectious Diseases*, 12, p. 101. doi: 10.1186/1471-2334-12-101.

Eckburg, P. B. *et al.* (2005) 'Diversity of the human intestinal microbial flora', *Science*, 308(5728), pp. 1635–1638. doi: 10.1126/science.1110591.

Eisfeld, A. J. *et al.* (2019) 'C57BL/6J and C57BL/6NJ Mice Are Differentially Susceptible to Inflammation-Associated Disease Caused by Influenza A Virus', *Frontiers in Microbiology*, 9, p. 3307. doi: 10.3389/fmicb.2018.03307.

Elzinga, J. *et al.* (2019) 'The Use of Defined Microbial Communities To Model Host-Microbe Interactions in the Human Gut', *Microbiology and Molecular Biology Reviews*, 83(2), pp. e00054-18. doi: 10.1128/mmbr.00054-18.

Escapa, I. F. *et al.* (2018) 'New Insights into Human Nostril Microbiome from the Expanded Human Oral Microbiome Database (eHOMD): a Resource for the Microbiome of the Human Aerodigestive Tract', *mSystems*. Edited by J. Xu, 3(6), pp. e00187-18. doi: 10.1128/mSystems.00187-18.

Faden, H. *et al.* (1997) 'Relationship between nasopharyngeal colonization and the development of otitis media in children. Tonawanda/Williamsville Pediatrics',

J Infect Dis, 175(6), pp. 1440–5. doi: 10.1086/516477.

Feng, T. *et al.* (2010) 'Microbiota innate stimulation is a prerequisite for T cell spontaneous proliferation and induction of experimental colitis', *The Journal of Experimental Medicine*, 207(6), pp. 1321–1332. doi: 10.1084/jem.20092253.

Fontaine, D. A. and Davis, D. B. (2016) 'Attention to Background Strain Is Essential for Metabolic Research: C57BL/6 and the International Knockout Mouse Consortium', *Diabetes*, 65(1), pp. 25–33. doi: 10.2337/db15-0982.

François, A. *et al.* (2016) 'Olfactory epithelium changes in germfree mice', *Scientific Reports*, 6, p. 24687. doi: 10.1038/srep24687.

Freeman, H. *et al.* (2006) 'Nicotinamide nucleotide transhydrogenase: A key role in insulin secretion', *Cell Metabolism*, 3(1), pp. 35–45. doi: 10.1016/j.cmet.2005.10.008.

Galipeau, H. J. *et al.* (2015) 'Intestinal microbiota modulates gluten-induced immunopathology in humanized mice', *American Journal of Pathology*, 185(11), pp. 2969–2982. doi: 10.1016/j.ajpath.2015.07.018.

Gamez, G. and Hammerschmidt, S. (2012) 'Combat pneumococcal infections: adhesins as candidates for protein-based vaccine development', *Current drug targets*, 13(3), pp. 323–337. Available at: https://www.ncbi.nlm.nih.gov/pubmed/22206255.

Ganz, T. (2002) 'Antimicrobial polypeptides in host defense of the respiratory tract', *The Journal of clinical investigation*, 109(6), pp. 693–697. doi: 10.1172/jci15218.

Gauguet, S. *et al.* (2015) 'Intestinal Microbiota of Mice Influences Resistance to Staphylococcus aureus Pneumonia', *Infection and immunity*, 83(10), pp. 4003–4014. doi: 10.1128/iai.00037-15.

Gibbings, S. L. *et al.* (2015) 'Transcriptome analysis highlights the conserved difference between embryonic and postnatal-derived alveolar macrophages', *Blood*, 126(11), pp. 1357–1366. doi: 10.1182/blood-2015-01-624809.

Gingles, N. A. *et al.* (2001) 'Role of genetic resistance in invasive pneumococcal infection: identification and study of susceptibility and resistance in inbred mouse strains', *Infection and immunity*, 69(1), pp. 426–434. doi: 10.1128/iai.69.1.426-434.2001.

van Ginkel, F. W. *et al.* (2003) 'Pneumococcal carriage results in ganglioside-mediated olfactory tissue infection', *Proceedings of the National Academy of Sciences*, 100(24), pp. 14363–14367. doi: 10.1073/pnas.2235844100.

Glendinning, L. *et al.* (2016) 'Variability of the sheep lung microbiota', *Applied and Environmental Microbiology*, 82(11), pp. 3225–3238. doi: 10.1128/AEM.00540-16.

Glennie, S. *et al.* (2016) 'Modulation of nasopharyngeal innate defenses by viral coinfection predisposes individuals to experimental pneumococcal carriage', *Mucosal Immunol*, 9(1), pp. 56–67. doi: 10.1038/mi.2015.35.

Glimstedt, G. (1959) 'The germfree animal as a research tool', *Annals of the New York Academy of Sciences*, 78(1), pp. 281–284. doi: 10.1111/j.1749-6632.1959.tb53112.x.

de Goffau, M. C. *et al.* (2018) 'Recognizing the reagent microbiome', *Nature Microbiology*, pp. 851–853. doi: 10.1038/s41564-018-0202-y.

Goggin, R. K. *et al.* (2018) 'Comparative Viral Sampling in the Sinonasal Passages; Different Viruses at Different Sites', *Frontiers in Cellular and Infection Microbiology*, 8, p. 334. doi: 10.3389/fcimb.2018.00334.

Gritzfeld, J. F. *et al.* (2011) 'Comparison between nasopharyngeal swab and nasal wash, using culture and PCR, in the detection of potential respiratory pathogens', *BMC Research Notes*, 4(1), p. 122. doi: 10.1186/1756-0500-4-122.

Gritzfeld, J. F. *et al.* (2013) 'Experimental human pneumococcal carriage', *J Vis Exp*, (72), p. 50115. doi: 10.3791/50115.

Harford, C. G. (1949) 'Effect of the Lesion Due To Influenza Virus on the Resistance of Mice To Inhaled Pneumococci', *Journal of Experimental Medicine*, 89(1), pp. 53–68. doi: 10.1084/jem.89.1.53.

Harrell Jr., F. E. and Dupont, C. (2019) 'Hmisc: Harrell Miscellaneous'. Available at: https://cran.r-project.org/package=Hmisc%7D.

Hartley, S. W. and Mullikin, J. C. (2015) 'QoRTs: A comprehensive toolset for quality control and data processing of RNA-Seq experiments', *BMC Bioinformatics*, 16(1), p. 224. doi: 10.1186/s12859-015-0670-5.

Hatcher, B. L., Hale, J. Y. and Briles, D. E. (2016) 'Free Sialic Acid Acts as a Signal That Promotes Streptococcus pneumoniae Invasion of Nasal Tissue and Nonhematogenous Invasion of the Central Nervous System', *Infection and Immunity*, 84(9), pp. 2607–2615. doi: 10.1128/iai.01514-15.

Hayashi, H., Sakamoto, M. and Benno, Y. (2002) 'Phylogenetic analysis of the human gut microbiota using 16S rDNA clone libraries and strictly anaerobic culture-based methods', *Microbiology and immunology*, 46(8), pp. 535–548. Available at: https://www.ncbi.nlm.nih.gov/pubmed/12363017.

Hentrich, K. *et al.* (2016) 'Streptococcus pneumoniae Senses a Human-like Sialic Acid Profile via the Response Regulator CiaR', *Cell Host and Microbe*, 20(3), pp. 307–317. doi: 10.1016/j.chom.2016.07.019.

Hilty, M. *et al.* (2010) 'Disordered microbial communities in asthmatic airway', *PLoS One*, 5(1), p. e8578. doi: 10.1371/journal.pone.0008578.

Hinojosa, E., Boyd, A. R. and Orihuela, C. J. (2009) 'Age-associated inflammation and toll-like receptor dysfunction prime the lungs for pneumococcal pneumonia', *J Infect Dis*, 200(4), pp. 546–54. doi: 10.1086/600870.

Hörmann, N. *et al.* (2014) 'Gut Microbial Colonization Orchestrates TLR2 Expression, Signaling and Epithelial Proliferation in the Small Intestinal Mucosa', *PLoS ONE*, 9(11), p. e113080. doi: 10.1371/journal.pone.0113080.

Hornick, E. E. *et al.* (2018) 'Nlrp12 Mediates Adverse Neutrophil Recruitment during Influenza Virus Infection', *The Journal of Immunology*, 200(3), pp. 1188–1197. doi: 10.4049/jimmunol.1700999.

Ichinohe, T. *et al.* (2011) 'Microbiota regulates immune defense against respiratory tract influenza A virus infection', *Proceedings of the National Academy of Sciences*, 108(13), pp. 5354–5359. doi: 10.1073/pnas.1019378108.

Iovino, F., Molema, G. and Bijlsma, J. J. E. (2014) 'Streptococcus pneumoniae

Interacts with pIgR Expressed by the Brain Microvascular Endothelium but Does Not Co-Localize with PAF Receptor', *PLoS ONE*, 9(5), p. e97914. doi: 10.1371/journal.pone.0097914.

Ivanov, I. I. *et al.* (2008) 'Specific microbiota direct the differentiation of IL-17-producing T-helper cells in the mucosa of the small intestine', *Cell Host Microbe*. 2008/10/16, 4(4), pp. 337–49. doi: 10.1016/j.chom.2008.09.009.

Ivanov, I. I. *et al.* (2009) 'Induction of intestinal Th17 cells by segmented filamentous bacteria', *Cell*, 139(3), pp. 485–498. doi: 10.1016/j.cell.2009.09.033.

Jalili-Firoozinezhad, S. *et al.* (2019) 'A complex human gut microbiome cultured in an anaerobic intestine-on-a-chip', *Nature Biomedical Engineering*, 3(7), pp. 520–531. doi: 10.1038/s41551-019-0397-0.

Jandhyala, S. M. *et al.* (2015) 'Role of the normal gut microbiota', *World journal of gastroenterology*, 21(29), pp. 8787–8803. doi: 10.3748/wjg.v21.i29.8787.

Janoff, E. N. *et al.* (2014) 'Pneumococcal IgA1 protease subverts specific protection by human IgA1', *Mucosal Immunology*, 7(2), pp. 249–256. doi: 10.1038/mi.2013.41.

Jensch, I. *et al.* (2010) 'PavB is a surface-exposed adhesin of Streptococcus pneumoniae contributing to nasopharyngeal colonization and airways infections', *Molecular microbiology*, 77(1), pp. 22–43. doi: 10.1111/j.1365-2958.2010.07189.x.

Johnson, N. P. A. S. and Mueller, J. (2002) 'Updating the Accounts: Global Mortality of the 1918-1920 "Spanish" Influenza Pandemic', *Bulletin of the History*

of Medicine, 76(1), pp. 105–115. doi: 10.1353/bhm.2002.0022.

Johswich, K. O. *et al.* (2013) 'In Vivo Adaptation and Persistence of Neisseria meningitidis within the Nasopharyngeal Mucosa', *PLoS Pathogens*. plos, 9(7), p. e1003509. doi: 10.1371/journal.ppat.1003509.

Jost, L. (2007) 'Partitioning diversity into independent alpha and beta components', *Ecology*, 88(10), pp. 2427–2439. Available at: https://www.ncbi.nlm.nih.gov/pubmed/18027744.

Juge, N., Tailford, L. and Owen, C. D. (2016) 'Sialidases from gut bacteria: a mini-review', *Biochemical Society Transactions*, 44(1), pp. 166–175. doi: 10.1042/bst20150226.

Kash, J. C. *et al.* (2011) 'Lethal Synergism of 2009 Pandemic H1N1 Influenza Virus and Streptococcus pneumoniae Coinfection Is Associated with Loss of Murine Lung Repair Responses', *mBio*, 2(5), pp. e00172-11. doi: 10.1128/mbio.00172-11.

Kasper, K. J. *et al.* (2014) 'Bacterial Superantigens Promote Acute Nasopharyngeal Infection by Streptococcus pyogenes in a Human MHC Class II-Dependent Manner', *PLoS Pathogens*, 10(5), p. e1004155. doi: 10.1371/journal.ppat.1004155.

Kellner, J. D. *et al.* (2009) 'Changing epidemiology of invasive pneumococcal disease in Canada, 1998-2007: update from the Calgary-area Streptococcus pneumoniae research (CASPER) study', *Clin Infect Dis*, 49(2), pp. 205–12. doi: 10.1086/599827.

Kellogg, J. (1917) ‘SHOULD THE COLON BE SACRIFICED OR MAY IT BE REFORMED?’, *Journal of the American Medical Association*, 58(26), p. 1957. doi: 10.1001/jama.1917.04270060365003.

Kietzman, C. C. *et al.* (2016) ‘Dynamic capsule restructuring by the main pneumococcal autolysin LytA in response to the epithelium’, *Nature Communications*, 7, p. 10859. doi: 10.1038/ncomms10859.

Kim, D. *et al.* (2016) ‘Nod2-mediated recognition of the microbiota is critical for mucosal adjuvant activity of cholera toxin’, *Nature Medicine*, 22(5), pp. 524–530. doi: 10.1038/nm.4075.

King, S. J., Hippe, K. R. and Weiser, J. N. (2006) ‘Deglycosylation of human glycoconjugates by the sequential activities of exoglycosidases expressed by Streptococcus pneumoniae’, *Molecular microbiology*, 59(3), pp. 961–974. doi: 10.1111/j.1365-2958.2005.04984.x.

Kirkeby, L. *et al.* (2000) ‘Immunoglobulins in Nasal Secretions of Healthy Humans: Structural Integrity of Secretory Immunoglobulin A1 (IgA1) and Occurrence of Neutralizing Antibodies to IgA1 Proteases of Nasal Bacteria’, *Clinical and Vaccine Immunology*, 7(1), pp. 31–39. doi: 10.1128/cdli.7.1.31-39.2000.

Kiser, K. B., Cantey-Kiser, J. M. and Lee, J. C. (1999) ‘Development and characterization of a Staphylococcus aureus nasal colonization model in mice’, *Infection and immunity*, 67(10), pp. 5001–5006. Available at: https://www.ncbi.nlm.nih.gov/pubmed/10496870.

Kissick, H. T. *et al.* (2014) 'The scavenger receptor MARCO modulates TLR-induced responses in dendritic cells', *PLoS ONE*, 9(8), p. e0104148. doi: 10.1371/journal.pone.0104148.

Kitada, K. and Oho, T. (2012) 'Effect of saliva viscosity on the co-aggregation between oral streptococci and Actinomyces naeslundii', *Gerodontology*, 29(2), pp. e981-7. doi: 10.1111/j.1741-2358.2011.00595.x.

Kraft, B. D. *et al.* (2014) 'Development of a novel preclinical model of pneumococcal pneumonia in nonhuman primates', *American journal of respiratory cell and molecular biology*, 50(5), pp. 995–1004. doi: 10.1165/rcmb.2013-0340oc.

Krishnan, S. *et al.* (2018) 'Amphiregulin-producing γδ T cells are vital for safeguarding oral barrier immune homeostasis', *Proceedings of the National Academy of Sciences*, 115(42), pp. 10738–10743. doi: 10.1073/pnas.1802320115.

Krone, C. L. *et al.* (2013) 'Impaired innate mucosal immunity in aged mice permits prolonged Streptococcus pneumoniae colonization', *Infect Immun*, 81(12), pp. 4615–25. doi: 10.1128/IAI.00618-13.

Krone, C. L. *et al.* (2014) 'Respiratory microbiota dynamics following Streptococcus pneumoniae acquisition in young and elderly mice.', *Infection and immunity*, 82(4), pp. 1725–31. doi: 10.1128/IAI.01290-13.

Kuczynski, J. *et al.* (2012) 'Experimental and analytical tools for studying the human microbiome', *Nature Reviews Genetics*, 13(1), pp. 47–58. doi:

10.1038/nrg3129.

Lau, J. T. *et al.* (2016) 'Capturing the diversity of the human gut microbiota through culture-enriched molecular profiling', *Genome Medicine*, 8(1), p. 72. doi: 10.1186/s13073-016-0327-7.

Laufer, A. S. *et al.* (2011) 'Microbial communities of the upper respiratory tract and otitis media in children', *mBio*, 2(1), pp. e00245-10. doi: 10.1128/mBio.00245-10.

Laurenzi, G. A., Potter, R. T. and Kass, E. H. (1961) 'Bacteriologic Flora of the Lower Respiratory Tract', *The New England Journal of Medicine*, 265(26), pp. 1273–1278. doi: 10.1056/nejm196112282652601.

Lavin, Y. *et al.* (2014) 'Tissue-Resident Macrophage Enhancer Landscapes Are Shaped by the Local Microenvironment', *Cell*, 159(6), pp. 1312–1326. doi: 10.1016/j.cell.2014.11.018.

LeBlanc, J. J. *et al.* (2017) 'Burden of vaccine-preventable pneumococcal disease in hospitalized adults: A Canadian Immunization Research Network (CIRN) Serious Outcomes Surveillance (SOS) network study', *Vaccine*, 35(29), pp. 3647–3654. doi: 10.1016/j.vaccine.2017.05.049.

Letunic, I. and Bork, P. (2016) 'Interactive tree of life (iTOL) v3: an online tool for the display and annotation of phylogenetic and other trees', *Nucleic acids research*, 44(W1), pp. W242–W245. doi: 10.1093/nar/gkw290.

Lewis, A. L. and Lewis, W. G. (2012) 'Mucosal sialoglycans and bacterial sialidases', *Cellular Microbiology*, 14(8), pp. 1174–1182. doi: 10.1111/j.1462-

5822.2012.01807.x.

Li, L. *et al.* (2013) 'Comparison among nasopharyngeal swab, nasal wash, and oropharyngeal swab for respiratory virus detection in adults with acute pharyngitis', *BMC Infectious Diseases*, 13(1), p. 281. doi: 10.1186/1471-2334-13-281.

Li, W. *et al.* (2014) 'Molecular characterization of skin microbiota between cancer cachexia patients and healthy volunteers.', *Microbial ecology*, 67(3), pp. 679–689. doi: 10.1007/s00248-013-0345-6.

Li, Y. *et al.* (2013) 'Surface charge of Streptococcus pneumoniae predicts serotype distribution', *Infection and Immunity*, 81(12), pp. 4519–4524. doi: 10.1128/IAI.00724-13.

Limoli, D. H. *et al.* (2011) 'BgaA acts as an adhesin to mediate attachment of some pneumococcal strains to human epithelial cells', *Microbiology (Reading, England)*, 157(Pt 8), pp. 2369–2381. doi: 10.1099/mic.0.045609-0.

von Linstow, M. L. *et al.* (2013) 'Neonatal airway colonization is associated with troublesome lung symptoms in infants', *Am J Respir Crit Care Med*, 188(8), pp. 1041–2. doi: 10.1164/rccm.201302-0395LE.

Liu, W. T. *et al.* (1997) 'Characterization of microbial diversity by determining terminal restriction fragment length polymorphisms of genes encoding 16S rRNA', *Applied and environmental microbiology*, 63(11), pp. 4516–4522. Available at: https://www.ncbi.nlm.nih.gov/pubmed/9361437.

Lombard, V. *et al.* (2014) 'The carbohydrate-active enzymes database (CAZy) in

2013', *Nucleic Acids Research*, 42, pp. D490-5. doi: 10.1093/nar/gkt1178.

Lozupone, C., Hamady, M. and Knight, R. (2006) 'UniFrac--an online tool for comparing microbial community diversity in a phylogenetic context.', *BMC bioinformatics*, 7, p. 371. doi: 10.1186/1471-2105-7-371.

Lu, L. *et al.* (2008) 'Species-Specific Interaction of Streptococcus pneumoniae with Human Complement Factor H', *The Journal of Immunology*, 181(10), pp. 7138–7146. doi: 10.4049/jimmunol.181.10.7138.

Lysenko, E. S. *et al.* (2005) 'The role of innate immune responses in the outcome of interspecies competition for colonization of mucosal surfaces', *PLoS Pathog*, 1(1), p. e1. doi: 10.1371/journal.ppat.0010001.

MacPherson, C. W. *et al.* (2017) 'Genome-Wide Immune Modulation of TLR3-Mediated Inflammation in Intestinal Epithelial Cells Differs between Single and Multi-Strain Probiotic Combination', *PLOS ONE*, 12(1), p. e0169847. doi: 10.1371/journal.pone.0169847.

Mandal, S. *et al.* (2015) 'Analysis of composition of microbiomes: a novel method for studying microbial composition', *Microbial Ecology in Health & Disease*, 26, p. 27663. doi: 10.3402/mehd.v26.27663.

Mardis, E. R. (2011) 'A decade's perspective on DNA sequencing technology', *Nature*, 470(7333), pp. 198–203. doi: 10.1038/nature09796.

Margolis, E., Yates, A. and Levin, B. R. (2010) 'The ecology of nasal colonization of streptococcus pneumoniae, haemophilus influenzae and staphylococcus aureus: The role of competition and interactions with host's immune response',

BMC Microbiology, 10, p. 59. doi: 10.1186/1471-2180-10-59.

Marik, P. E. and Kaplan, D. (2003) 'Aspiration pneumonia and dysphagia in the elderly', *Chest*, 124(1), pp. 328–336. doi: 10.1378/chest.124.1.328.

Marks, L. R. *et al.* (2013) 'Interkingdom Signaling Induces Streptococcus pneumoniae Biofilm Dispersion and Transition from Asymptomatic Colonization to Disease', *mBio*, 4(4), pp. e00438-13. doi: 10.1128/mbio.00438-13.

Martin, M. (2011) 'Cutadapt removes adapter sequences from high-throughput sequencing reads', *EMBnet.journal*, 17(1), p. 10. doi: 10.14806/ej.17.1.200.

McCombs, J. E. and Kohler, J. J. (2016) 'Pneumococcal Neuraminidase Substrates Identified through Comparative Proteomics Enabled by Chemoselective Labeling', *Bioconjugate Chemistry*, 27(4), pp. 1013–1022. doi: 10.1021/acs.bioconjchem.6b00050.

McCullers, J. A. and Bartmess, K. C. (2003) 'Role of Neuraminidase in Lethal Synergism between Influenza Virus and Streptococcus pneumoniae', *The Journal of Infectious Diseases*, 187(6), pp. 1000–1009. doi: 10.1086/368163.

McCullers, J. A. and Rehg, J. E. (2002) 'Lethal Synergism between Influenza Virus and Streptococcus pneumoniae: Characterization of a Mouse Model and the Role of Platelet-Activating Factor Receptor', *The Journal of Infectious Diseases*, 186(3), pp. 341–350. doi: 10.1086/341462.

McFall-Ngai, M. *et al.* (2013) 'Animals in a bacterial world, a new imperative for the life sciences', *Proceedings of the National Academy of Sciences*, 110(9), pp. 3229–3236. doi: 10.1073/pnas.1218525110.

McMurdie, P. J. and Holmes, S. (2013) ‘phyloseq: an R package for reproducible interactive analysis and graphics of microbiome census data’, *PLOS ONE*. 2013/05/01, 8(4), p. e61217. doi: 10.1371/journal.pone.0061217.

Memish, Z. A. *et al.* (2015) ‘Impact of the Hajj on pneumococcal transmission’, *Clinical microbiology and infection : the official publication of the European Society of Clinical Microbiology and Infectious Diseases*, 21(1), pp. e11-18. doi: 10.1016/j.cmi.2014.07.005.

Metchnikoff, E. (1891) ‘Etudes sure l’immunité’, *Ann Inst Pasteur (Paris*, 5, pp. 465–478. Available at: https://www.biodiversitylibrary.org/item/22256#page/497/mode/1up.

Metchnikoff, E. and Williams, H. S. (1912) ‘Why not live forever’, *Cosmopolitan*, 53(5), pp. 436–46. Available at: http://scholar.google.com/scholar?q=Why not live forever&btnG=&hl=en&num=20&as_sdt=0%2C22.

Mika, M. *et al.* (2016) ‘The nasal microbiota in infants with cystic fibrosis in the first year of life: a prospective cohort study’, *Lancet Respir Med*, 4(8), pp. 627–63. doi: 10.1016/S2213-2600(16)30081-9.

Mirza, S. *et al.* (2016) ‘The effects of differences in pspA alleles and capsular types on the resistance of Streptococcus pneumoniae to killing by apolactoferrin.’, *Microbial pathogenesis*, 99, pp. 209–219. doi: 10.1016/j.micpath.2016.08.029.

Misharin, A. V. *et al.* (2013) ‘Flow cytometric analysis of macrophages and dendritic cell subsets in the mouse lung’, *American Journal of Respiratory Cell*

and Molecular Biology, 49(4), pp. 503–510. doi: 10.1165/rcmb.2013-0086MA.

Misharin, A. V. *et al.* (2017) 'Monocyte-derived alveolar macrophages drive lung fibrosis and persist in the lung over the life span', *The Journal of Experimental Medicine*, 214(8), pp. 2387–2404. doi: 10.1084/jem.20162152.

Møller, M. E. *et al.* (2017) 'Sinus bacteriology in patients with cystic fibrosis or primary ciliary dyskinesia: A systematic review', *American Journal of Rhinology and Allergy*, 31(5), pp. 293–298. doi: 10.2500/ajra.2017.31.4461.

Moncla, B. J. and Braham, P. (1989) 'Detection of sialidase (neuraminidase) activity in Actinomyces species by using 2'-(4-methylumbelliferyl)alpha-D-N-acetylneuraminic acid in a filter paper spot test', *Journal of clinical microbiology*, 27(1), pp. 182–184. Available at: https://www.ncbi.nlm.nih.gov/pubmed/2643620.

Moon, C. *et al.* (2015) 'Vertically transmitted faecal IgA levels determine extra-chromosomal phenotypic variation', *Nature*, 521(7550), pp. 90–93. doi: 10.1038/nature14139.

Morens, D. M., Taubenberger, J. K. and Fauci, A. S. (2008) 'Predominant Role of Bacterial Pneumonia as a Cause of Death in Pandemic Influenza: Implications for Pandemic Influenza Preparedness', *The Journal of Infectious Diseases*, 198(7), pp. 962–970. doi: 10.1086/591708.

Morris, A. *et al.* (2013) 'Comparison of the respiratory microbiome in healthy nonsmokers and smokers', *Am J Respir Crit Care Med*, 187(10), pp. 1067–75. doi: 10.1164/rccm.201210-1913OC.

Morrow, A. *et al.* (2007) 'The burden of pneumococcal disease in the Canadian

population before routine use of the seven-valent pneumococcal conjugate vaccine', *Canadian Journal of Infectious Diseases and Medical Microbiology*, 18(2), pp. 121–127. doi: 10.1155/2007/713576.

Muyzer, G., de Waal, E. C. and Uitterlinden, A. G. (1993) 'Profiling of complex microbial populations by denaturing gradient gel electrophoresis analysis of polymerase chain reaction-amplified genes coding for 16S rRNA.', *Applied and environmental microbiology*, 59(3), pp. 695–700. Available at: https://www.ncbi.nlm.nih.gov/pubmed/7683183.

Natividad, J. M. M. *et al.* (2012) 'Commensal and Probiotic Bacteria Influence Intestinal Barrier Function and Susceptibility to Colitis in Nod1−/−;Nod2−/− Mice', *Inflammatory Bowel Diseases*, 18(8), pp. 1434–1446. doi: 10.1002/ibd.22848.

Nayfach, S. *et al.* (2019) 'New insights from uncultivated genomes of the global human gut microbiome', *Nature*, 568(7753), pp. 505–510. doi: 10.1038/s41586-019-1058-x.

Nelson, A. L. *et al.* (2007) 'Capsule enhances pneumococcal colonization by limiting mucus-mediated clearance', *Infection and Immunity*, 75(1), pp. 83–90. doi: 10.1128/IAI.01475-06.

Ngo, C. C. *et al.* (2016) 'Predominant Bacteria Detected from the Middle Ear Fluid of Children Experiencing Otitis Media: A Systematic Review', *PloS one*, 11(3), p. e0150949. doi: 10.1371/journal.pone.0150949.

van Nimwegen, F. A. *et al.* (2011) 'Mode and place of delivery, gastrointestinal microbiota, and their influence on asthma and atopy.', *The Journal of allergy and*

clinical immunology, 128(5), pp. 948-55.e1–3. doi: 10.1016/j.jaci.2011.07.027.

Nishikawa, T. *et al.* (2012) 'Bacterial Neuraminidase Rescues Influenza Virus Replication from Inhibition by a Neuraminidase Inhibitor', *PLoS ONE*. Edited by S. Pöhlmann, 7(9), p. e45371. doi: 10.1371/journal.pone.0045371.

Nöllmann, M. *et al.* (2004) 'The Role of Cholesterol in the Activity of Pneumolysin, a Bacterial Protein Toxin', *Biophysical Journal*, 86(5), pp. 3141–3151. doi: 10.1016/s0006-3495(04)74362-3.

Norin, E. and Midtvedt, T. (2010) 'Intestinal microflora functions in laboratory mice claimed to harbor a "normal" intestinal microflora. Is the SPF concept running out of date?', *Anaerobe*, 16(3), pp. 311–313. doi: 10.1016/j.anaerobe.2009.10.006.

Numminen, E. *et al.* (2015) 'Climate induces seasonality in pneumococcal transmission', *Scientific Reports*. doi: 10.1038/srep11344.

Oksanen, J. *et al.* (2019) 'vegan: Community Ecology Package'. Available at: https://cran.r-project.org/package=vegan.

Orihuela, C. J. *et al.* (2004) 'Tissue-specific contributions of pneumococcal virulence factors to pathogenesis', *The Journal of infectious diseases*, 190(9), pp. 1661–1669. doi: 10.1086/424596.

Palacios, G. *et al.* (2009) 'Streptococcus pneumoniae Coinfection Is Correlated with the Severity of H1N1 Pandemic Influenza', *PLoS ONE*, 4(12), p. e0008540. doi: 10.1371/journal.pone.0008540.

Palma, G. De *et al.* (2015) 'Microbiota and host determinants of behavioural

phenotype in maternally separated mice', *Nature Communications*, 6(1), p. 7735. doi: 10.1038/ncomms8735.

Pasolli, E. *et al.* (2019) 'Extensive Unexplored Human Microbiome Diversity Revealed by Over 150,000 Genomes from Metagenomes Spanning Age, Geography, and Lifestyle', *Cell*, 176(3), pp. 649-662.e20. doi: 10.1016/j.cell.2019.01.001.

Peltola, V. T., Murti, K. G. and McCullers, J. A. (2005) 'Influenza Virus Neuraminidase Contributes to Secondary Bacterial Pneumonia', *The Journal of Infectious Diseases*, 192(2), pp. 249–257. doi: 10.1086/430954.

Peterson, J. *et al.* (2009) 'The NIH Human Microbiome Project', *Genome Research*, 19(12), pp. 2317–2323. doi: 10.1101/gr.096651.109.

Pettigrew, M. M. *et al.* (2011) 'Viral-bacterial interactions and risk of acute otitis media complicating upper respiratory tract infection', *Journal of clinical microbiology*, 49(11), pp. 3750–3755. doi: 10.1128/jcm.01186-11.

Pettigrew, M. M. *et al.* (2014) 'Dynamic Changes in the Streptococcus pneumoniae Transcriptome during Transition from Biofilm Formation to Invasive Disease upon Influenza A Virus Infection', *Infection and Immunity*, 82(11), pp. 4607–4619. doi: 10.1128/iai.02225-14.

Porter, J. R. (1976) 'Antony van Leeuwenhoek: tercentenary of his discovery of bacteria', *Bacteriological reviews*, 40(2), pp. 260–269. Available at: https://www.ncbi.nlm.nih.gov/pubmed/786250.

Pracht, D. *et al.* (2005) 'PavA of Streptococcus pneumoniae modulates

adherence, invasion, and meningeal inflammation', *Infection and immunity*, 73(5), pp. 2680–2689. doi: 10.1128/iai.73.5.2680-2689.2005.

Prevaes, S. M. *et al.* (2016) 'Development of the Nasopharyngeal Microbiota in Infants with Cystic Fibrosis', *Am J Respir Crit Care Med*, 193(5), pp. 504–15. doi: 10.1164/rccm.201509-1759OC.

Puchta, A. *et al.* (2014) 'Characterization of Inflammatory Responses During Intranasal Colonization with Streptococcus pneumoniae', *Journal of Visualized Experiments*, (83), p. e50490. doi: 10.3791/50490.

Puchta, A. *et al.* (2016) 'TNF Drives Monocyte Dysfunction with Age and Results in Impaired Anti-pneumococcal Immunity', *PLOS Pathogens*. Edited by D. J. Philpott, 12(1), p. e1005368. doi: 10.1371/journal.ppat.1005368.

Qin, J. *et al.* (2010) 'A human gut microbial gene catalogue established by metagenomic sequencing', *Nature*, 464(7285), pp. 59–65. doi: 10.1038/nature08821.

Quast, C. *et al.* (2013) 'The SILVA ribosomal RNA gene database project: improved data processing and web-based tools', *Nucleic acids research*, 41, pp. D590–D596. doi: 10.1093/nar/gks1219.

R Core Team (2018) 'R: A Language and Environment for Statistical Computing'. Vienna, Austria: R Foundation for Statistical Computing. Available at: https://www.r-project.org/.

Radin, J. N. *et al.* (2005) '-Arrestin 1 Participates in Platelet-Activating Factor Receptor-Mediated Endocytosis of Streptococcus pneumoniae', *Infection and*

Immunity, 73(12), pp. 7827–7835. doi: 10.1128/IAI.73.12.7827-7835.2005.

Rajendra, K. C. *et al.* (2017) 'Temporal upregulation of host surface receptors provides a window of opportunity for bacterial adhesion and disease', *Microbiology*, 163(4), pp. 421–430. doi: 10.1099/mic.0.000434.

Rasmussen, T. S. *et al.* (2019) 'Mouse Vendor Influence on the Bacterial and Viral Gut Composition Exceeds the Effect of Diet', *Viruses*, 11(5), p. 435. doi: 10.3390/v11050435.

Rayner, C. F. *et al.* (1995) 'Interaction of pneumolysin-sufficient and -deficient isogenic variants of Streptococcus pneumoniae with human respiratory mucosa', *Infection and immunity*, 63(2), pp. 442–447. Available at: https://www.ncbi.nlm.nih.gov/pubmed/7822008.

Reyes, L. F. *et al.* (2016) 'A Non-Human Primate Model of Severe Pneumococcal Pneumonia', *PLOS ONE*, 11(11), p. e0166092. doi: 10.1371/journal.pone.0166092.

Richard, A. L. *et al.* (2014) 'TLR2 Signaling Decreases Transmission of Streptococcus pneumoniae by Limiting Bacterial Shedding in an Infant Mouse Influenza A Co-infection Model', *PLoS Pathogens*, 10(8), p. e1004339. doi: 10.1371/journal.ppat.1004339.

Rigottier-Gois, L. (2013) 'Dysbiosis in inflammatory bowel diseases: the oxygen hypothesis', *The ISME Journal*, 7(7), pp. 1256–1261. doi: 10.1038/ismej.2013.80.

Rijneveld, A. W. *et al.* (2002) 'Urokinase Receptor Is Necessary for Adequate Host Defense Against Pneumococcal Pneumonia', *The Journal of Immunology*,

168(7), pp. 3507–3511. doi: 10.4049/jimmunol.168.7.3507.

Rijneveld, A. W. *et al.* (2004) 'Improved Host Defense against Pneumococcal Pneumonia in Platelet-Activating Factor Receptor–Deficient Mice', *The Journal of Infectious Diseases*, 189(4), pp. 711–716. doi: 10.1086/381392.

Roberts, S. A. and Freed, D. L. (1977) 'Neonatal IgA secretion enhanced by breast feeding', *Lancet*, 2(8048), p. 1131. doi: 10.1016/s0140-6736(77)90576-1.

Robertson, S. J. *et al.* (2019) 'Comparison of Co-housing and Littermate Methods for Microbiota Standardization in Mouse Models', *Cell Reports*, 27(6), pp. 1910-1919.e2. doi: 10.1016/j.celrep.2019.04.023.

Robinson, M. D., McCarthy, D. J. and Smyth, G. K. (2010) 'edgeR: a Bioconductor package for differential expression analysis of digital gene expression data', *Bioinformatics*, 26(1), pp. 139–140. doi: 10.1093/bioinformatics/btp616.

Roche, A. M. *et al.* (2015) 'Antibody blocks acquisition of bacterial colonization through agglutination', *Mucosal Immunology*, 8(1), pp. 176–185. doi: 10.1038/mi.2014.55.

Rogers, G. B. *et al.* (2006) 'Use of 16S rRNA gene profiling by terminal restriction fragment length polymorphism analysis to compare bacterial communities in sputum and mouthwash samples from patients with cystic fibrosis', *Journal of Clinical Microbiology*. doi: 10.1128/JCM.02282-05.

Romero-Steiner, S. *et al.* (1999) 'Reduction in functional antibody activity against Streptococcus pneumoniae in vaccinated elderly individuals highly correlates with

decreased IgG antibody avidity', *Clinical infectious diseases : an official publication of the Infectious Diseases Society of America*, 29(2), pp. 281–288. doi: 10.1086/520200.

Romero-Steiner, S. *et al.* (2003) 'Inhibition of Pneumococcal Adherence to Human Nasopharyngeal Epithelial Cells by Anti-PsaA Antibodies', *Clinical and Vaccine Immunology*, 10(2), pp. 246–251. doi: 10.1128/cdli.10.2.246-251.2003.

Rosshart, S. P. *et al.* (2017) 'Wild Mouse Gut Microbiota Promotes Host Fitness and Improves Disease Resistance', *Cell*, 171(5), pp. 1015-1028.e13. doi: 10.1016/j.cell.2017.09.016.

Round, J. L. and Mazmanian, S. K. (2009) 'The gut microbiota shapes intestinal immune responses during health and disease', *Nature Reviews Immunology*. doi: 10.1038/nri2515.

Russell, S. L. *et al.* (2012) 'Early life antibiotic-driven changes in microbiota enhance susceptibility to allergic asthma', *EMBO reports*, 13(5), pp. 440–447. doi: 10.1038/embor.2012.32.

Russell, S. L. *et al.* (2013) 'Perinatal antibiotic treatment affects murine microbiota, immune responses and allergic asthma', *Gut Microbes*, 4(2), pp. 158–164. doi: 10.4161/gmic.23567.

Sahin-Yilmaz, A. and Naclerio, R. M. (2011) 'Anatomy and Physiology of the Upper Airway', *Proceedings of the American Thoracic Society*, 8(1), pp. 31–39. doi: 10.1513/pats.201007-050RN.

Salter, S. J. *et al.* (2014) 'Reagent and laboratory contamination can critically

impact sequence-based microbiome analyses', *BMC Biology*, 12, p. 87. doi: 10.1186/s12915-014-0087-z.

Sanchez, C. J. *et al.* (2011) 'Streptococcus pneumoniae in Biofilms Are Unable to Cause Invasive Disease Due to Altered Virulence Determinant Production', *PLoS ONE*, 6(12), p. e0028738. doi: 10.1371/journal.pone.0028738.

Sandgren, A. *et al.* (2005) 'Virulence in mice of pneumococcal clonal types with known invasive disease potential in humans', *The Journal of infectious diseases*, 192(5), pp. 791–800. doi: 10.1086/432513.

Schliep, K. P. (2011) 'phangorn: Phylogenetic analysis in R', *Bioinformatics*, 27(4), pp. 592–593. doi: 10.1093/bioinformatics/btq706.

Schloss, P. D. *et al.* (2009) 'Introducing mothur: Open-Source, Platform-Independent, Community-Supported Software for Describing and Comparing Microbial Communities', *Applied and Environmental Microbiology*, 75(23), pp. 7537–7541. doi: 10.1128/AEM.01541-09.

Schloss, P. D. (2010) 'The Effects of Alignment Quality, Distance Calculation Method, Sequence Filtering, and Region on the Analysis of 16S rRNA Gene-Based Studies', *PLoS Computational Biology*. Edited by J. A. Eisen, 6(7), p. e1000844. doi: 10.1371/journal.pcbi.1000844.

Schneeman, T. A. *et al.* (2005) 'Regulation of the Polymeric Ig Receptor by Signaling through TLRs 3 and 4: Linking Innate and Adaptive Immune Responses', *The Journal of Immunology*, 175(1), pp. 376–384. doi: 10.4049/jimmunol.175.1.376.

Schneider, C. A., Rasband, W. S. and Eliceiri, K. W. (2012) 'NIH Image to ImageJ: 25 years of image analysis', *Nature Methods*, 9(7), pp. 671–675. doi: 10.1038/nmeth.2089.

Schuijt, T. J. *et al.* (2016) 'The gut microbiota plays a protective role in the host defence against pneumococcal pneumonia', *Gut*, 65(4), pp. 575–583. doi: 10.1136/gutjnl-2015-309728.

Segal, L. N. *et al.* (2013) 'Enrichment of lung microbiome with supraglottic taxa is associated with increased pulmonary inflammation', *Microbiome*, 1(1), p. 19. doi: 10.1186/2049-2618-1-19.

Segata, N. *et al.* (2011) 'Metagenomic biomarker discovery and explanation', *Genome biology*, 12(6), p. R60. doi: 10.1186/gb-2011-12-6-r60.

Selva, L. *et al.* (2009) 'Killing niche competitors by remote-control bacteriophage induction', *Proc Natl Acad Sci U S A*, 106(4), pp. 1234–8. doi: 10.1073/pnas.0809600106.

Shahangian, A. *et al.* (2009) 'Type I IFNs mediate development of postinfluenza bacterial pneumonia in mice', *J Clin Invest*, 119(7), pp. 1910–1920. doi: 10.1172/JCI35412.

Shak, J. R. *et al.* (2014) 'Impact of experimental human pneumococcal carriage on nasopharyngeal bacterial densities in healthy adults', *PLOS ONE*, 9(6), p. e0098829. doi: 10.1371/journal.pone.0098829.

Shen, P. *et al.* (2016) 'Cigarette Smoke Attenuates the Nasal Host Response to Streptococcus pneumoniae and Predisposes to Invasive Pneumococcal Disease

in Mice', *Infect Immun*, 84(5), pp. 1536–1547. doi: 10.1128/IAI.01504-15.

Sibley, C. D. *et al.* (2011) 'Culture Enriched Molecular Profiling of the Cystic Fibrosis Airway Microbiome', *PLoS ONE*. Edited by P. J. Planet, 6(7), p. e22702. doi: 10.1371/journal.pone.0022702.

Siegel, S. J., Roche, A. M. and Weiser, J. N. (2014) 'Influenza promotes pneumococcal growth during coinfection by providing host sialylated substrates as a nutrient source', *Cell Host Microbe*, 16(1), pp. 55–67. doi: 10.1016/j.chom.2014.06.005.

Siegel, S. J., Tamashiro, E. and Weiser, J. N. (2015) 'Clearance of Pneumococcal Colonization in Infants Is Delayed through Altered Macrophage Trafficking', *PLOS Pathogens*. Edited by C. J. Orihuela, 11(6), p. e1005004. doi: 10.1371/journal.ppat.1005004.

Siegel, S. J. and Weiser, J. N. (2015) 'Mechanisms of Bacterial Colonization of the Respiratory Tract', *Annual Review of Microbiology*, 69(1), pp. 425–444. doi: 10.1146/annurev-micro-091014-104209.

Simon, M. M. *et al.* (2013) 'A comparative phenotypic and genomic analysis of C57BL/6J and C57BL/6N mouse strains', *Genome Biology*, 14(7), p. R82. doi: 10.1186/gb-2013-14-7-r82.

Sluijs, K. F. van der *et al.* (2006) 'Involvement of the platelet-activating factor receptor in host defense against Streptococcus pneumoniae during postinfluenza pneumonia', *American Journal of Physiology-Lung Cellular and Molecular Physiology*, 290(1), pp. L194-9. doi: 10.1152/ajplung.00050.2005.

Smith, P. M. *et al.* (2013) 'The Microbial Metabolites, Short-Chain Fatty Acids, Regulate Colonic Treg Cell Homeostasis', *Science*, 341(6145), pp. 569–573. doi: 10.1126/science.1241165.

Sommer, J. U. *et al.* (2011) 'ENT manifestations in patients with primary ciliary dyskinesia: prevalence and significance of otorhinolaryngologic co-morbidities', *Eur Arch Otorhinolaryngol*, 268(3), pp. 383–8. doi: 10.1007/s00405-010-1341-9.

Southam, D. S. *et al.* (2002) 'Distribution of intranasal instillations in mice: effects of volume, time, body position, and anesthesia', *American Journal of Physiology-Lung Cellular and Molecular Physiology*, 282(4), pp. L833-9. doi: 10.1152/ajplung.00173.2001.

Stearns, J. C. *et al.* (2011) 'Bacterial biogeography of the human digestive tract', *Scientific Reports*, 1, p. 170. doi: 10.1038/srep00170.

Stearns, J. C. *et al.* (2015) 'Culture and molecular-based profiles show shifts in bacterial communities of the upper respiratory tract that occur with age.', *The ISME journal*, 9(5), pp. 1246–59. doi: 10.1038/ismej.2014.250.

de Steenhuijsen Piters, W. A. *et al.* (2016) 'Dysbiosis of upper respiratory tract microbiota in elderly pneumonia patients', *The ISME Journal*, 10(1), pp. 97–108. doi: 10.1038/ismej.2015.99.

Stewart, E. J. (2012) 'Growing Unculturable Bacteria', *Journal of Bacteriology*, 194(16), pp. 4151–4160. doi: 10.1128/JB.00345-12.

Sun, K. *et al.* (2004) 'An Important Role for Polymeric Ig Receptor-Mediated Transport of IgA in Protection against Streptococcus pneumoniae

Nasopharyngeal Carriage', *The Journal of Immunology*, 173(7), pp. 4576–4581. doi: 10.4049/jimmunol.173.7.4576.

Sun, K. and Metzger, D. W. (2008) 'Inhibition of pulmonary antibacterial defense by interferon-γ during recovery from influenza infection', *Nature Medicine*, 14(5), pp. 558–564. doi: 10.1038/nm1765.

Taylor, C. E. and Toms, G. L. (1984) 'Immunoglobulin concentrations in nasopharyngeal secretions', *Arch Dis Child*, 59(1), pp. 48–53. doi: 10.1136/adc.59.1.48.

Teo, S. M. *et al.* (2015) 'The infant nasopharyngeal microbiome impacts severity of lower respiratory infection and risk of asthma development', *Cell Host Microbe*, 17(5), pp. 704–15. doi: 10.1016/j.chom.2015.03.008.

Thevaranjan, N. *et al.* (2016) 'Streptococcus pneumoniae Colonization Disrupts the Microbial Community within the Upper Respiratory Tract of Aging Mice', *Infection and Immunity*. Edited by A. Camilli, 84(4), pp. 906–916. doi: 10.1128/IAI.01275-15.

Thevaranjan, N. *et al.* (2017) 'Age-Associated Microbial Dysbiosis Promotes Intestinal Permeability, Systemic Inflammation, and Macrophage Dysfunction', *Cell Host and Microbe*, 21(4), pp. 455–466. doi: 10.1016/j.chom.2017.03.002.

Thompson, G. R. and Trexler, P. C. (1971) 'Gastrointestinal structure and function in germ-free or gnotobiotic animals.', *Gut*, 12(3), pp. 230–235. doi: 10.1136/gut.12.3.230.

Thornton, C. S. *et al.* (2015) 'Prevalence and impact of Streptococcus

pneumoniae in adult cystic fibrosis patients: a retrospective chart review and capsular serotyping study', *BMC Pulmonary Medicine*, 15(1), p. 49. doi: 10.1186/s12890-015-0041-z.

Thurston, T. L. M. *et al.* (2012) 'Galectin 8 targets damaged vesicles for autophagy to defend cells against bacterial invasion', *Nature*, 482(7385), pp. 414–418. doi: 10.1038/nature10744.

Tocheva, A. S. *et al.* (2011) 'Declining serotype coverage of new pneumococcal conjugate vaccines relating to the carriage of Streptococcus pneumoniae in young children', *Vaccine*, 29(26), pp. 4400–4404. doi: 10.1016/j.vaccine.2011.04.004.

Tuomanen, E. I. (2000) 'Pathogenesis of pneumococcal inflammation: otitis media', *Vaccine*, 19 Suppl 1, pp. S38-40. Available at: https://www.ncbi.nlm.nih.gov/pubmed/11163461.

Uchiyama, S. *et al.* (2009) 'The surface-anchored NanA protein promotes pneumococcal brain endothelial cell invasion', *The Journal of experimental medicine*, 206(9), pp. 1845–1852. doi: 10.1084/jem.20090386.

Ulland, T. K. *et al.* (2016) 'Nlrp12 mutation causes C57BL/6J strain-specific defect in neutrophil recruitment', *Nature Communications*, 7(1), p. 13180. doi: 10.1038/ncomms13180.

Velazquez, E. M. *et al.* (2019) 'Endogenous Enterobacteriaceae underlie variation in susceptibility to Salmonella infection', *Nature Microbiology*, 4(6), pp. 1057–1064. doi: 10.1038/s41564-019-0407-8.

Venkataraman, A. *et al.* (2015) 'Application of a neutral community model to assess structuring of the human lung microbiome', *mBio*, 6(1), pp. e02284-14. doi: 10.1128/mBio.02284-14.

Verhelst, R. *et al.* (2004) 'Cloning of 16S rRNA genes amplified from normal and disturbed vaginal microflora suggests a strong association between Atopobium vaginae, Gardnerella vaginalis and bacterial vaginosis.', *BMC microbiology*, 4, p. 16. doi: 10.1186/1471-2180-4-16.

Verhoeven, D., Nesselbush, M. and Pichichero, M. E. (2013) 'Lower nasopharyngeal epithelial cell repair and diminished innate inflammation responses contribute to the onset of acute otitis media in otitis-prone children', *Med Microbiol Immunol*, 202(4), pp. 295–302. doi: 10.1007/s00430-013-0293-2.

Virolainen, A. *et al.* (1994) 'Comparison of PCR assay with bacterial culture for detecting Streptococcus pneumoniae in middle ear fluid of children with acute otitis media', *Journal of Clinical Microbiology*, 32(11), pp. 2667–2670. Available at: http://www.ncbi.nlm.nih.gov/pubmed/7852553 (Accessed: 27 July 2019).

Walter, N. D. *et al.* (2009) 'Holiday spikes in pneumococcal disease among older adults', *N Engl J Med*, 361(26), pp. 2584–2585. doi: 10.1056/NEJMc0904844.

Wang, H. *et al.* (2018) 'TLR4 deficiency reduces pulmonary resistance to Streptococcus pneumoniae in gut microbiota-disrupted mice', *PLoS ONE*, 13(12), p. e0209183. doi: 10.1371/journal.pone.0209183.

Wang, Q. *et al.* (2007) 'Naive Bayesian Classifier for Rapid Assignment of rRNA Sequences into the New Bacterial Taxonomy', *Applied and Environmental*

Microbiology, 73(16), pp. 5261–5267. doi: 10.1128/AEM.00062-07.

Wanner, A., Salathe, M. and O'Riordan, T. G. (1996) 'Mucociliary clearance in the airways', *Am J Respir Crit Care Med*, 154(6 Pt 1), pp. 1868–902. doi: 10.1164/ajrccm.154.6.8970383.

Warnes, G. R. *et al.* (2019) 'gplots: Various R Programming Tools for Plotting Data'. Available at: https://cran.r-project.org/package=gplots.

Webster, L. T. (1933) 'INHERITED AND ACQUIRED FACTORS IN RESISTANCE TO INFECTION II. A COMPARISON OF MICE INHERENTLY RESISTANT OR SUSCEPTIBLE TO BACILLUS ENTERITIDIS INFECTION WITH RESPECT TO FERTILITY, WEIGHT, AND SUSCEPTIBILITY TO VARIOUS ROUTES AND TYPES OF INFECTION', *The Journal of Experimental Medicine*, 57(5), pp. 819–843. doi: 10.1084/jem.57.5.819.

Wei, T. and Simko, V. (2017) 'R Package "corrplot": Visualization of a Correlation Matrix'. Available at: https://github.com/taiyun/corrplot.

Weiser, J. N. *et al.* (1994) 'Phase variation in pneumococcal opacity: Relationship between colonial morphology and nasopharyngeal colonization', *Infection and Immunity*, 62(6), pp. 2582–2589. Available at: http://www.ncbi.nlm.nih.gov/pubmed/8188381 (Accessed: 27 July 2019).

Weiser, J. N. *et al.* (2001) 'Changes in availability of oxygen accentuate differences in capsular polysaccharide expression by phenotypic variants and clinical isolates of Streptococcus pneumoniae', *Infection and Immunity*, 69(9), pp. 5430–5439. doi: 10.1128/IAI.69.9.5430-5439.2001.

Weiser, J. N. *et al.* (2003) 'Antibody-enhanced pneumococcal adherence requires IgA1 protease', *Proceedings of the National Academy of Sciences*, 100(7), pp. 4215–4220. doi: 10.1073/pnas.0637469100.

Weyrich, L. S. *et al.* (2014) 'Resident Microbiota Affect Bordetella pertussis Infectious Dose and Host Specificity', *Journal of Infectious Diseases*, 209(6), pp. 913–921. doi: 10.1093/infdis/jit597.

Whelan, F. J. *et al.* (2014) 'The loss of topography in the microbial communities of the upper respiratory tract in the elderly.', *Annals of the American Thoracic Society*, 11(4), pp. 513–21. doi: 10.1513/AnnalsATS.201310-351OC.

Wren, J. T. *et al.* (2017) 'Pneumococcal Neuraminidase A (NanA) Promotes Biofilm Formation and Synergizes with Influenza A Virus in Nasal Colonization and Middle Ear Infection', *Infection and Immunity*, 85(4), pp. e01044-16. doi: 10.1128/iai.01044-16.

Wu, H.-Y. *et al.* (1997) 'Establishment of aStreptococcus pneumoniaenasopharyngeal colonization model in adult mice', *Microbial Pathogenesis*, 23(3), pp. 127–137. doi: 10.1006/mpat.1997.0142.

Wyllie, A. L. *et al.* (2014) 'Streptococcus pneumoniae in saliva of Dutch primary school children', *PLoS ONE*, 9(7), p. 0102045. doi: 10.1371/journal.pone.0102045.

Xu, G. *et al.* (2011) 'Three Streptococcus pneumoniae Sialidases: Three Different Products', *Journal of the American Chemical Society*, 133(6), pp. 1718–1721. doi: 10.1021/ja110733q.

Yan, M. *et al.* (2013) 'Nasal microenvironments and interspecific interactions influence nasal microbiota complexity and S. aureus carriage', *Cell Host Microbe*, 14(6), pp. 631–640. doi: 10.1016/j.chom.2013.11.005.

Yende, S. *et al.* (2005) 'Preinfection systemic inflammatory markers and risk of hospitalization due to pneumonia', *Am J Respir Crit Care Med*, 172(11), pp. 1440–6. doi: 10.1164/rccm.200506-888OC.

Yissachar, N. *et al.* (2017) 'An Intestinal Organ Culture System Uncovers a Role for the Nervous System in Microbe-Immune Crosstalk', *Cell*, 168(6), pp. 1135–1148. doi: 10.1016/j.cell.2017.02.009.

Yu, G. *et al.* (2015) 'Nested PCR Biases in Interpreting Microbial Community Structure in 16S rRNA Gene Sequence Datasets', *PLOS ONE*. Edited by D. Ercolini, 10(7), p. e0132253. doi: 10.1371/journal.pone.0132253.

Yu, S. *et al.* (2008) 'Influence of nasal structure on the distribution of airflow in nasal cavity.', *Rhinology*, 46(2), pp. 137–143. Available at: https://www.ncbi.nlm.nih.gov/pubmed/18575016.

Yun, Y. *et al.* (2014) 'Environmentally determined differences in the murine lung microbiota and their relation to alveolar architecture', *PLOS ONE*, 9(12), p. e0113466. doi: 10.1371/journal.pone.0113466.

Zafar, M. A. *et al.* (2016) 'Infant Mouse Model for the Study of Shedding and Transmission during Streptococcus pneumoniae Monoinfection', *Infection and Immunity*, 84(9), pp. 2714–2722. doi: 10.1128/iai.00416-16.

Zeng, M. Y., Inohara, N. and Nuñez, G. (2017) 'Mechanisms of inflammation-

driven bacterial dysbiosis in the gut', *Mucosal Immunology*, 10(1), pp. 18–26. doi: 10.1038/mi.2016.75.

Zeppa, J. J. *et al.* (2016) 'Nasopharyngeal infection of mice with Streptococcus pyogenes and in vivo detection of superantigen activity', in *Methods in Molecular Biology*. doi: 10.1007/978-1-4939-3344-0_8.

Zhang, D. *et al.* (2015) 'Neutrophil ageing is regulated by the microbiome', *Nature*, 525, pp. 528–532. doi: 10.1038/nature15367.

Zhang, J. R. *et al.* (2000) 'The polymeric immunoglobulin receptor translocates pneumococci across nasopharyngeal human epithelial cells', *Cell*, 102(6), pp. 827–837. doi: 10.1016/S0092-8674(00)00071-4.

Zhang, Z., Clarke, T. B. and Weiser, J. N. (2009) 'Cellular effectors mediating Th17-dependent clearance of pneumococcal colonization in mice', *J Clin Invest*, 119(7), pp. 1899–909. doi: 10.1172/JCI36731.

Chapter 6: Figures and Tables

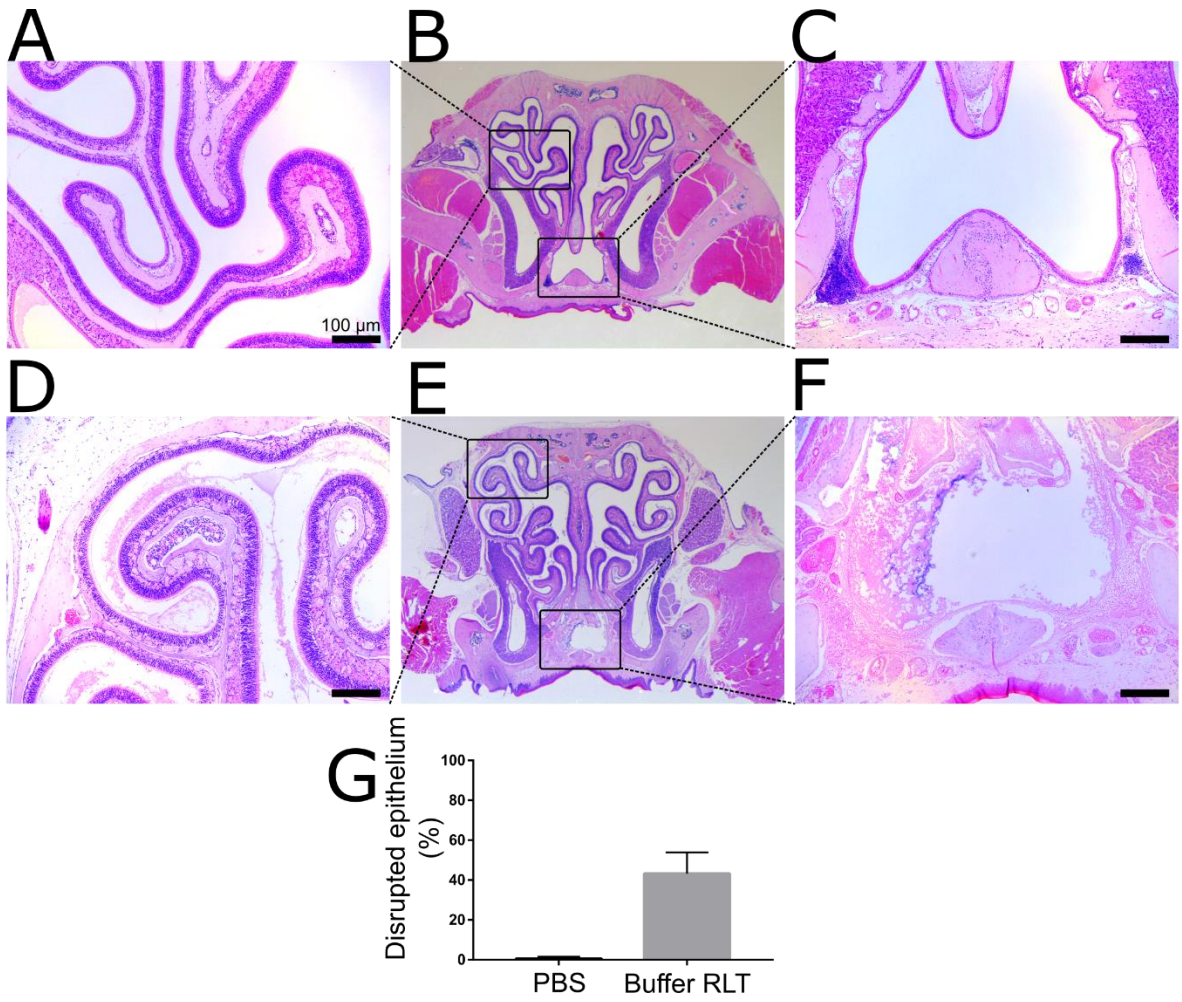

Figure 4– Nasal wash does not effectively sample the nasal turbinates.
Hematoxylin and eosin-stained cross-sections demonstrate that nasal washes with PBS do not disrupt the epithelial layer (A-C). Buffer RLT washes greatly disrupt the nasopharyngeal space (E&F) but not the nasal turbinates (D). Quantification of the disrupted epithelial lining demonstrates only half of the tissue is disrupted by Buffer RLT nasal washes, indicating that this space is assessed during nasal wash (G).

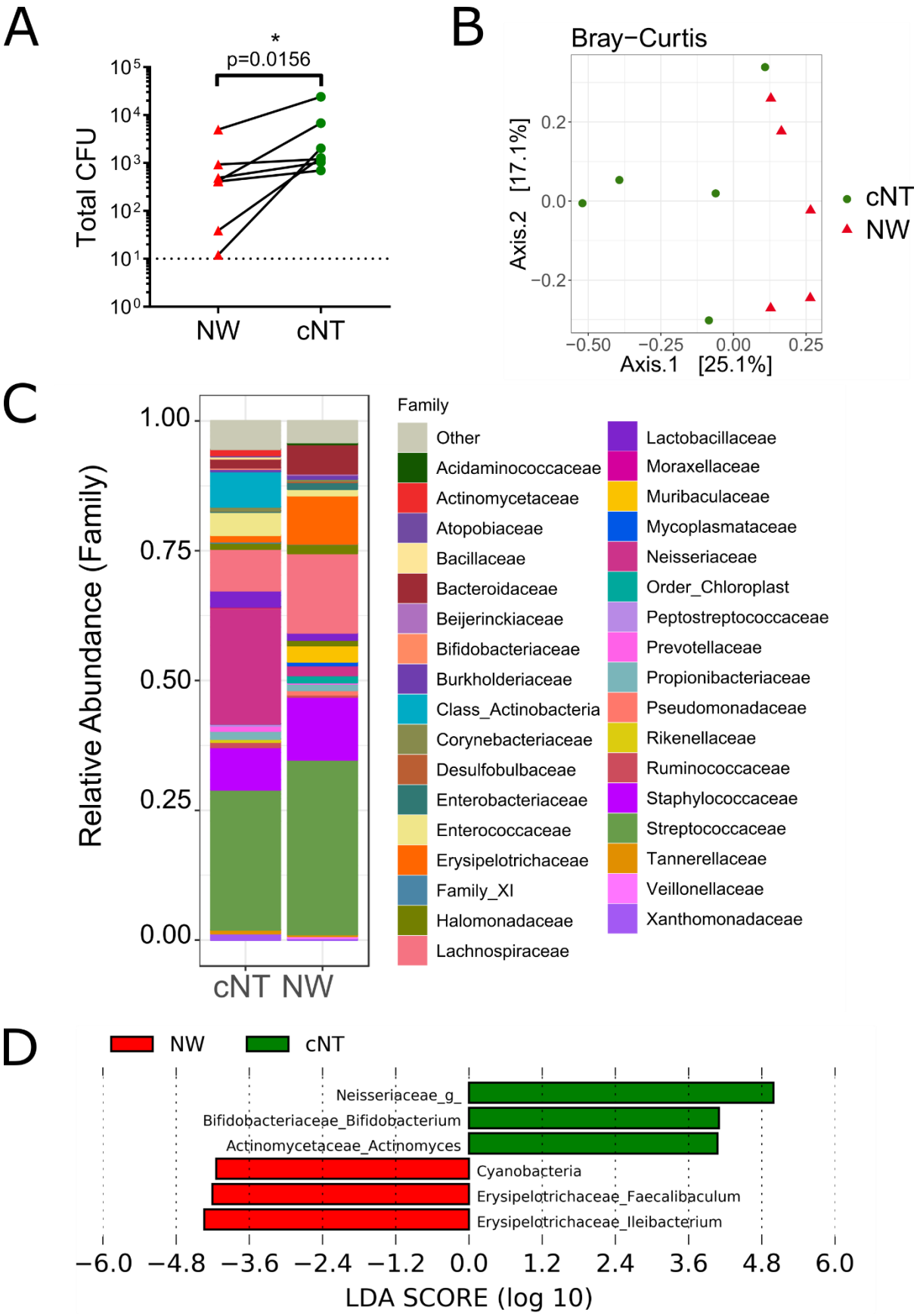
A
*
p=0.0156
Total CFU
NW
cNT
B
Bray−Curtis
Axis.2 [17.1%]
Axis.1 [25.1%]
cNT
NW
C
Relative Abundance (Family)
cNT NW
Family
Other
Acidaminococcaceae
Actinomycetaceae
Atopobiaceae
Bacillaceae
Bacteroidaceae
Beijerinckiaceae
Bifidobacteriaceae
Burkholderiaceae
Class_Actinobacteria
Corynebacteriaceae
Desulfobulbaceae
Enterobacteriaceae
Enterococcaceae
Erysipelotrichaceae
Family_XI
Halomonadaceae
Lachnospiraceae
Lactobacillaceae
Moraxellaceae
Muribaculaceae
Mycoplasmataceae
Neisseriaceae
Order_Chloroplast
Peptostreptococcaceae
Prevotellaceae
Propionibacteriaceae
Pseudomonadaceae
Rikenellaceae
Ruminococcaceae
Staphylococcaceae
Streptococcaceae
Tannerellaceae
Veillonellaceae
Xanthomonadaceae
D
NW
cNT
Neisseriaceae_g_
Bifidobacteriaceae_Bifidobacterium
Actinomycetaceae_Actinomyces
Cyanobacteria
Erysipelotrichaceae_Faecalibaculum
Erysipelotrichaceae_Ileibacterium
LDA SCORE (log 10)

Figure 5– Nasal tissue extraction is essential for complete microbiota assessment.

Nasal washes were collected, followed by tissue collection on the same mice, followed by V3 16S rRNA gene high throughput sequencing. Nasal tissue had significantly more bacteria than nasal washes (A). Nasal tissue microbial communities clustered separately from nasal wash communities (Bray-Curtis PERMANOVA, $p<0.05$) (B). Nasal tissue microbiota were enriched in Neisseriaceae, *Bifidobacterium*, and *Actinomyces*, while nasal washes were enriched in Erysipelotrichaceae and Cyanobacteria (C; LEfSe).

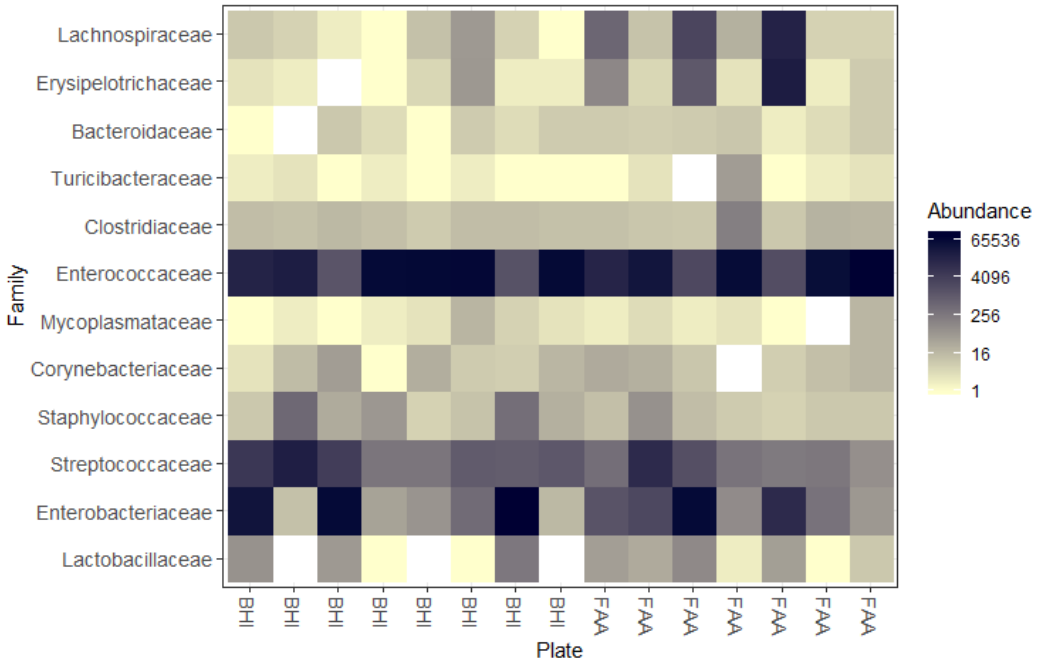

Figure 6 – Dominant bacterial groups in culture of SPF nasal microbiota. Nasal microbiota was cultivated on BHI and FAA plates and colonies were pooled into one DNA extraction tube per culture condition per mouse. Streptococcaceae, Enterococcaceae, Enterobacteraceae, Staphylococcaceae, and Corynebacteriaceae are commonly cultured across multiple mice. Colours are indicative of how many sequencings reads per sample were detected.

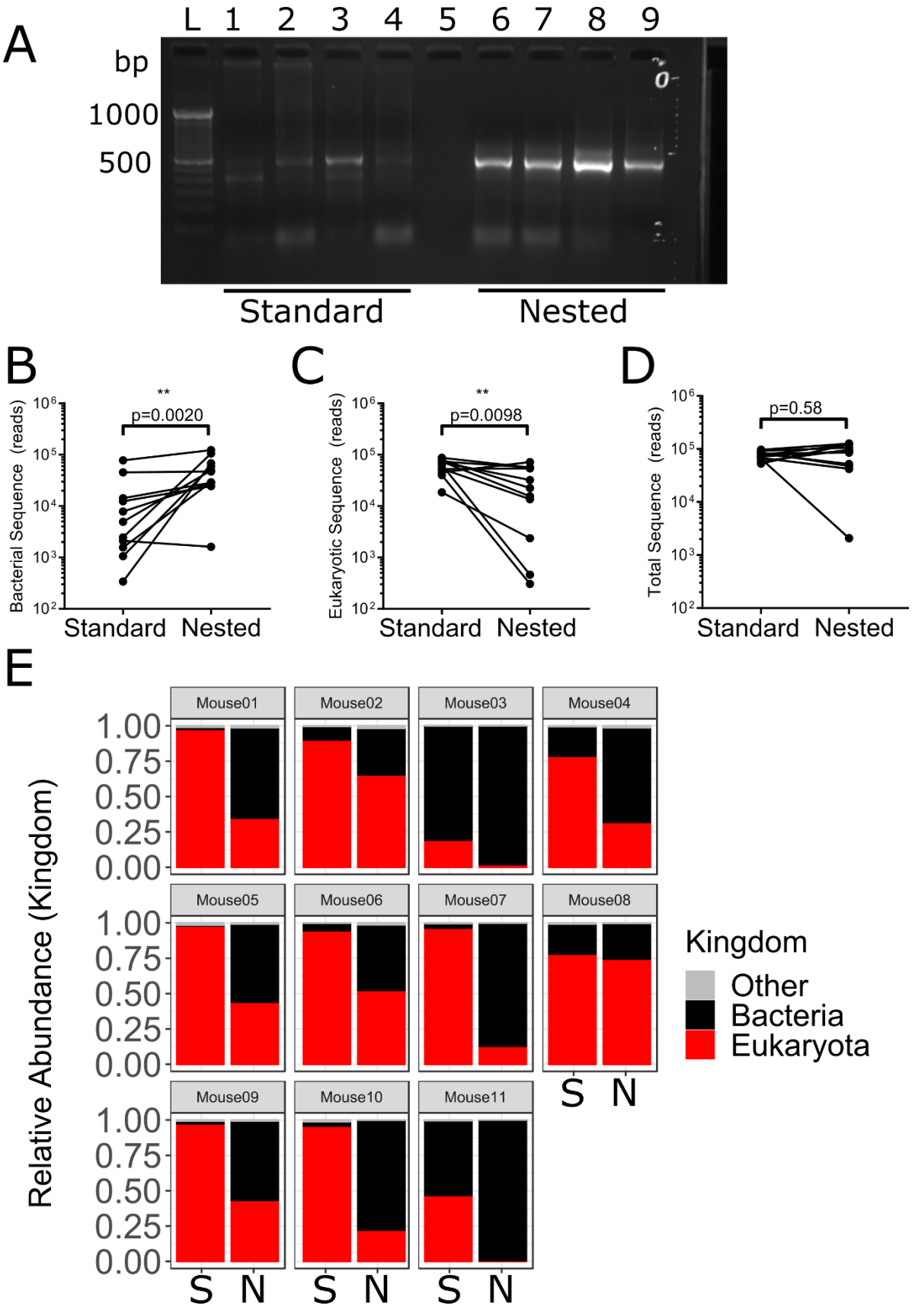
A
L 1 2 3 4 5 6 7 8 9
bp
1000
500
Standard
Nested
B
Bacterial Sequence (reads)
**
p=0.0020
Standard Nested
C
Eukaryotic Sequence (reads)
**
p=0.0098
Standard Nested
D
Total Sequence (reads)
p=0.58
Standard Nested
E
Relative Abundance (Kingdom)
Mouse01
Mouse02
Mouse03
Mouse04
Mouse05
Mouse06
Mouse07
Mouse08
Mouse09
Mouse10
Mouse11
1.00
0.75
0.50
0.25
0.00
S N
Kingdom
Other
Bacteria
Eukaryota

Figure 7 – Nested PCR improves bacterial read count in murine nasal tissue microbiota analysis.

DNA was extracted from murine nasal tissue and subjected to standard one-step or nested two-step PCR. (A) Nested PCR (lanes 6-9) improved yield of the expected band size compared to standard PCR (lanes 1-4). Nested PCR improved the number of bacterial reads (B) and decreased the eukaryotic reads (C) compared to standard PCR. Total reads were not different between standard and nested PCR (D). (E) Nested PCR (N) improved the relative abundance of bacterial reads in individual mouse samples compared to standard PCR (S). ** indicates significance $p<0.01$, Wilcoxon matched-pairs signed rank test.

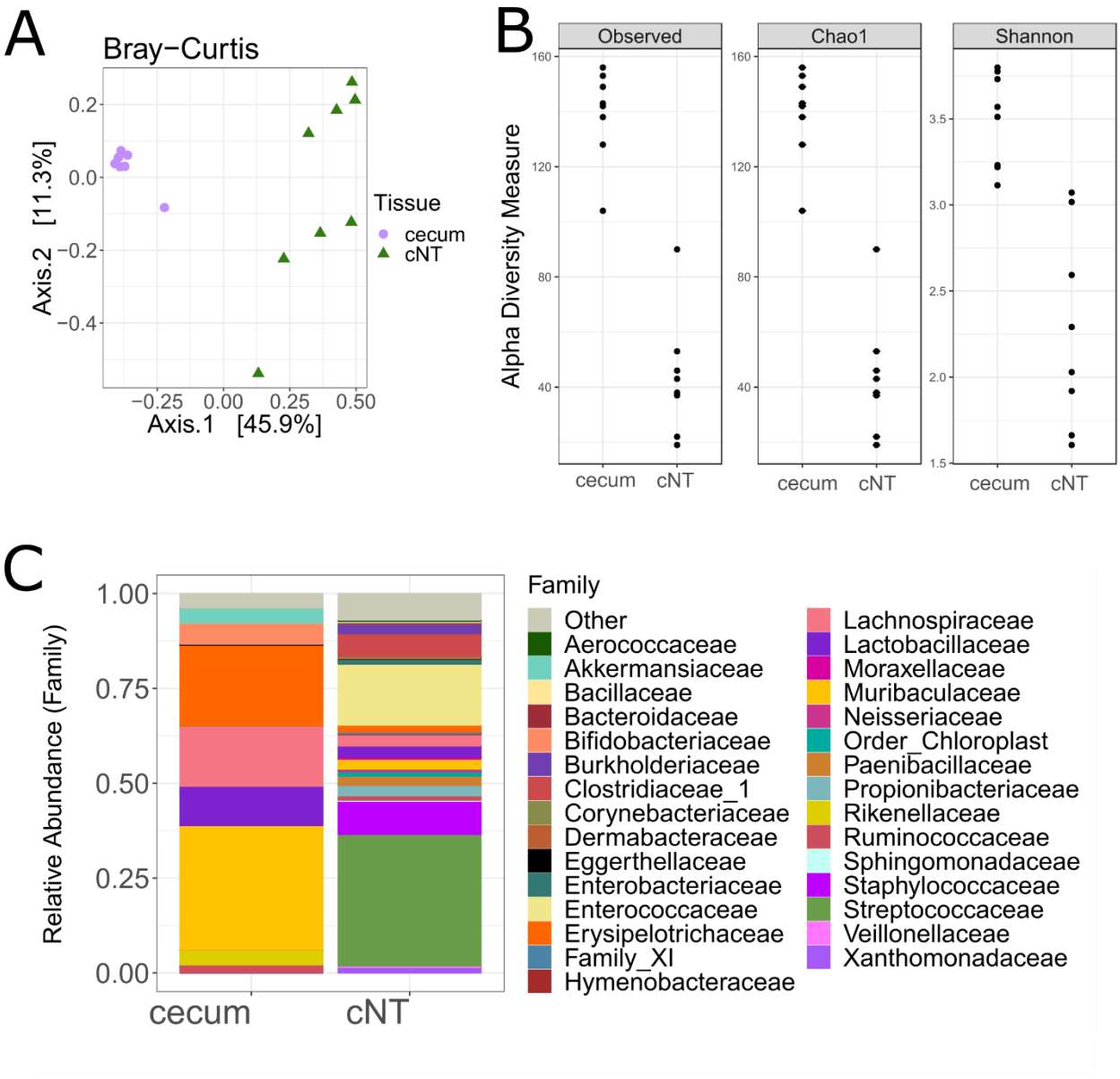

Figure 8 – Murine nasal microbiota is distinct from gut microbiota.

DNA was extracted from nasal and cecal tissues (N=9 mice) and the V3 region of the 16S rRNA gene was sequenced. (A) The microbial communities were distinct between the nasal and cecal microbiota (PERMANOVA $p<0.001$) . (B) The alpha-diversity metrics demonstrate greatly increased richness in the cecal microbiota compared to the nasal microbiota (Mann-Whitney test, $p<0.001$). (C) Taxa summary comparing the Family level identifications of cecal and nasal microbiota.

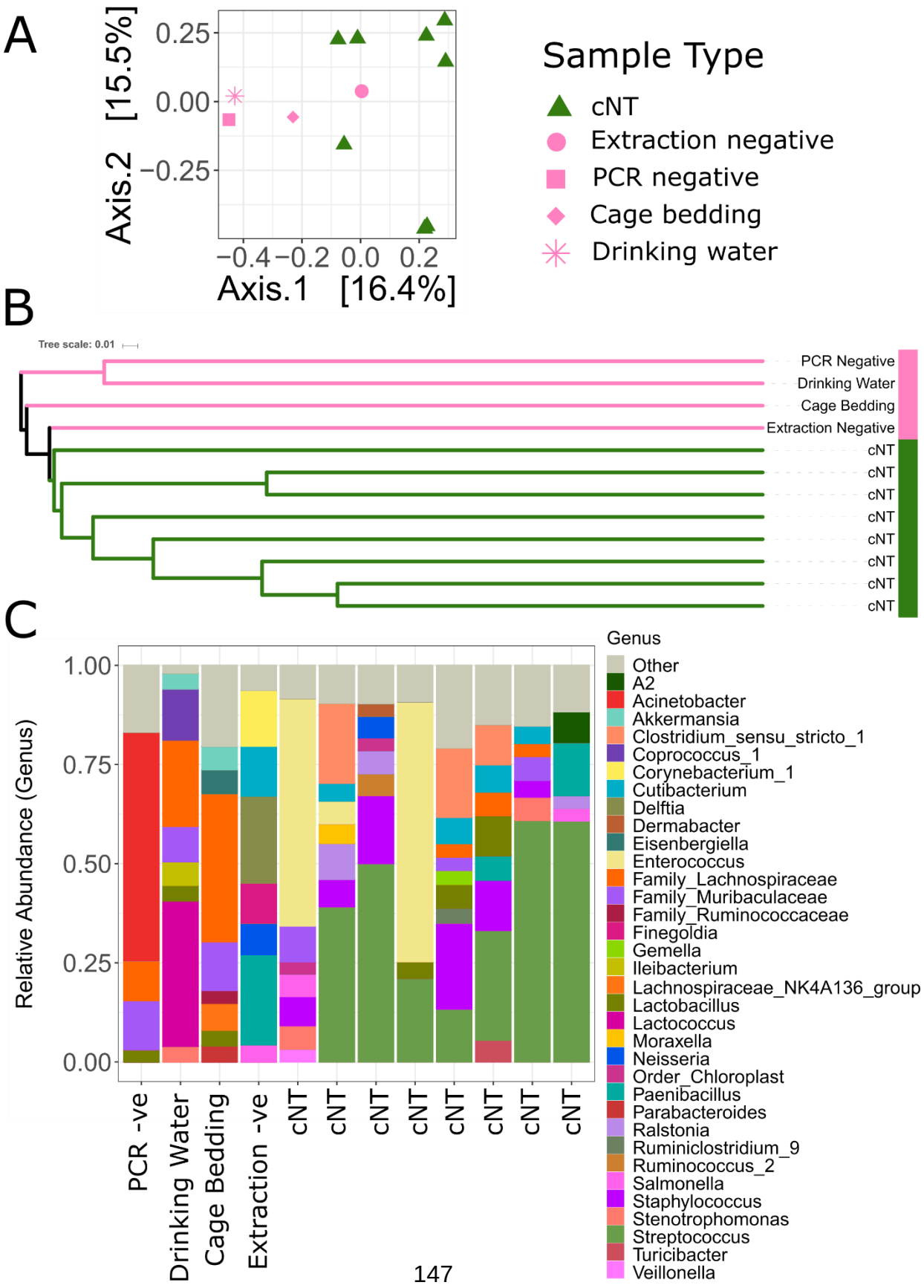
A
Axis.2 [15.5%]
0.25
0.00
−0.25
−0.4 −0.2 0.0 0.2
Axis.1 [16.4%]
Sample Type
cNT
Extraction negative
PCR negative
Cage bedding
Drinking water
B
Tree scale: 0.01
PCR Negative
Drinking Water
Cage Bedding
Extraction Negative
cNT
C
Relative Abundance (Genus)
1.00
0.75
0.50
0.25
0.00
PCR -ve
Drinking Water
Cage Bedding
Extraction -ve
Genus
Other
A2
Acinetobacter
Akkermansia
Clostridium_sensu_stricto_1
Coprococcus_1
Corynebacterium_1
Cutibacterium
Delftia
Dermabacter
Eisenbergiella
Enterococcus
Family_Lachnospiraceae
Family_Muribaculaceae
Family_Ruminococcaceae
Finegoldia
Gemella
Ileibacterium
Lachnospiraceae_NK4A136_group
Lactobacillus
Lactococcus
Moraxella
Neisseria
Order_Chloroplast
Paenibacillus
Parabacteroides
Ralstonia
Ruminiclostridium_9
Ruminococcus_2
Salmonella
Staphylococcus
Stenotrophomonas
Streptococcus
Turicibacter
Veillonella

Figure 9 – Sequencing and extraction negatives are distinct from nasal microbiota.

DNA was extracted from nasal tissues, bedding material, drinking water, PBS exposed to surgical tools, or water used in place of template prior to amplification and sequencing of the V3 region of the 16S rRNA gene. (A) The communities were distinct via Bray- Curtis PCoA (PERMANOVA $p<0.05$, $R^2 = 0.138$). (B) UPGMA tree based on Bray-Curtis distances demonstrate the negatives are distinct from the nasal tissue microbiota. (C) Taxonomic summaries of the negatives contain several different taxa compared to the nasal tissue.

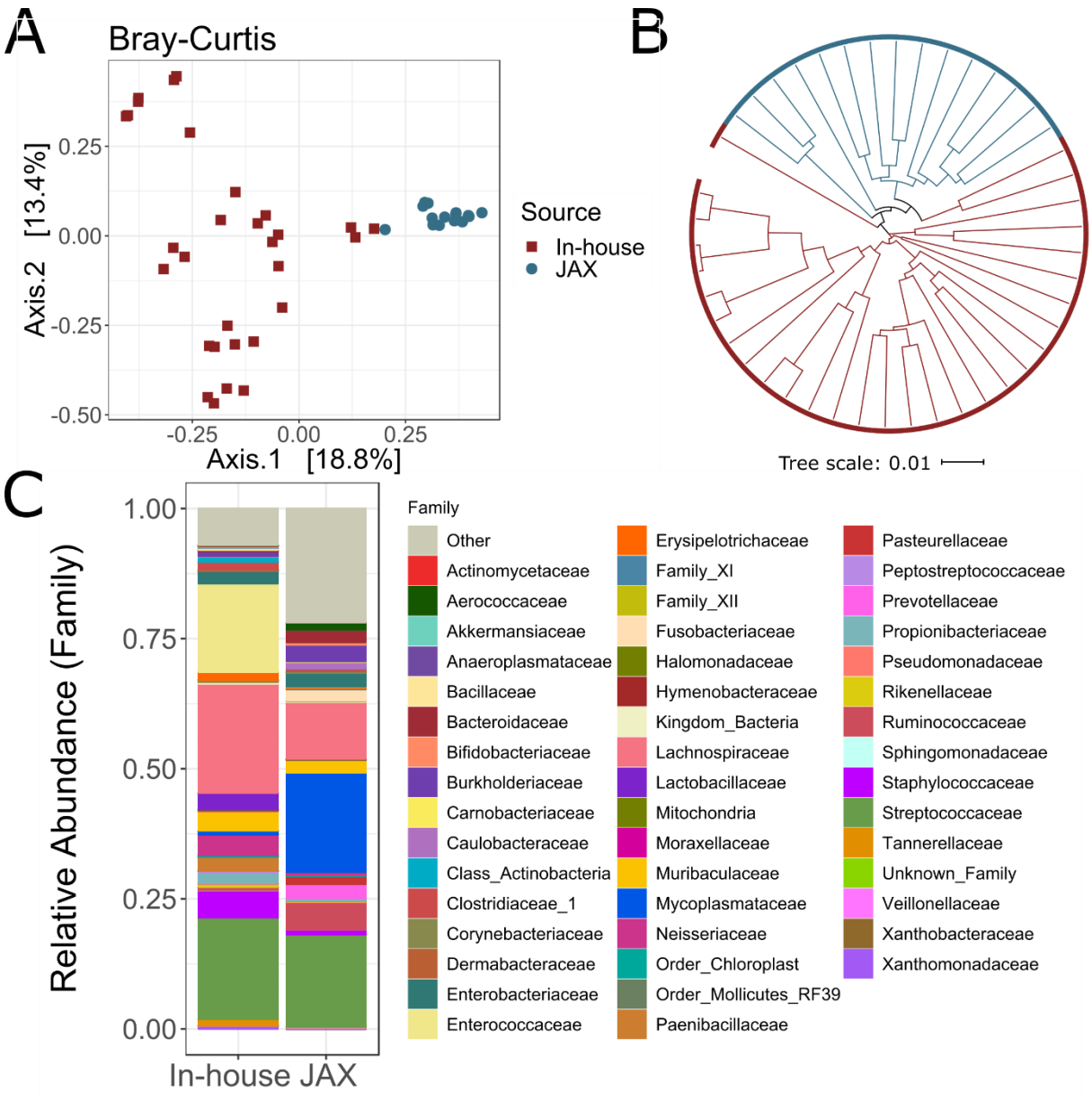
A
Bray-Curtis
Axis.2 [13.4%]
0.25
0.00
-0.25
-0.50
-0.25
0.00
0.25
Axis.1 [18.8%]
Source
In-house
JAX
B
Tree scale: 0.01
C
Relative Abundance (Family)
1.00
0.75
0.50
0.25
0.00
In-house JAX
Family
Other
Actinomycetaceae
Aerococcaceae
Akkermansiaceae
Anaeroplasmataceae
Bacillaceae
Bacteroidaceae
Bifidobacteriaceae
Burkholderiaceae
Carnobacteriaceae
Caulobacteraceae
Class_Actinobacteria
Clostridiaceae_1
Corynebacteriaceae
Dermabacteraceae
Enterobacteriaceae
Enterococcaceae
Erysipelotrichaceae
Family_XI
Family_XII
Fusobacteriaceae
Halomonadaceae
Hymenobacteraceae
Kingdom_Bacteria
Lachnospiraceae
Lactobacillaceae
Mitochondria
Moraxellaceae
Muribaculaceae
Mycoplasmataceae
Neisseriaceae
Order_Chloroplast
Order_Mollicutes_RF39
Paenibacillaceae
Pasteurellaceae
Peptostreptococcaceae
Prevotellaceae
Propionibacteriaceae
Pseudomonadaceae
Rikenellaceae
Ruminococcaceae
Sphingomonadaceae
Staphylococcaceae
Streptococcaceae
Tannerellaceae
Unknown_Family
Veillonellaceae
Xanthobacteraceae
Xanthomonadaceae
D
Observed
Shannon
Simpson
Alpha Diversity Measure
In-house JAX
In-house JAX
In-house JAX
E
Mycoplasma
Relative Abundance
In-house
Jackson
F
Lactobacillus
Relative Abundance
In-house
Jackson

Figure 10 – Source of mice impacts nasal microbiota composition.

The nasal microbiota of C57BL/6J ordered directly from Jackson Laboratories were compared to C57BL/6J mice bred in-house for several generations. JAX mice had a significantly distinct microbiota composition (A; PERMANOVA, $p<0.0001$). (B) Bray-Curtis distance tree demonstrates the clustering of mice from Jackson Laboratories compared to mice bred in-house. (C) Taxa summary at the Family level comparing nasal microbiota of in-house bred mice to JAX mice. (D) Alpha-diversity is increased in Jackson Laboratories murine nasal microbiota compared to in-house bred mice, as measured by Observed species, Chao1, and Shannon diversity (Mann-Whitney, $p<0.001$). LEfSe analysis revealed 109 genera within the nasal microbiota that were significantly different between in-house mice and Jackson Laboratories. The nasal microbiota of mice from Jackson were enriched in *Mycoplasma* (E) and decreased in *Lactobacillus* (F) species compared to mice bred in-house.

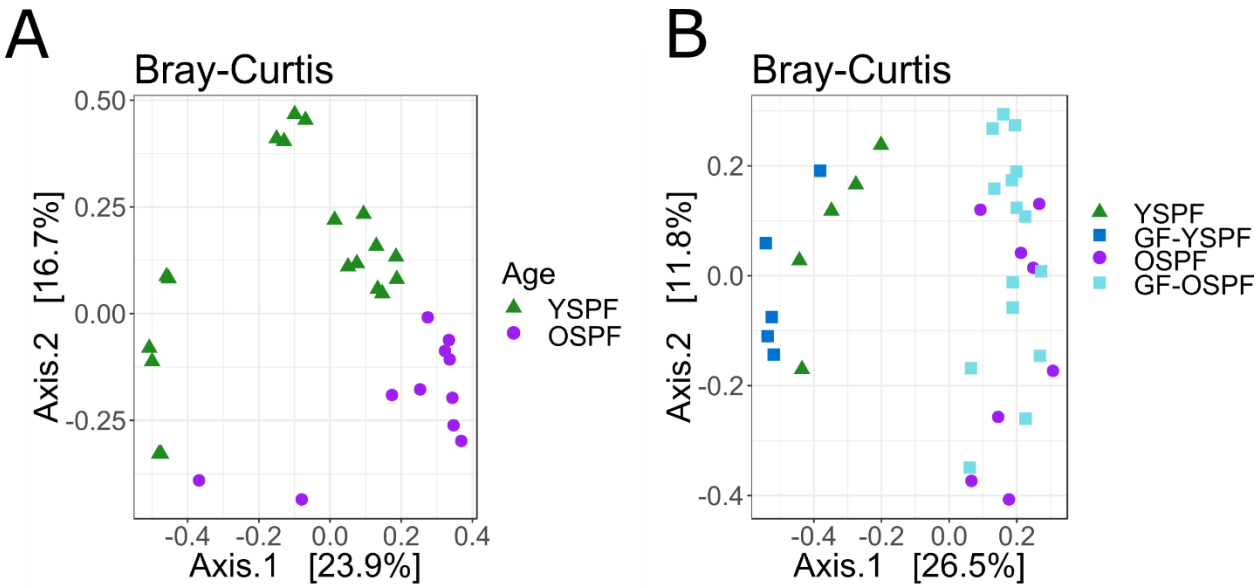
A
Bray-Curtis
0.50
0.25
0.00
-0.25
Axis.2 [16.7%]
-0.4 -0.2 0.0 0.2 0.4
Axis.1 [23.9%]
Age
YSPF
OSPF
B
Bray-Curtis
0.2
0.0
-0.2
-0.4
Axis.2 [11.8%]
-0.4 -0.2 0.0 0.2
Axis.1 [26.5%]
YSPF
GF-YSPF
OSPF
GF-OSPF

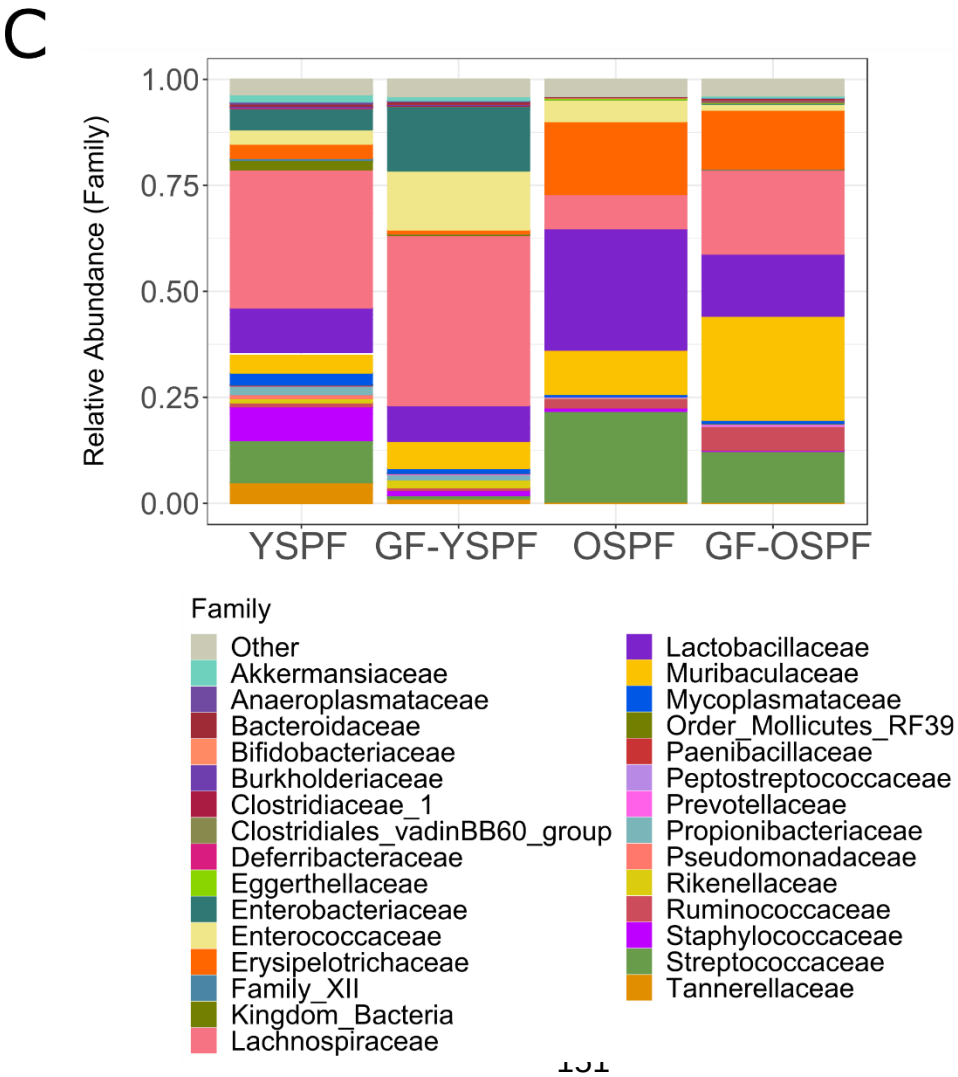
C
Relative Abundance (Family)
1.00
0.75
0.50
0.25
0.00
YSPF
GF-YSPF
OSPF
GF-OSPF
Family
Other
Akkermansiaceae
Anaeroplasmataceae
Bacteroidaceae
Bifidobacteriaceae
Burkholderiaceae
Clostridiaceae_1
Clostridiales_vadinBB60_group
Deferribacteraceae
Eggerthellaceae
Enterobacteriaceae
Enterococcaceae
Erysipelotrichaceae
Family_XII
Kingdom_Bacteria
Lachnospiraceae
Lactobacillaceae
Muribaculaceae
Mycoplasmataceae
Order_Mollicutes_RF39
Paenibacillaceae
Peptostreptococcaceae
Prevotellaceae
Propionibacteriaceae
Pseudomonadaceae
Rikenellaceae
Ruminococcaceae
Staphylococcaceae
Streptococcaceae
Tannerellaceae

Figure 11 – Young and old mice have distinct nasal microbiota, which can be transferred to germ-free mice by cohousing.

Nasal tissue was collected from young (3-4 months old) and old (18-22 months old) mice and the microbiota was measured via 16S rRNA gene sequencings. Community composition was distinct between young (green triangles) and old mice (purple circles) (A). When these mice were cohoused with germ-free mice (squares), the microbiota from young (dark blue) was still distinct from old (light blue) (B). Family level identification of bacteria demonstrate the similarities between the SPF and cohoused GF mice.

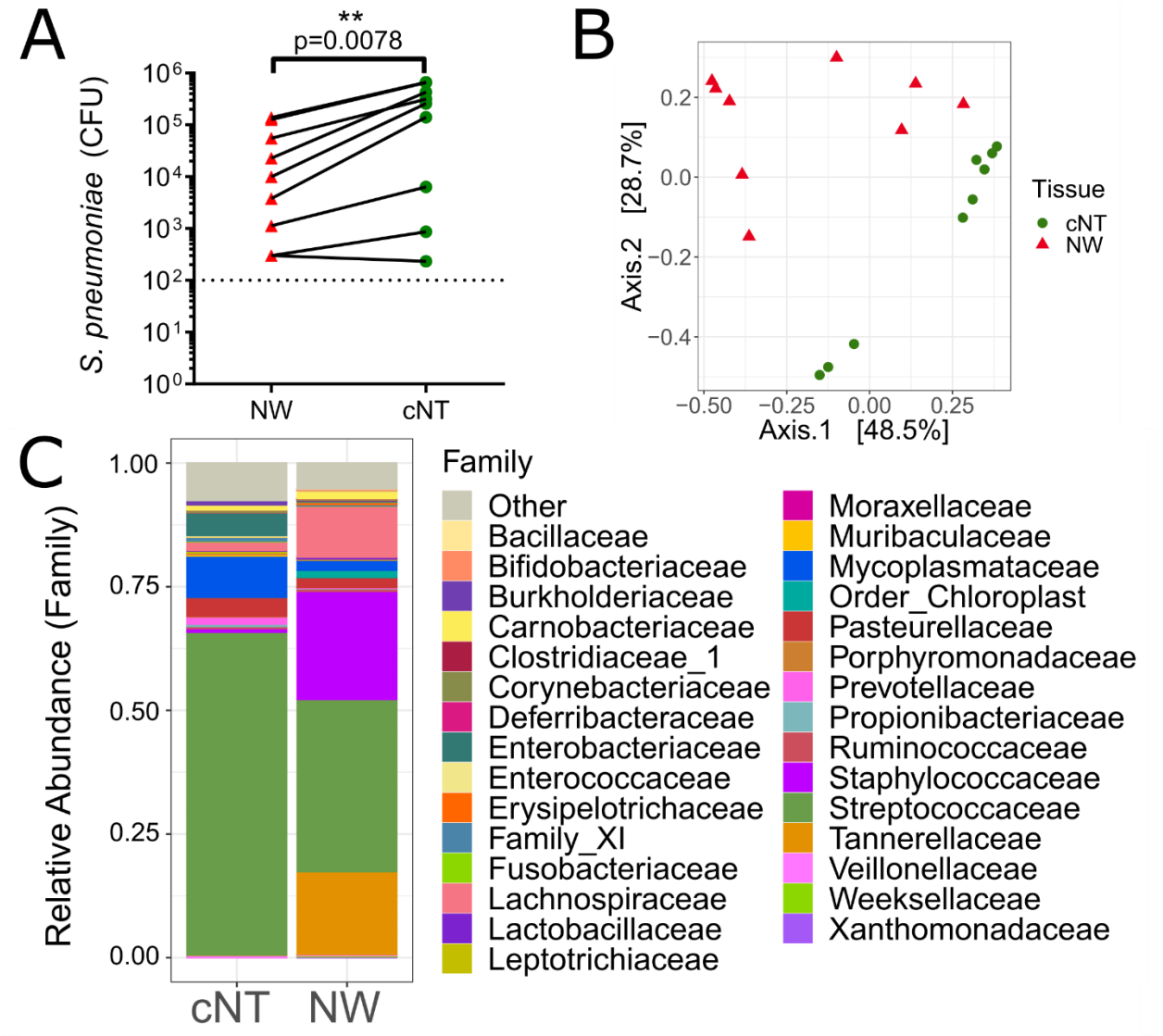

Figure 12 – *Streptococcus pneumoniae* dominates the nasal microbiota during colonization.

Female C57BL/6J mice were intranasally colonized with 10^7 CFU of *S. pneumoniae* and sacrificed 3 days later for collection of nasal washes and complete nasal tissues (N=8). (A) Nasal tissue had significantly higher pneumococcal load compared to nasal washes (p = 0.0078, Wilcoxon match-paired signed rank test). (B)The nasal tissue microbiota was distinct from the nasal wash microbiota (PERMANOVA, p = 0.0002). (C) Summary taxa plot of nasal tissue microbiota community (dominated by Streptococcaceae and Mycoplasmataceae) and nasal wash microbiota (dominated by Tannerellaceae, Streptococcaceae and Staphylococcaceae).

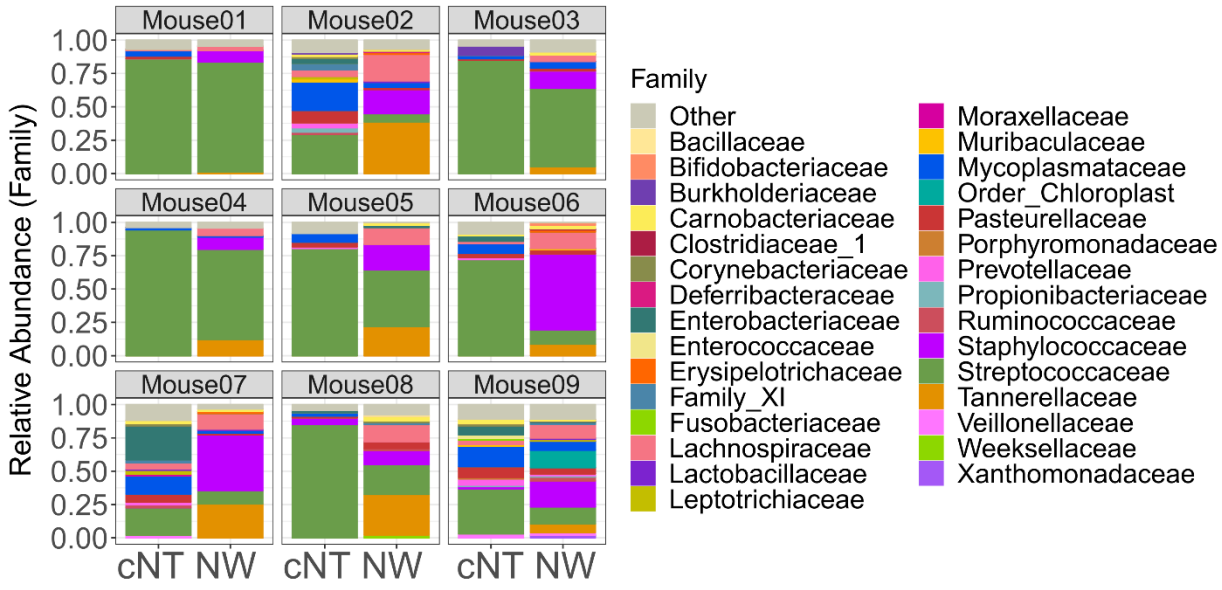

Figure 13– Individual taxa plots of nasal tissue and wash from S. pneumoniae colonized mice.

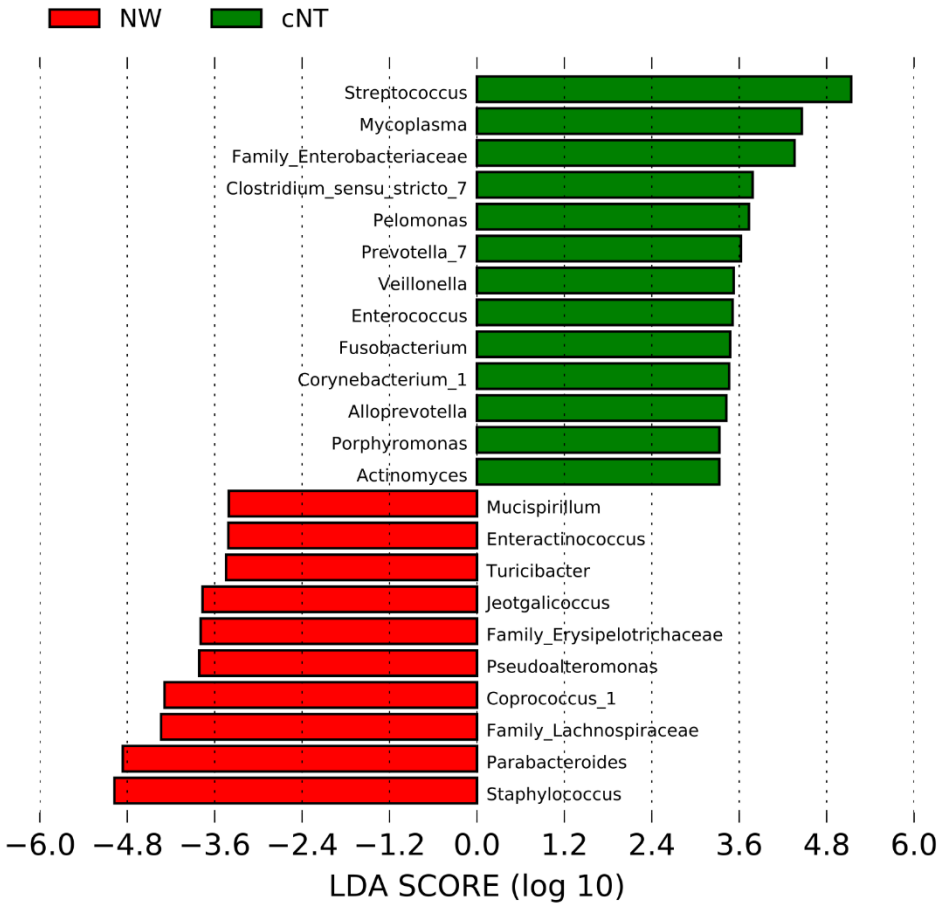

Figure 14 – LEfSe results of nasal wash and tissue microbiota differences in S. pneumoniae colonized mice.

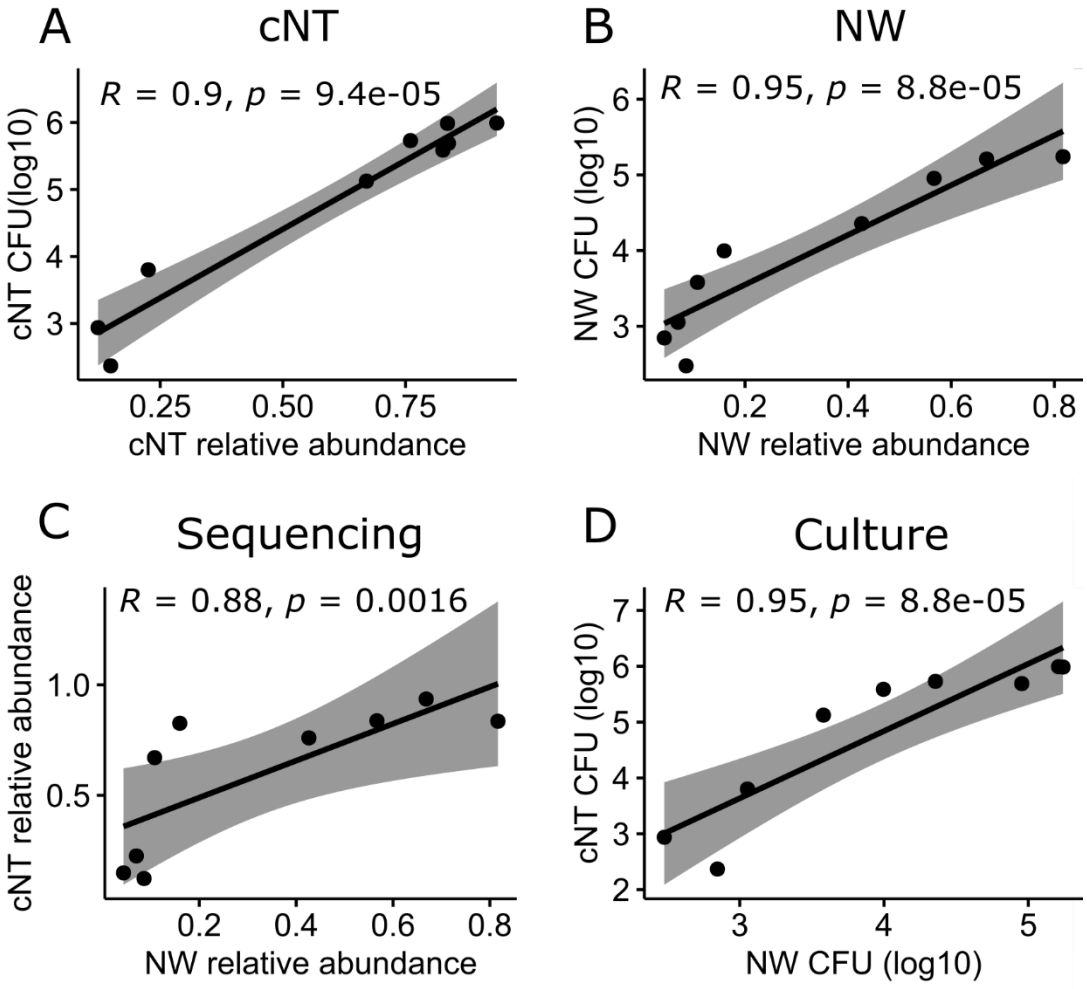

Figure 15 – Strong correlations between cultured and *S. pneumoniae* and *Streptococcus* ASV relative abundance.

Mice were inoculated with *S. pneumoniae* and 3 days later nasal washes and tissues were collected. Spearman correlations between cultured and sequenced *Streptococcus* in the nasal tissue (A) and nasal wash (B) were strong. *Streptococcus* ASV abundance (C) and cultured *S. pneumoniae* (D) strongly correlated in the nasal tissue and wash (Spearman correlations, each dot represents one mouse, n=9).

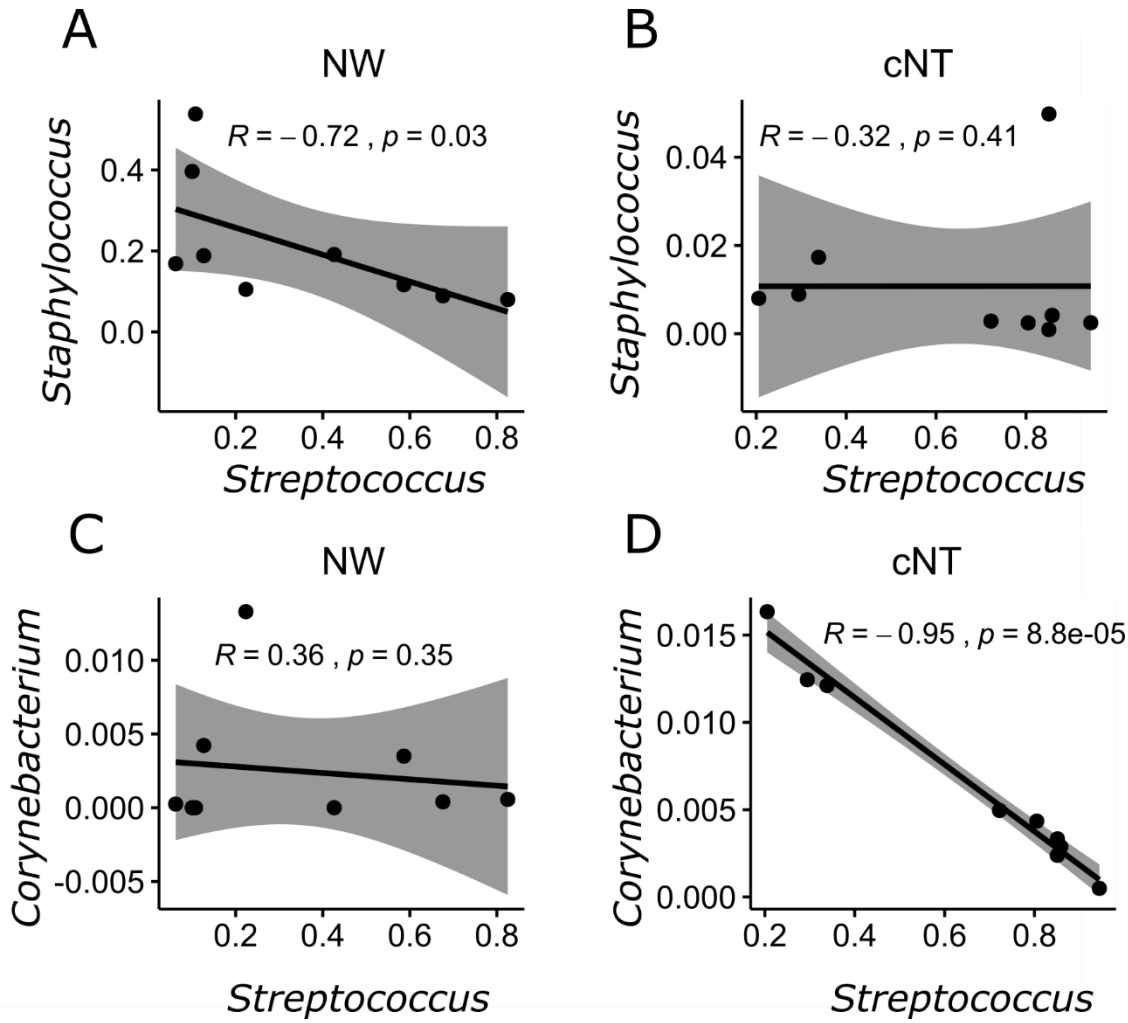

Figure 16 – Microbiota interactions depend on nasal sampling method. Spearman correlations of relative abundances of ASVs representing *Streptococcus* and *Staphylococcus* (A,B) or *Corynebacterium* (C,D) species. *Staphylococcus* and *Streptococcus* species have a negative correlation in the nasal washes (A), but not nasal tissue (B). Conversely, *Corynebacterium* species have a negative correlation in the nasal tissue (D), but not the nasal wash (C). Each dot represents relative abundance within one animal, from either nasal wash or tissue (n=9).

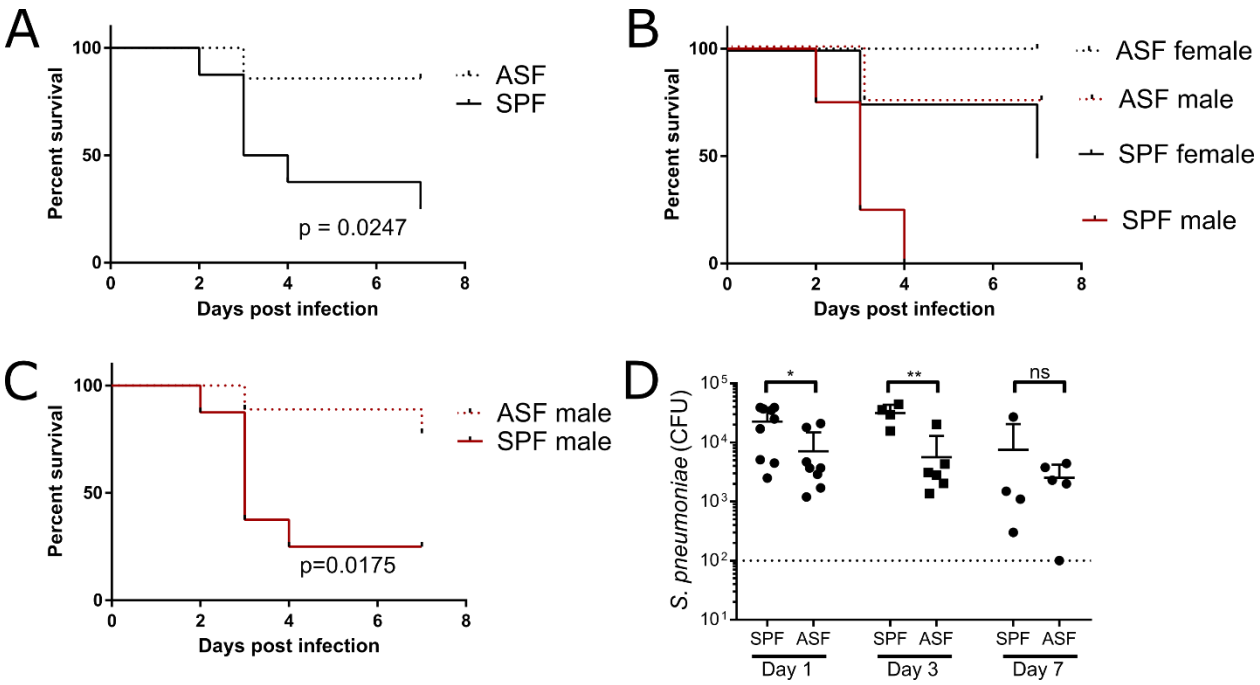

Figure 17 – ASF mice exhibit less mortality compared to SPF mice during pneumococcal exposure.

SPF and ASF (n=9) male and female mice were intranasally inoculated with *S. pneumoniae* P1547. (A) SPF mice exhibited significantly more mortality compared to ASF mice. (B) All male SPF mice died during the course of infection. (C) SPF male mice (n=8) have significantly more mortality than ASF male mice (n=9) post-pneumococcal inoculation. (D) SPF mice had significantly higher nasal pneumococcal density 1 and 3 days post-inoculation. *p*-values are indicated from log-rank Mantel-Cox tests or two-way ANOVA, Sidak's multiple comparison test, dotted line indicates limit of detection.

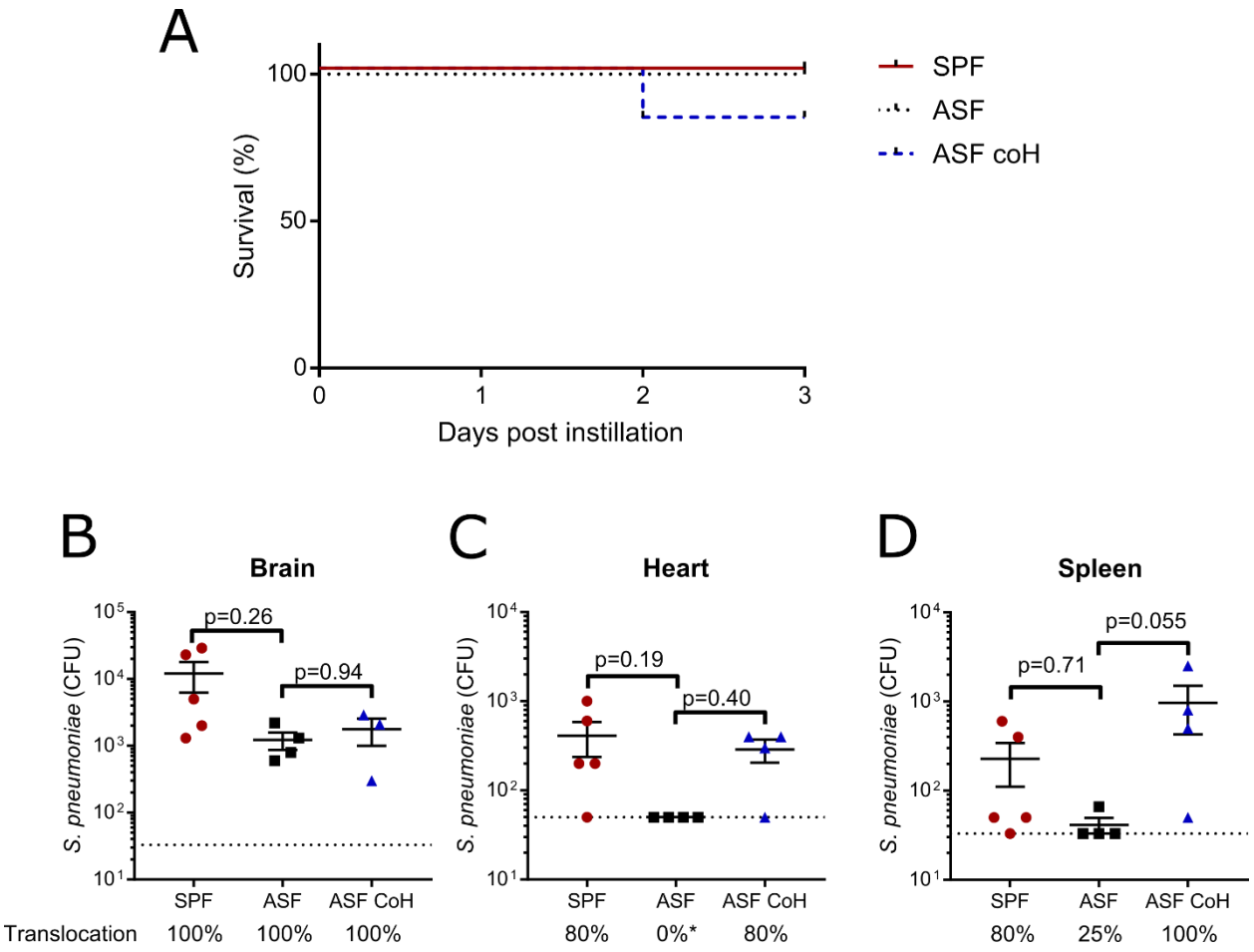

Figure 18 – ASF mice have lower incidence of pneumococcal spread.

ASF, SPF, and ASF mice cohoused with SPF mice for 3 weeks (ASF-CoH) were exposed to *S. pneumoniae* P1547 via lung instillation. (A) Survival was similar across all groups over 3 days, though one ASF-CoH was removed at day 2. All mice had cultivable *S. pneumoniae* in the brain (B) but ASF mice had lower incidence of heart translocation (C; $p<0.05$). (D) Translocation to the spleen was only detected in one ASF mouse, as compared to SPF (80%) and ASF-CoH (100%) mice. * indicates $p<0.05$, Fisher's exact test of translocation, dotted line represents limit of detection. Comparison of bacterial density was insignificant, *p*-values from Kruskal-Wallis analysis with Dunn's post-hoc test.

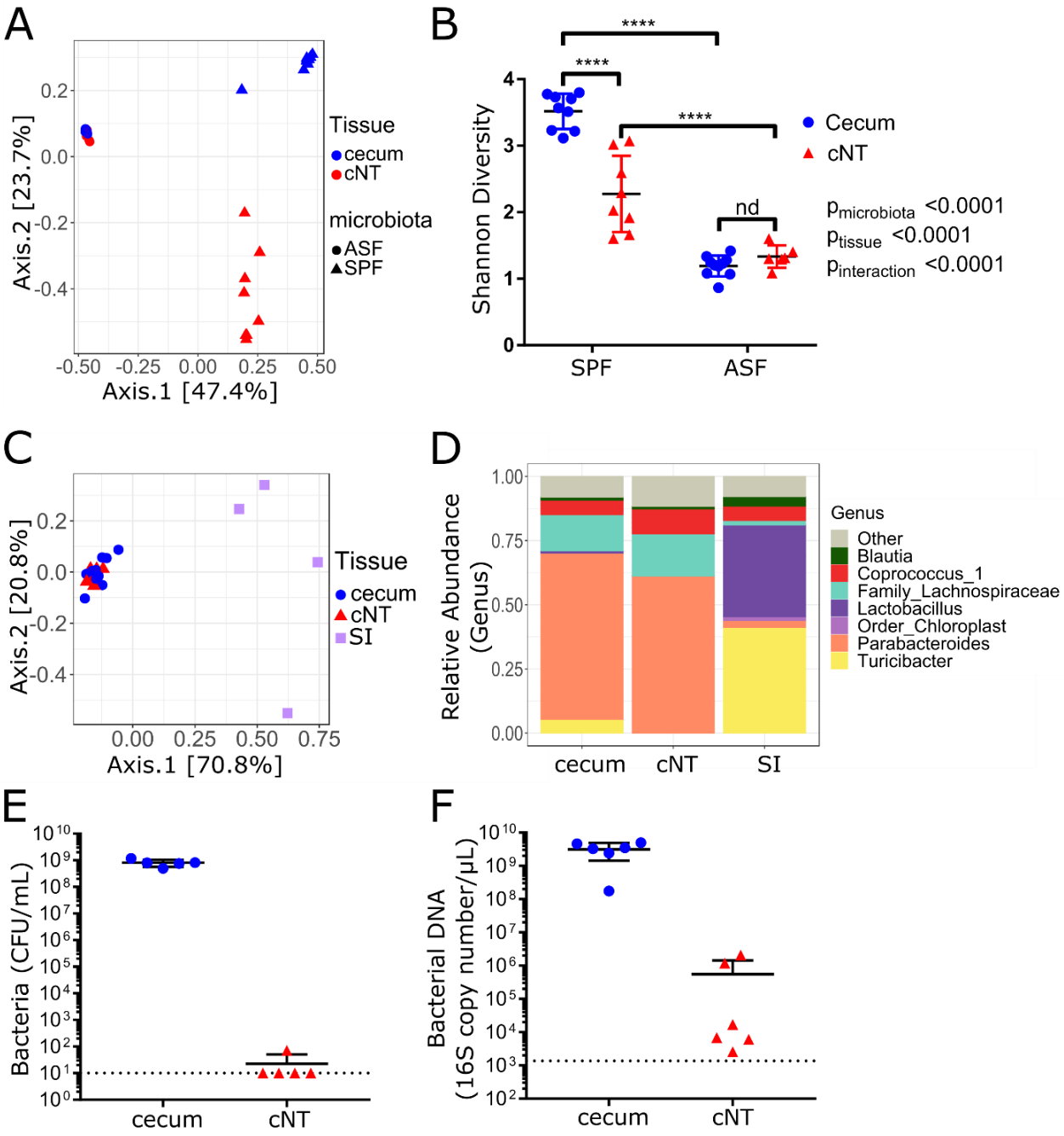

Figure 19 – ASF mice do not have cultivable nasal microbiota.

Nasal and gut tissues were collected from SPF and ASF mice for bacterial culture and DNA analysis. (A) 16S rRNA gene sequencing revealed a lack of distinction between tissue sites in ASF compared to SPF mice. (B) ASF mice have a greatly decreased α-diversity in their gut and nasal tissue compared to SPF mice, but no difference in diversity between tissue sites. (C) ASF mice do have distinction between small intestinal and cecal microbiota, suggesting that

this difference is not due to low complexity microbiota. (D) The community composition of nasal and cecal tissues are very similar compared to the small intestinal community. ASF mice did not have cultivable bacteria (E) but do have detectable bacterial DNA (F) in the nasal tissue. n=4-10 mice, **** indicates $p<0.0001$, two-way ANOVA, Sidak's multiple comparison test, dotted line indicates limit of detection.

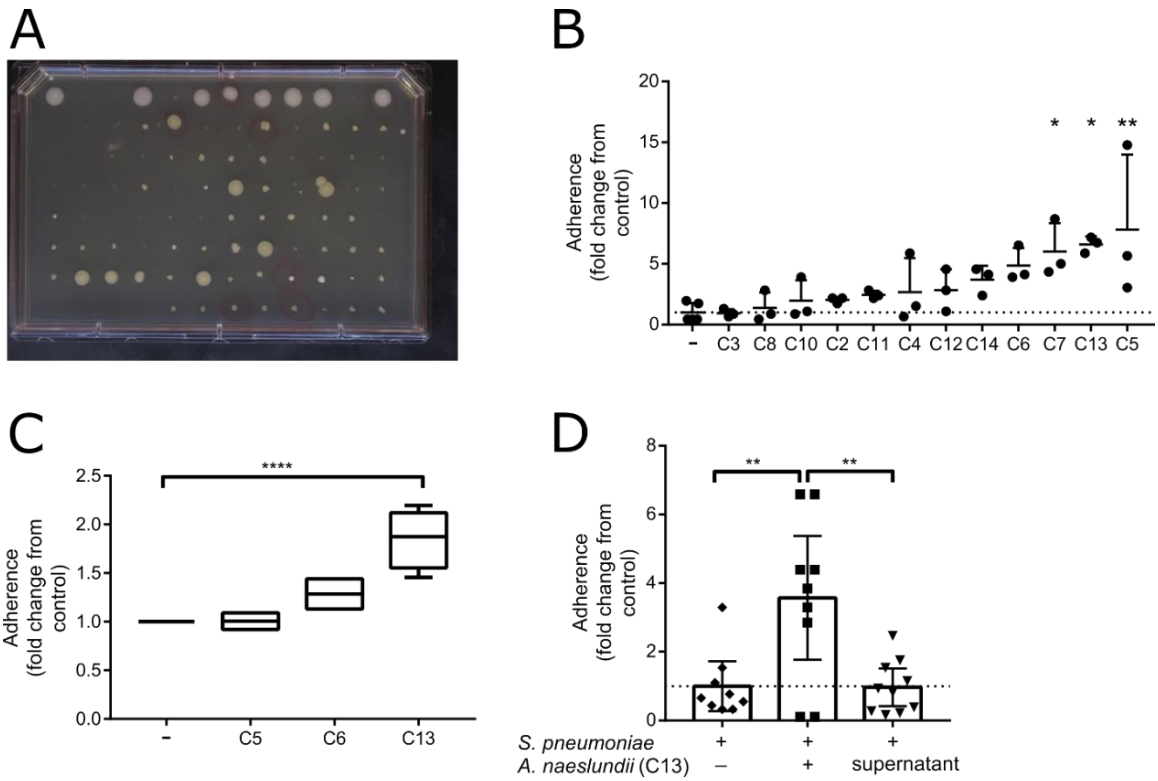

Figure 20 – *Actinomyces naeslundii* enhances pneumococcal adherence to epithelial cells *in vitro*.

(A) Nasal microbiota were cultured and isolated from SPF mice. (B) Distinct microbiota isolates were incubated with human pharyngeal carcinoma cells (Detroit-562) for 1 hour prior to incubation with S. pneumoniae P1547. Adherent pneumococci were counted from washed, trypsinized cells plated on selective media. (C) Isolate C13 reproducibly enhanced pneumococcal adherence across multiple experiments. (D) Bacterial cells of isolate C13, Actinomyces naeslundii, but not filtered supernatants enhanced pneumococcal adherence. Dots represent individual wells in experiments (n=3-10), dotted line represents control adherence. * indicates $p<0.05$, ** indicates $p<0.01$, **** indicates $p<0.0001$, ANOVA with Dunn's post-hoc test.

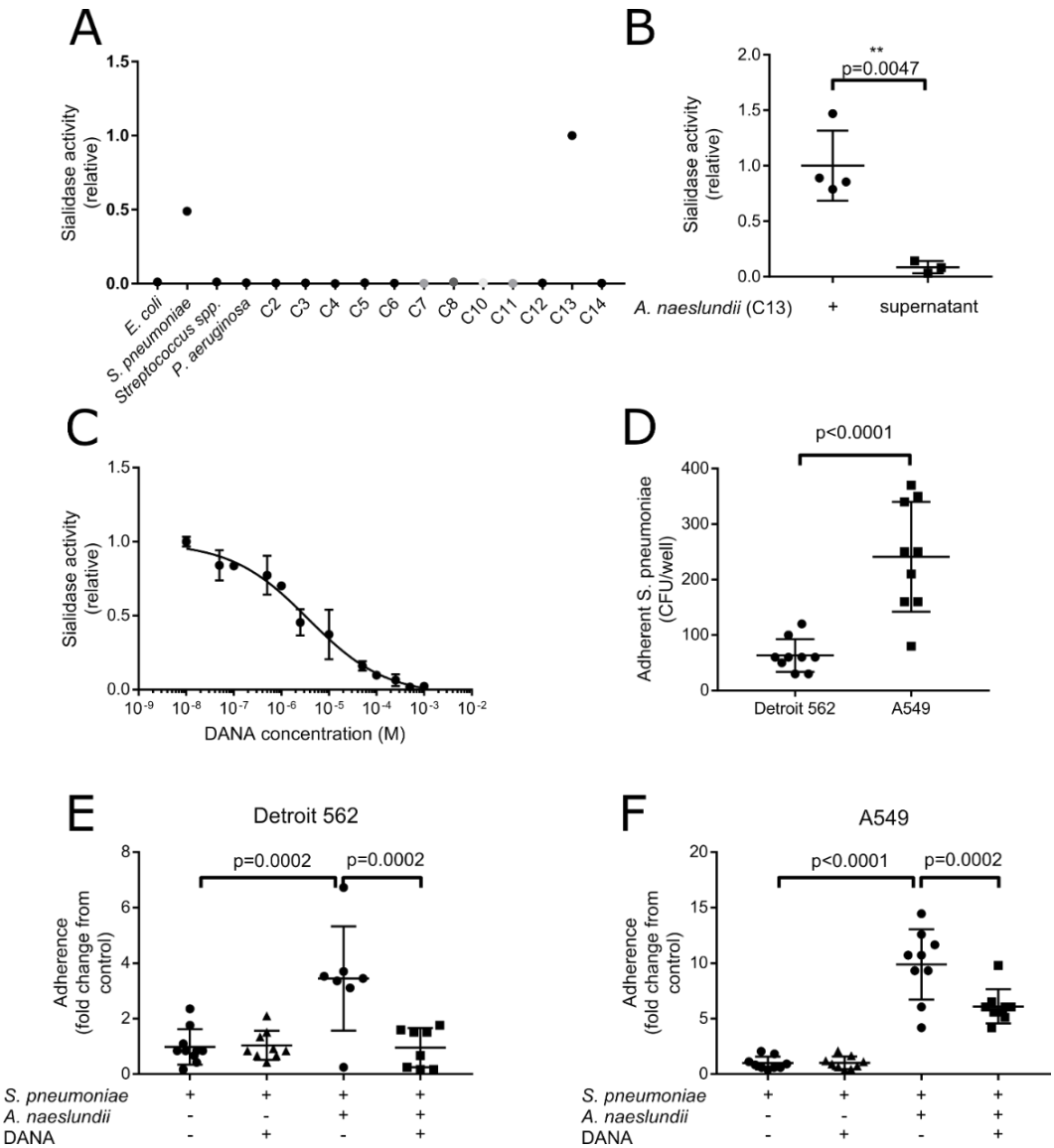

Figure 21 – Sialidase activity from *Actinomyces naeslundii* enhances pneumococcal adherence to epithelial cells *in vitro*.

(A) Bacterial isolates were screened for sialidase activity using a fluorescence-based 96-well plate assay. *S. pneumoniae* P1547 and isolate C13, *Actinomyces naeslundii*, possess sialidase activity. (B) Filtered supernatant from *A. naeslundii* lost sialidase activity. (C) Sialidase activity from *A. naeslundii* was sensitive to the pan-sialidase inhibitor DANA, with an IC50 of 3.66 µM. (D) *S. pneumoniae* is more adherent to lung (A549) compared to pharyngeal (Detroit-562) cells *in vitro*. Potentiation of pneumococcal adherence by *A. naeslundii* was inhibited by DANA (500 µM) in Detroit-562 (E) and A549 cells (F). Dots represent individual wells and are representative plots from at least 3 independent experiments. *p*-values are indicated from a one-way ANOVA with Dunn's post-hoc test.

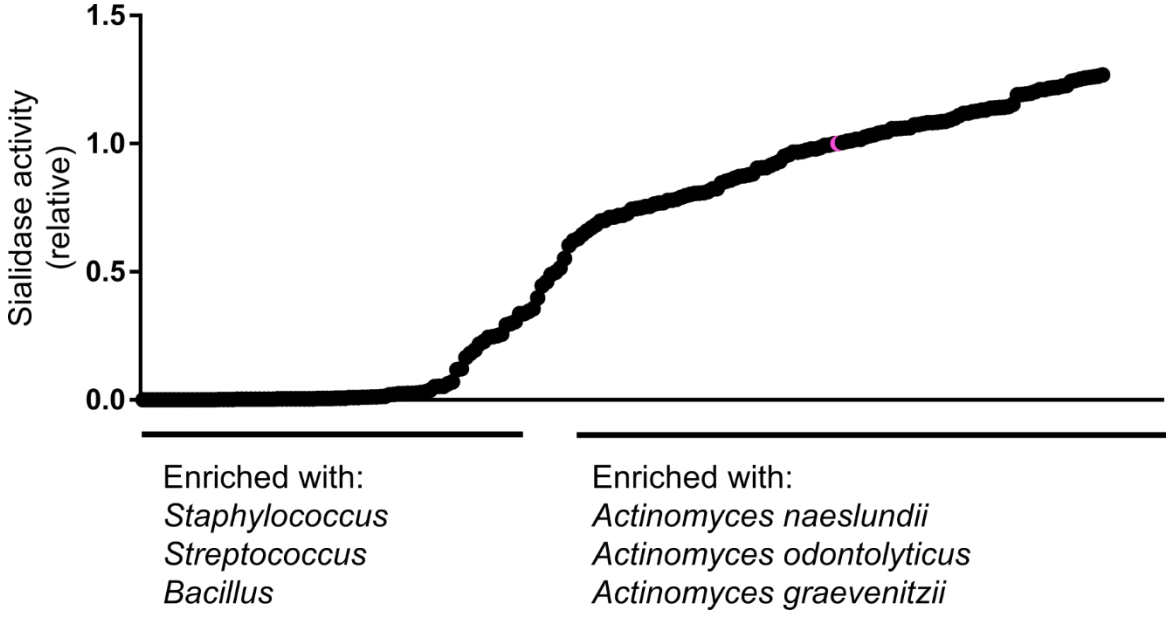

Figure 22 – Sialidase activity is conserved across *Actinomyces* genera.
150 isolates from a human respiratory microbial isolate collection were cultured on BHI agar for 48 hours prior to screening for sialidase activity. *Actinomyces* species expressed high sialidase activity, whereas members of *Staphylococcus*, *Streptococcus*, and *Bacillus* species had low expression. The pink dot is the reference strain, C13 *A. naeslundii*, isolated from mouse studies.

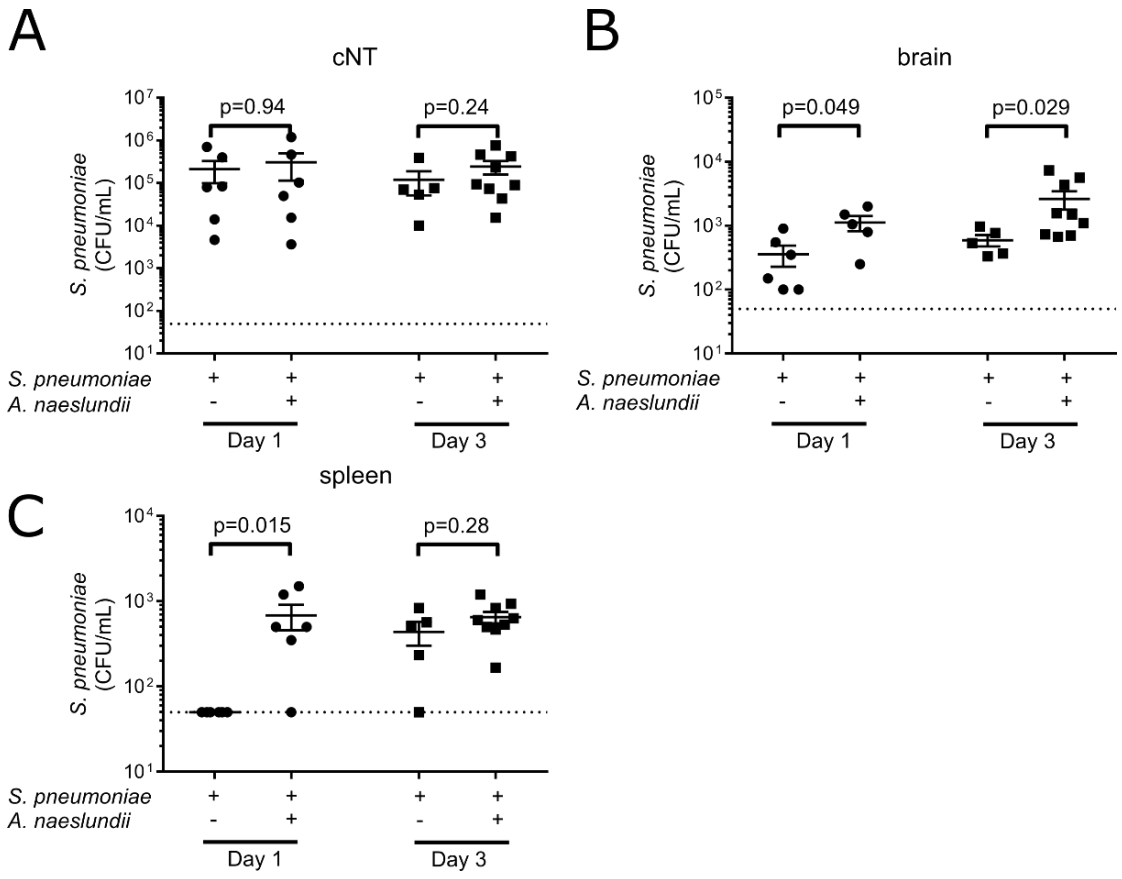

Figure 23 – *Actinomyces naeslundii* colonization enhances pneumococcal translocation to the brain and spleen.

SPF mice were colonized with *A. naeslundii* intranasally 24 hours prior to *S. pneumoniae* P1547 colonization. *A. naeslundii* had no effect on pneumococcal burden in the nasal tissue (A). Pneumococcal translocation was enhanced to the brain (B) and spleen (C) at early timepoints, but by day 3 SPF mice had similar levels. Dots represent individual mice (n=5-9), dotted line represents limit of detection. *p*-values are indicated from Mann-Whitney non-parametric t-tests.

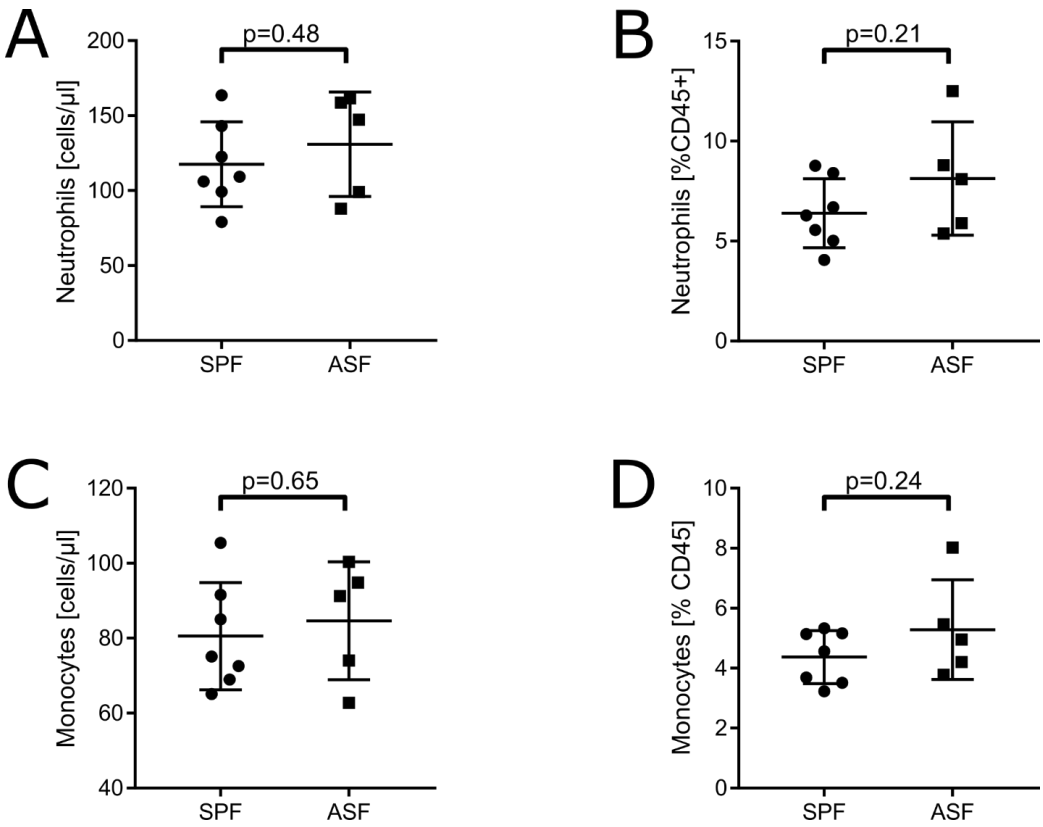

Figure 24 – SPF and ASF mice have similar neutrophil and monocyte composition in the blood.

Blood from SPF (n=7) and ASF (n=5) was collected and stained to quantify neutrophils and monocytes via flow cytometry. SPF and ASF mice have similar neutrophil total counts (A), and as a composition of all CD45 (B). Blood monocytes counts (C) and proportions (D) were similar between ASF and SPF mice. Each dot represents one animal, *p* values are indicated from unpaired Student's t-test.

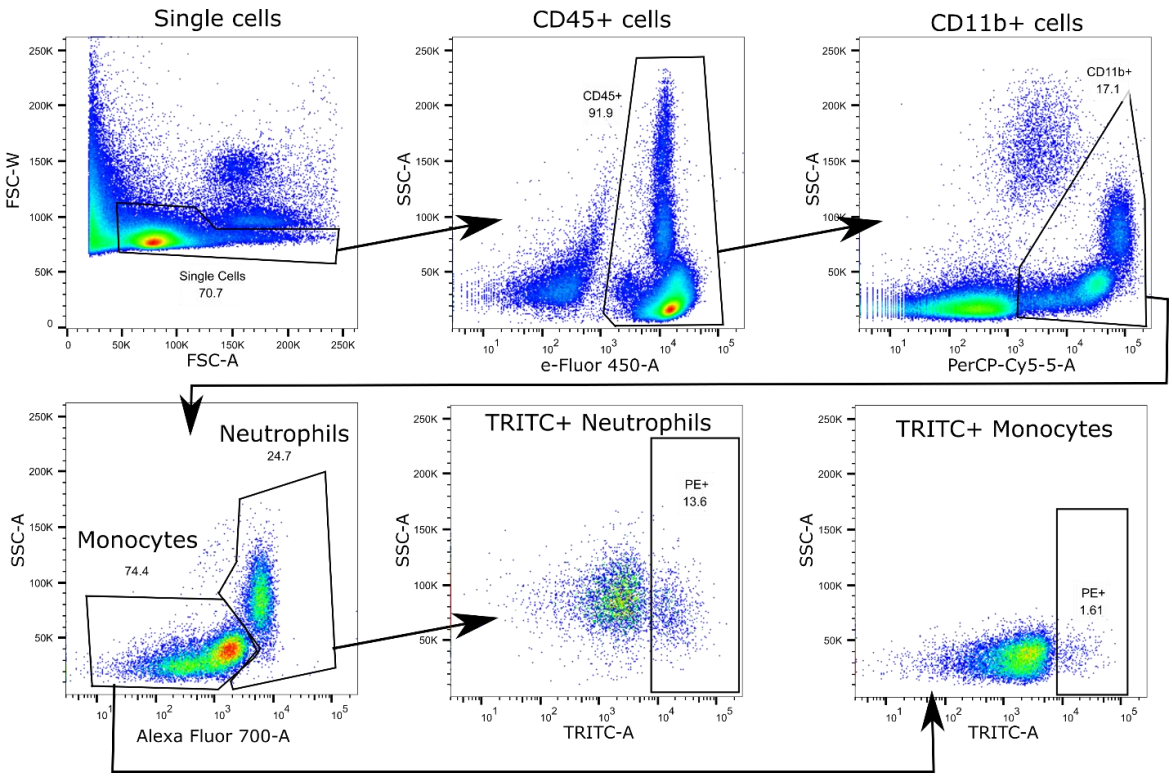

Figure 25 – Gating strategy for *S. pneumoniae*-positive neutrophils and monocytes from mouse blood.

Blood was incubated with TRITC-labelled *S. pneumoniae* prior to cell staining and flow cytometry. CD45+ single cells were assed for Cd11b and Ly6G to differentiate monocytes and neutrophils, prior to assessing bound/internalized *S. pneumoniae*.

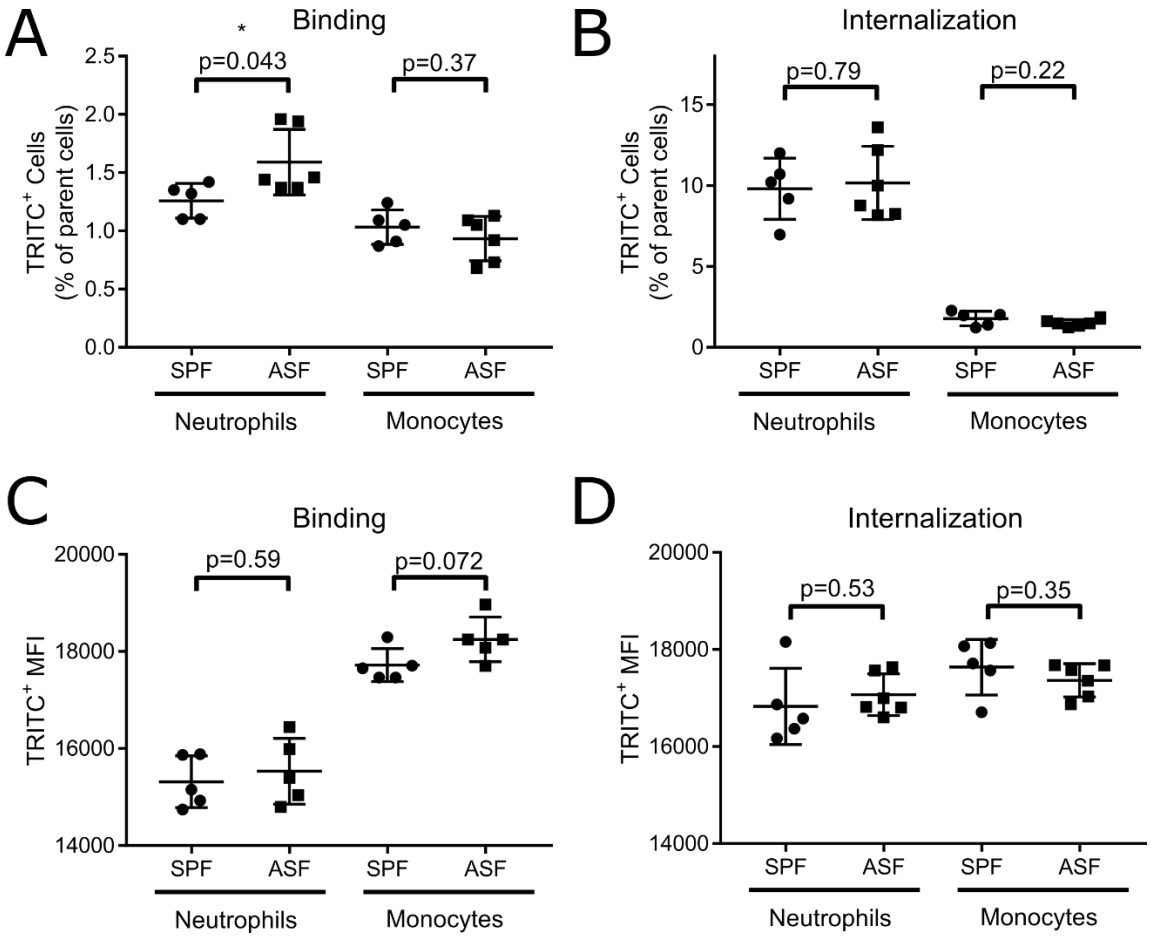

Figure 26 – Neutrophils from ASF mice have slightly increased pneumococcal binding.

Whole blood from SPF (n=5) and ASF (n=6) mice was incubated for 1 hour with TRITC-labelled, heat-killed *S. pneumoniae* for binding and internalization. Cells were stained to differentiate neutrophils ad monocytes by flow cytometry, as well as to quantify bacterial association (geometric mean fluorescence intensity: C,D). * indicates $p < 0.05$, unpaired Student's t-test.

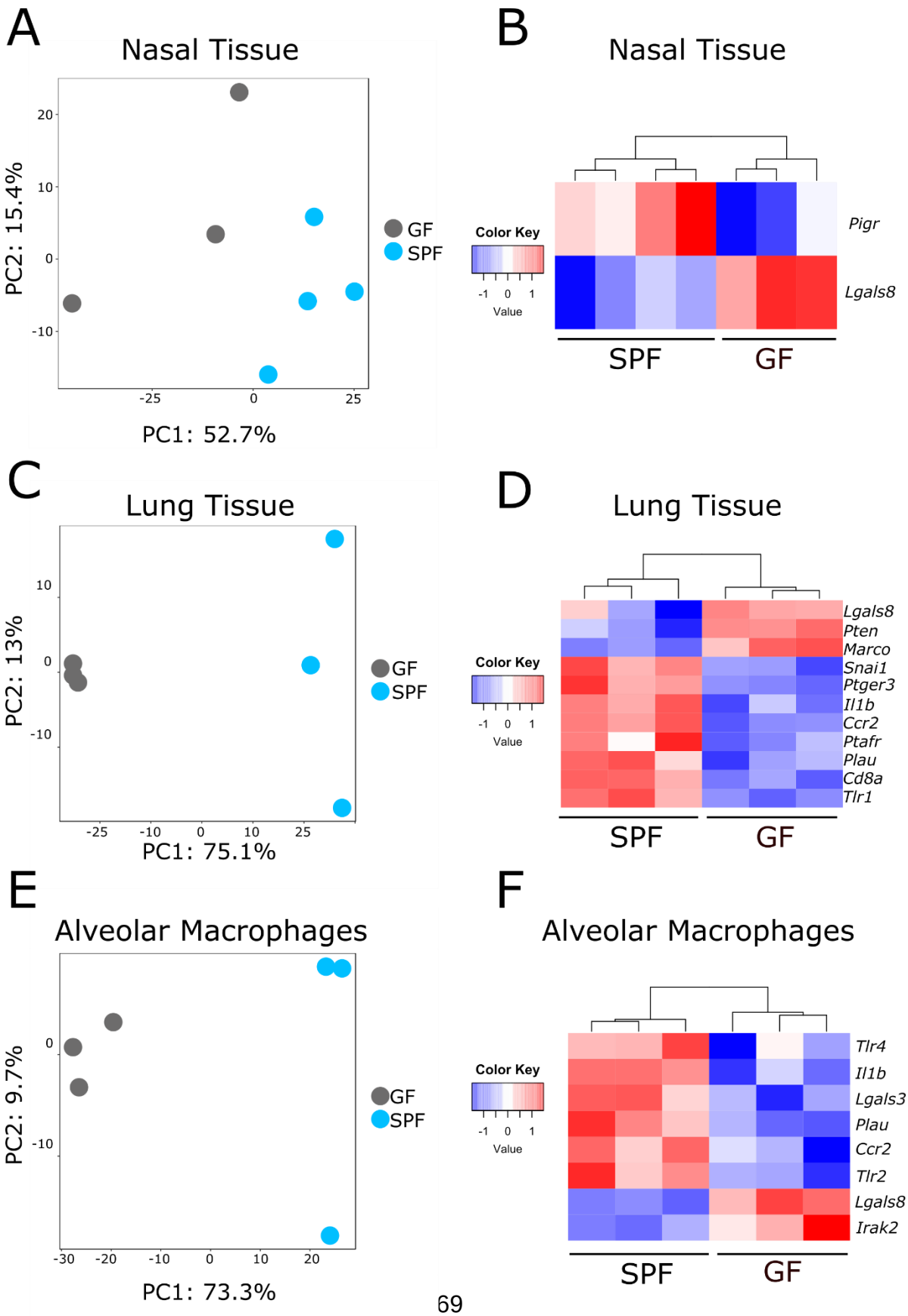
A
Nasal Tissue
PC2: 15.4%
PC1: 52.7%
GF
SPF
B
Nasal Tissue
Color Key
Value
Pigr
Lgals8
SPF
GF
C
Lung Tissue
PC2: 13%
PC1: 75.1%
GF
SPF
D
Lung Tissue
Color Key
Value
Lgals8
Pten
Marco
Snai1
Ptger3
Il1b
Ccr2
Ptafr
Plau
Cd8a
Tlr1
SPF
GF
E
Alveolar Macrophages
PC2: 9.7%
PC1: 73.3%
GF
SPF
F
Alveolar Macrophages
Color Key
Value
Tlr4
Il1b
Lgals3
Plau
Ccr2
Tlr2
Lgals8
Irak2
SPF
GF

Figure 27 – The microbiota alters host gene expression in the respiratory system, including genes important for *S. pneumoniae* infection.

Nasal (A-B) and lung (C-D) tissues, and alveolar macrophages (E-F), were collected from GF and SPF mice and prepared for transcriptomic analysis. Principal component analysis revealed that nasal (A), lung (C), and alveolar macrophage (E) gene expression profiles distinguished GF from SPF mice. Table 1 contains genes of importance identified from murine pneumococcal infections. All genes present in heatmaps (B,D,F) passed a false discover rate (FDR) of 0.05 after generalized linear model statistical tests performed in edgeR.

Table 1 – Identified isolates from URT microbiota of SPF mice

Identified colonies
Actinomyces naeslundii
Bacillus licheniformis
Staphylococcus caprae
Staphylococcus epidermidis
Staphylococcus saprophyticus
Staphylococcus warneri
Staphylococcus xylosus
Kocuria/Kytococcus species
Kocuria/Rothia species

Table 2 – Important genes during pneumococcal colonization and infection

Pneumococcal disease	Genes
Protective	*Ccl2, Ccr2, Cd4, Cerk, Cldn7, Cldn10, Ctsg, Elane, Fcna, Fcnb, Ifng, Il10, Il17a, Il1b, Il22ra1,Irak, Irak2, Lgals3, Lgals8, Marco, Nik, Nlrp3, Nod1, Nod2, Plaur, Prf1,Rip2, Tab2, Tak1,Tcra-j, Tlr1, Tlr2, Tlr4,Tnfrsf1a*
Deleterious	*Cd14, Ifna, Ifnb, Ifnar, Pten, Ptger3, Plau, Snai1*
Mixed reports	*Cd8a, Pigr, Ptafr, Tnfa*

Table 3 – Significantly different genera in the URT microbiota of in-house mice versus Jackson Laboratories

Genus	Enriched	LDA	*p*-value
Mycoplasma	JAX	4.91	2.38E-07
Fusobacterium	JAX	4.12	2.72E-04
Faecalibacterium	JAX	4.10	3.19E-05
Bacteroides	JAX	4.10	4.51E-06
Burkholderia_Caballeronia_Paraburkholderia	JAX	4.09	1.60E-02
Family_Caulobacteraceae	JAX	3.89	3.59E-11
Blautia	JAX	3.87	4.74E-06
Aerococcus	JAX	3.85	1.58E-04
Corynebacterium_1	JAX	3.80	1.80E-07
Bifidobacterium	JAX	3.77	2.96E-05
Haemophilus	JAX	3.74	5.88E-05
Prevotella_9	JAX	3.69	9.41E-05
Roseburia	JAX	3.65	1.13E-03
Actinobacillus	JAX	3.63	1.73E-09
Escherichia_Shigella	JAX	3.63	1.30E-03
Prevotella_7	JAX	3.63	4.73E-05
Eisenbergiella	JAX	3.62	1.93E-05
Lactococcus	JAX	3.60	2.35E-03
Gemella	JAX	3.60	9.64E-05
Pseudobutyrivibrio	JAX	3.60	2.52E-05
Methylobacterium	JAX	3.56	9.63E-08
Pluralibacter	JAX	3.54	2.55E-03
Acidibacter	JAX	3.50	2.60E-10
Neisseria	JAX	3.45	6.35E-05
Veillonella	JAX	3.41	1.21E-04
Family_Mitochondria	JAX	3.40	3.25E-06
Kingdom_Bacteria	JAX	3.40	1.92E-05
Pseudomonas	JAX	3.38	4.57E-04
Subdoligranulum	JAX	3.35	5.18E-04
Prevotella	JAX	3.34	5.80E-05
Lachnospira	JAX	3.34	1.78E-03
Prevotella_2	JAX	3.33	8.15E-06
Granulicatella	JAX	3.32	1.11E-04
Ruminococcus_1	JAX	3.30	6.92E-06

Family_Ruminococcaceae	JAX	3.27	1.82E-03
Fusicatenibacter	JAX	3.27	3.59E-03
Peptoniphilus	JAX	3.25	5.48E-04
Lachnospiraceae_NK4A136_group	JAX	3.25	7.78E-03
Ralstonia	JAX	3.24	4.74E-07
Porphyromonas	JAX	3.24	3.11E-05
Parvimonas	JAX	3.24	1.92E-04
Coprococcus_2	JAX	3.21	3.42E-03
Peptostreptococcus	JAX	3.21	1.67E-04
Clostridioides	JAX	3.20	9.91E-03
Lachnospiraceae_UCG_001	JAX	3.18	4.07E-02
Holdemanella	JAX	3.13	3.70E-02
Leptotrichia	JAX	3.13	3.68E-05
Dialister	JAX	3.12	8.04E-06
Bacillus	JAX	3.10	2.69E-04
Acetatifactor	JAX	3.10	1.13E-03
Acinetobacter	JAX	3.09	7.47E-03
Family_Peptostreptococcaceae	JAX	3.09	6.36E-04
Finegoldia	JAX	3.06	1.29E-02
Jeotgalicoccus	JAX	3.01	4.77E-02
Flavonifractor	JAX	3.01	6.47E-04
Collinsella	JAX	3.00	1.50E-02
Sutterella	JAX	2.96	5.40E-05
Ruminococcaceae_UCG_014	JAX	2.95	8.08E-03
Facklamia	JAX	2.92	3.68E-02
Atopostipes	JAX	2.92	1.63E-03
Ruminococcaceae_UCG_002	JAX	2.92	4.76E-03
Ruminiclostridium_9	JAX	2.91	1.21E-02
Hydrotalea	JAX	2.90	3.68E-05
Alkalispirillum	JAX	2.89	9.74E-03
Ezakiella	JAX	2.87	6.47E-04
Bradyrhizobium	JAX	2.87	9.74E-03
Oligella	JAX	2.87	3.68E-02
Tannerella	JAX	2.84	6.47E-04
Rothia	JAX	2.83	4.91E-02
Family_Family_XIII	JAX	2.82	2.55E-03
Lachnospiraceae_UCG_004	JAX	2.81	2.55E-03
Family_Xanthobacteraceae	JAX	2.81	3.68E-02

Vibrionimonas	JAX	2.81	2.55E-03
Haliangium	JAX	2.79	3.68E-02
Treponema_2	JAX	2.79	8.55E-04
Campylobacter	JAX	2.78	2.55E-03
Ruminiclostridium_6	JAX	2.78	5.90E-03
Christensenellaceae_R_7_group	JAX	2.78	3.78E-04
Ruminococcaceae_UCG_005	JAX	2.77	1.36E-02
Negativicoccus	JAX	2.77	3.68E-02
ASF356	JAX	2.75	3.68E-02
Family_Coriobacteriales_Incertae_Sedis	JAX	2.73	3.68E-02
Class_Bacteroidia	JAX	2.73	9.74E-03
Oscillospira	JAX	2.72	6.47E-04
Selenomonas_3	JAX	2.71	2.55E-03
Intestinimonas	JAX	2.71	3.68E-02
Butyricicoccus	JAX	2.70	3.16E-03
Flavobacterium	JAX	2.70	3.68E-02
Bergeyella	JAX	2.63	3.68E-02
Lysinibacillus	JAX	2.61	3.68E-02
Ruminococcaceae_UCG_009	JAX	2.59	3.68E-02
Megasphaera	JAX	2.59	9.74E-03
Prevotella_6	JAX	2.58	3.68E-02
Tepidimonas	JAX	2.57	9.74E-03
Catenibacterium	JAX	2.57	3.68E-02
Trueperella	JAX	2.54	3.68E-02
Dolosigranulum	JAX	2.53	9.74E-03
Family_Chitinophagaceae	JAX	2.48	3.68E-02
Merdibacter	JAX	2.43	3.68E-02
Enterococcus	In-house	4.97	1.74E-04
Family_Neisseriaceae	In-house	4.26	4.77E-03
Lactobacillus	In-house	4.20	5.75E-03
Paenibacillus	In-house	4.11	2.23E-03
Clostridium_sensu_stricto_1	In-house	3.78	3.13E-03
Salmonella	In-house	3.40	3.65E-02
Ileibacterium	In-house	3.39	2.68E-02
Ruminococcus_2	In-house	3.00	1.24E-02
Erysipelotrichaceae_UCG_003	In-house	2.73	6.10E-03
Anaeroplasma	In-house	2.69	2.01E-02